THE ASTROPHYSICAL JOURNAL

AN INTERNATIONAL REVIEW OF SPECTROSCOPY AND ASTRONOMICAL PHYSICS

VOLUME 85 APRIL 1937 NUMBER 3

OBSERVATIONS OF B-TYPE STARS IN THE RED AND INFRA-RED REGIONS OF THE SPECTRUM

JOHN S. HALL

ABSTRACT

The difference in magnitude between ζ and ϵ Persei has been determined throughout a spectral region of more than 5000 A with a photoelectric photometer used in conjunction with an objective grating.

When these observations are combined with those by Kienle and by Mrs. Rudnick, the difference in magnitude between these two stars is, to a first approximation, proportional to the frequency. These data therefore do not definitely disprove the hypothesis that the peculiar color of ζ is either partly or entirely due to a temperature difference between these two stars. If this coloring is attributed to matter in interstellar space, the wave-length exponent in the attenuation term is near unity in the observed spectral region. A more literal interpretation of the data suggests that this exponent increases from about 1.2 in the visual to 1.6 in the infra-red.

Infra-red colors and magnitudes of 19 B stars have been determined. A comparison of the color excesses computed from these data with those given by Stebbins and Huffer also indicates that this exponent is near unity.

It has been shown in a previous paper[1] that certain early-type stars measured in the infra-red region of the spectrum were much redder than the average star of the same spectral type. The same stars were known to be highly colored, from measures in the blue and yellow regions of the spectrum.

In an effort to determine the attenuation coefficient as a function of the wave-length, the effective energy of ζ Persei was compared with that of ϵ Persei over a long spectral range, on five different nights at the Sproul Observatory.

Since this program was started, Mrs. Rudnick, at the Yerkes Ob-

[1] *Ap. J.*, **79**, 177, 1934.

servatory, has published a paper[2] on this subject and has based her conclusions mainly on her spectrophotometric observations of these two stars. Kienle[3] has also made spectrophotometric comparisons of these stars. Three similar comparisons have been made in the blue and the red regions by the Greenwich observers Greaves, Davidson, and Martin.[4] The Sproul data were derived in an entirely different manner and cover a much longer spectral region than former comparisons.

Spectra were produced by a fine-wire objective grating. A spectrometer in the focal plane separated the two first-order spectra into definite energy units of known wave-length and reflected them to the photoelectric cell. This method has been described in a previous paper.[5]

Since these two stars are only a little more than eight degrees apart in the sky, and since they were observed near the zenith, the corrections for differential extinction were negligibly small.

Since I was interested in the difference in magnitude of these two stars as a function of the wave-length, it was important to know whether the scale of the photometer changed with the wave-length. From former laboratory tests I found that the observed response of the cell was linear if an incandescent lamp was used as a source. Since the two stars are about equally bright visually, it seemed more important to check the scale at 10,000 A, where ζ Persei is about 0.6 mag. brighter than ϵ and the observed electrometer deflections are small. The scale of the photometer was checked in this region in the following manner: the two first-order spectra of ζ Persei were focused on their respective slits, which were displaced from the central image at such a distance that their centers corresponded to 10,000 A. The slits were 2 mm or 980 A wide. The response was then measured with first one and then the other slit covered, and again with both slits open. This process was repeated with no star in the field, in order to determine the response due to background and other effects. After the stellar observations were corrected for background, it was found that the total response from the separate slits equaled the combined effective energy, within the error of observation. This

[2] *Ibid.*, **83**, 394, 1936.

[3] *M.N.*, **88**, 700, 1928.

[4] *Ibid.*, p. 702.

[5] *Ap. J.*, **84**, 372, 1936.

process was completed four times, and the mean scale factor was 1.00 ± 0.02 (probable error).

Figure 1 shows the photoelectric response as a function of the wave-length, according to the observations of December 7, 1936. Since the slit-widths were 2.00 mm wide, the effective wave-lengths were not exactly the same as the wave-length of the center of the slit, which is the abscissa of the curves. It is evident from the number of observations that each spectral region was measured twice.

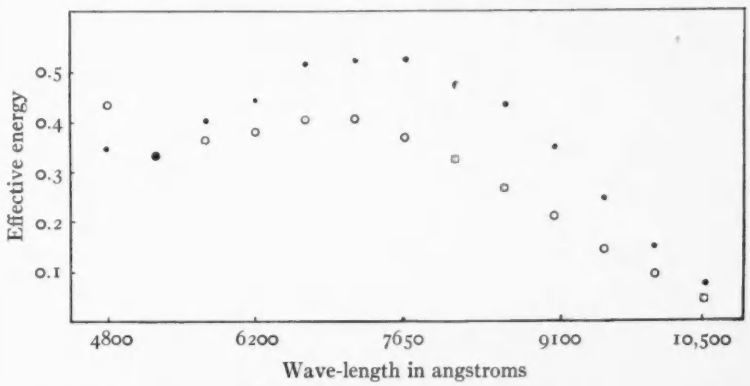

FIG. 1.—The photoelectric response in eyepiece divisions per second is plotted against the wave-length of the center of the slits. ζ Persei is represented by dots, and ϵ Persei by circles. If the positions of the slits were numbered from 1 to 13, beginning at the left, these data were observed in the order 1, 3, 5, 7, 9, 11, 13, 12, 10, 8, 6, 4, 2,1. Readings with the standard lamp in position, and also readings due to background were made at each end of the stellar sequence.

These observations are sufficiently numerous to enable one to determine by a graphical process the wave-length which equally divides the effective energy for each setting of the slits. When this wave-length is known, a smoothed curve through the points may be used to determine the corrections to the observed energy in order to reduce it to its value at the wave-length corresponding to the center of the slits. I have carried through this procedure and found that these corrections are 0.04 mag. or less, except for the last three points in the infra-red. Since we are primarily concerned with the *difference in magnitude* between these two stars as a function of the wave-length, the corrections to be applied to the measured magnitude differences are very small, except for observations beyond 10,000 A.

These differential corrections are given in the next to the last column of Table 1. The wave-length of the center of the slits, which in view of these corrections may be considered as the effective wave-length, is given in the first column of Table 1.

The small grating mentioned in the footnote of Table 1 is the one mentioned in the former paper.[5] The large grating gives

TABLE 1*

Wave-Length (μ)	Magnitude Differences: ζ Persei − ϵ Persei								
	1936 Jan. 25	1936 Feb. 8	1936 Nov. 29	1936 Dec. 7	1936 Dec. 22	Weighted Mean	Weight	Diff. Corr.	Final Mean
0.428	.....	.....	+0^{M}28	.....	.....	+0^{M}28	0.5	.....	.....
0.477	+0^{M}21	+0^{M}16	+ .31	+0^{M}24	+0^{M}18	+ .21	4.0	−0^{M}02	+0^{M}19
0.525	.....	+ .06	− .01	.00	.....	+ .02	2.5	.00	+ .02
0.573	− .09	− .05	.19	− .12	− .07	− .10	4.0	+ .01	− .09
0.621	.....	.17	.14	.18	.....	.17	2.5	+ .01	.16
0.669	.24	.24	.28	.27	.34	.28	4.0	.00	.28
0.717	.....	.25	.35	.28	.....	.28	2.5	.00	.28
0.765	.37	.32	.37	.39	.42	.37	4.0	.00	.37
0.813	.....	.48	.35	.42	.....	.43	2.5	.00	.43
0.862	.50	.46	.53	.52	.42	.48	4.0	− .01	.49
0.910	.....	.58	(.30)	.56	.....	.57	2.0	− .01	.58
0.958	0.51	0.64	.52	.60	0.54	.57	4.5	+ .01	.56
0.982	.....	.....	0.66	.....	.....	.66	0.5	.00	
1.007	.....	.....	.....	.52	.....	.52	1.0	+ .01	0.62
1.055	.....	.....	.....	0.64	.....	0.64	1.0	−0.08	
Slit-widths	2 mm	2 mm	1 mm	2 mm	2 mm	.....	.....	.....	.....
Grating	Small	Small	Large	Large	Small	.....	.....	.....	.....
Number of readings	1	2	1	2	2	.....	.....	.....	.....

* No observations were made on January 25 of the region beyond 0.862μ. The value 0.51 at 0.958μ was derived from a recent comparison in this spectral region. The value in parentheses has been assigned zero weight in forming the mean magnitude difference.

a similar dispersion at the focus but covers 0.9 instead of 0.4 of the objective. The hydrogen emission lines $H\alpha$ and $H\beta$ in γ Cassiopeia have been seen and photographed with this grating in front of the 24-inch objective. The dispersion as derived from a single exposure of this star appears to be near 483 instead of 480 A per mm. The use of the former value, which was used for the smaller grating, does not noticeably change the results of this paper. Except for the observations of February 8, the focal length was changed in such a way that the slits were always in reasonably good focus for the par-

PLATE III

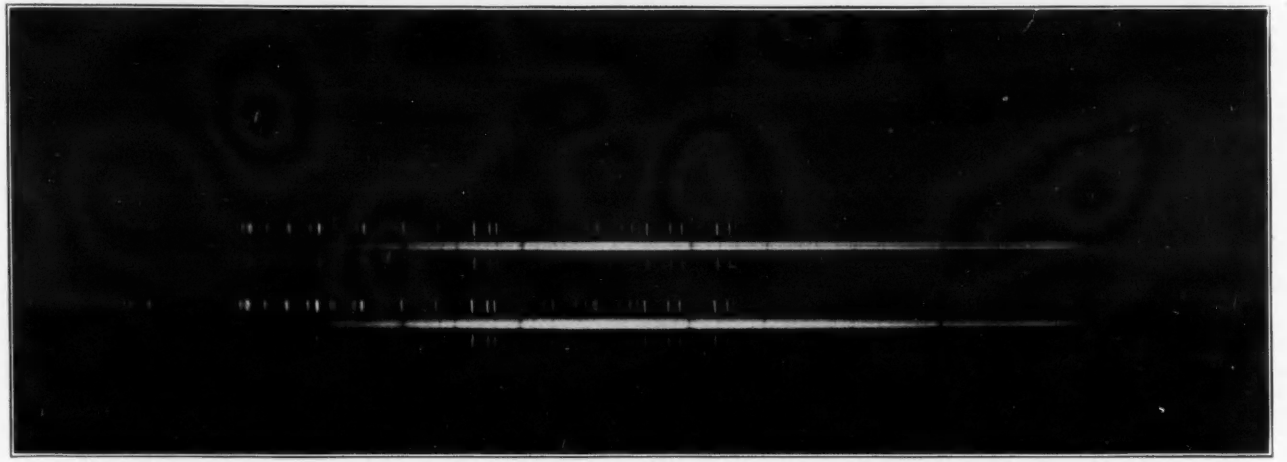

SPECTROGRAMS OF ζ AND ϵ PERSEI SECURED BY DR. MOHLER AT THE COOK OBSERVATORY
The lines in ζ are slightly sharper than those in ϵ Persei

ticular wave-length bands passing through them. On February 8 the focus was fixed at a mean value for all readings. The two nights on which only one reading was made for each position of the slits were given half-weight in forming the mean magnitude differences. In general, since these single readings average longer than 30 seconds in duration, they are equivalent to at least two short readings. Except for these two nights, when the telescope was pointed at each star but once, the first star was always reobserved. The transparency was excellent on all five nights.

Both ζ and ϵ Persei have companions which share their proper motions of 13″ and 9″ separation, respectively. Their respective visual magnitudes are 9.3 and 8.3. Both are on the edge of the field striking the cathode of the cell. Since, according to descriptions in Burnham's catalogue, neither companion is reddish in color, it is highly improbable that they influence the results by an appreciable amount.

The final mean magnitude differences of Table 1 are plotted against the frequency in Figure 2. If ϵ and ζ radiate as black bodies with temperatures of 22,500° and 10,000° K, respectively, and if the theoretical curve were fitted to the straight line at its mid-point, the extreme values of this curve would fall 0.04 mag. below the straight line at each end. These data do not definitely refute the hypothesis that the peculiar color of ζ is due to an unusually low temperature of this B1 star.

The color of ϵ Persei has been found to be normal for its spectral class in both the violet and the infra-red regions of the spectrum. The spectral type and absolute magnitude found by Edwards[6] for ζ Persei are B1ss and -3.2. The corresponding data for ϵ Persei are B1s and -2.9. Rimmer[7] has classified both ζ and ϵ Persei as B1s and has assigned an absolute magnitude of -2.5 to both stars. However, Struve and others have shown that ζ Persei has strong interstellar lines, and is therefore very luminous. Plate III shows that the spectra of these stars are very similar. It is therefore reasonable to suppose that the distribution of energy is the same function of the wave-length for each of them, and that the observed reddening of ζ is due to selective absorption or scattering of its initial energy by

[6] *M.N.*, **87**, 377, 1927. [7] *Commonwealth Solar Obs. Mem. 2*, 1930.

particles in interstellar space. If we let $e^{-k\lambda^{-\alpha}+c}$ be the transmission coefficient of intervening particles, then the observed difference in magnitude between these two stars is

$$\Delta m_\lambda = -(2.5\ log\ e)k\lambda^{-\alpha} + D\ . \qquad (1)$$

The coefficient k is a function of the properties of the intervening medium and is assumed to be independent of λ. According to

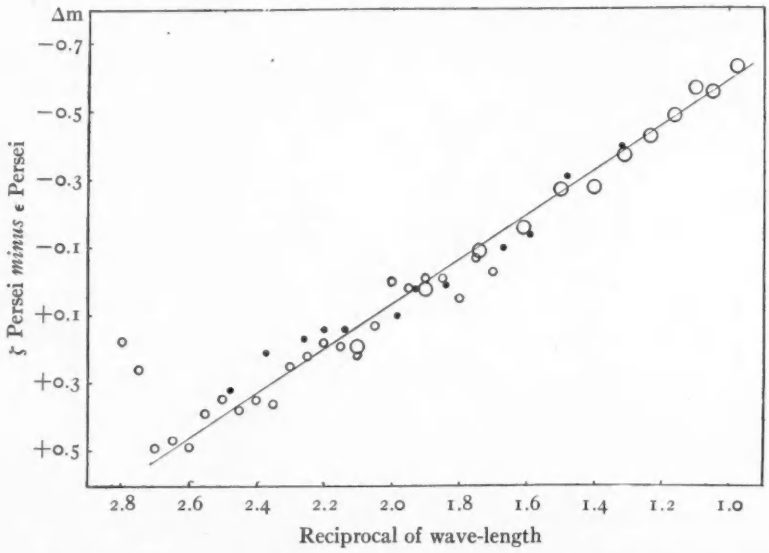

FIG. 2.—The observed magnitude differences are plotted against the frequency. Observations by Kienle are represented by small circles, and those by Mrs. Rudnick are denoted by dots. The large circles are the final mean differences given in Table 1. No systematic adjustment has been made between the three sets of data. Kienle has attributed the two discordant observations at the extreme left of the diagram to unusually heavy absorption near the head of the Balmer series in ϵ Persei. The data of the Greenwich observers are not shown. Their mean gradient of 0.62 agrees very closely with the value 0.61 indicated by the straight line in this figure.

Schoenberg and Jung,[8] this assumption is valid for gases and non-absorbing spheres and is a much better approximation in the red than in the violet for small metallic particles. The constant D is independent of λ, and its value depends on the luminosities and distances of the two stars, as well as on the general absorption.

[8] *A.N.*, **253**, 266, 1934.

The data are well represented if a is set equal to unity. The value of k is then -0.61, and D equals -1.25 mag. If the slight upward curvature indicated in Figure 2 is real, a increases with λ and its rate of increase depends on the value assumed for D, as Mrs. Rudnick has shown. I have recently discussed these data from this point of view in a paper read before the American Astronomical Society. One would not expect D to exceed the lowest observed Δm, namely, -0.6 mag. In view of spectroscopic and other data, we may reasonably assume that D is -1.0 mag. In this case a increases from 1.2 in the visual region to 1.6 in the infra-red. Schoenberg and Jung, as well as Schalén,[9] have shown by theoretical reasoning that a may have a value near unity. Gerasimovič[10] was apparently the first to suspect this to be the case. Struve, Keenan, and Hynek[11] have found evidence that a is near 2. Schalén[9] finds that the λ^{-1} law fits the observational data in the photographic and visual regions better than Rayleigh scattering or the λ^{-4} law. Since Δm is near -0.6 mag. at 10,000 A and $+0.3$ mag. at 4250 A, the total photographic absorption is at least 0.9 mag.

The unusual color of ζ Persei has been discussed from two points of view: as a low-temperature phenomenon and as the result of selective absorption or scattering in interstellar space. Kreiken's[12] recent suggestion that a considerable portion of the reddening in B stars may be attributed to stellar rotation does not seem to be valid in the case of this star. Miss Westgate[13] finds that the rotational velocity of ϵ is slightly greater than that of ζ.

It seems important to separate stellar from interstellar reddening. It may be possible to do this by carefully studying the colors and spectra of the companions of B stars which share the proper motions of their primaries. In the case of ζ Persei, for example, since the early B stars are among the bluest stars known, we would not expect to find its companion to be bluer than ζ, which appears yellow. If this were the case, it would imply that some of the reddening is of stellar origin. According to Burnham's catalogue, this companion is "ashen." It is very difficult, with my present photometric equip-

[9] *Medd. Upsala Obs.*, **64**, 1936.

[10] *Zs. f. Ap.*, **4**, 265, 1932.

[11] *Ap. J.*, **79**, 1, 1934.

[12] *A.N.*, **261**, 202, 1936.

[13] *Ap. J.*, **77**, 142, 1933.

ment, to measure the color of this companion. HD 170740 is another reddened B star with a ninth-magnitude companion.

In 1934 Stebbins and Huffer[14] published the results of an extensive color survey of early B-type stars. The effective wave-lengths of their colors are in the blue and the violet regions of the spectrum. In October, 1935, I observed the colors and magnitudes of 19 B-type stars which had been selected on the basis of their results. Eight comparison stars of later spectral types were also observed. The effective wave-lengths of these colors are 6110 A and 8000 A, and of the magnitudes, 8000 A. These wave-lengths were derived from contemporaneous observations of Vega with the objective grating.[5] Since these B stars were all observed at small zenith distances, their colors and magnitudes were reduced to the zenith by means of the extinction coefficients formerly found for Ko stars.[5]

The results of these observations are shown in Table 2. The various columns are, respectively: the HD number of the star, the mean color, the number of nights on which the star was observed, the visual magnitude, the infra-red magnitude, the spectral type, Stebbins and Huffer's color excess, and a color excess E_c derived from the filter measures at effective wave-lengths 6110 A and 8000 A. A third color excess, E_m, given in the final column is derived from colors formed by taking the difference between the visual and infra-red magnitudes. For the stars observed more than once the average deviation from the mean for the observed colors is 0.02 mag., and for the magnitudes, 0.03 mag.

Since Ko stars whose infra-red magnitudes have already been published were observed on the same nights as were the B-type stars, the zero point and magnitude scale of these stars are the same as for the Ko stars. In forming the color excesses, the mean colors of each spectral type were derived from a curve involving the comparison stars and B stars whose color excesses, as given by Stebbins and Huffer, are less than +0.04 mag. The mean differences in magnitude were derived in the same way with the same stars in the derivation of E_m.

The two observed magnitudes of HD 223960 are very discordant. Evidently on one of these nights a near-by K5 star (HD 223866) of similar visual magnitude was mistaken for the Bo star. As I had

[14] *Pub. Washburn Obs.*, **15**, Part 5, 1934.

relied entirely on the circles of the telescope in locating these stars, I have recently looked up the visual magnitudes and spectra of the stars in the vicinity of those observed B stars which are fainter

TABLE 2

Star HD	C	N	Magnitude		Sp.	Color Excess		
			Vis.	Infra-Red		E_s	E_c	E_m
3940	+0M18	1	7.40	6.04	B5	+0M40	+0M63	+1M43
3950	− .32	1	6.93	6.62	Bo	.14	.20	+0.59
14372	.38	1	6.08	6.07	B7	.00	.04	−0.01
14818	.15	1	6.24	5.67	B1	.27	.36	+0.81
206165	.25	2	4.87	4.24	B2	.22	.25	0.82
206672	.48	2	4.78	4.68	B3	.03	.00	0.25
207563	.48	1	6.16	6.15	B3	.03	.00	0.16
207793	.18	1	6.56	5.90	B2	.26	.32	0.85
210839	.25	1	5.19	4.59	O6	.19	+ .31	+1.04
212222	.49	1	6.27	6.34	B7	.00	− .07	−0.09
214993	.50	3	5.18	5.32	B1	.00	+ .01	+0.10
216014	.17	3	6.83	6.34	Bo	.27	.35	0.77
215200	.32	2	5.84	5.56	B3	.12	+ .16	0.43
216916	.49	1	5.54	5.61	B3	.02	− .01	0.08
218342	.06	1	7.46	6.75	B2	.30	+ .44	+0.90
218344	.49	1	7.17	7.41	B3	.01	− .01	−0.09
218376	.45	1	4.93	4.81	B1	.03	+ .06	+0.36
223229	− .50	2	5.84	6.06	B3	.03	− .02	−0.07
223960?	+ .11	1	6.98	5.69	Bo	+0.43	+(0.63)	+(1.57)
223866?	+0.18	1	6.92	5.30	K5	.....	.....	.....
	Comparison Stars							
8723	−0.15	1	5.32	4.75	F1	.....	.....	.....
8763	+ .14	1	5.63	4.25	K1	.....	.....	.....
11443	− .18	1	3.58	2.78	F2	.....	.....	.....
11973	.26	1	4.83	4.33	A5	.....	.....	.....
12869	.28	1	5.08	4.95	Ao	.....	.....	.....
214994	.38	1	4.85	4.78	A2	.....	.....	.....
215182	.00	1	3.10	2.24	G2	.....	.....	.....
220657	−0.09	1	4.57	3.76	F6	.....	.....	.....

than 6.00 mag. It appears highly improbable that any other B-star was misidentified. If we let C be the observed color and M_r the observed infra-red magnitude, then the visual magnitude may be computed by the empirical formula

$$M_v = M_r + 2.30C + 1^{M}02 .$$

The average difference between the computed and the observed visual magnitudes for the B stars is 0.09, and the largest difference is 0.18 mag. This procedure affords a partial check of the identity of the stars, since the visual magnitudes were taken from the HD catalogue.

In the notation of equation (1) the color excess

$$E = \Delta m_{\lambda_1} - \Delta m_{\lambda_2} = -(2.5 \log e)k(\lambda_1^{-\alpha} - \lambda_2^{-\alpha}),$$

where $\lambda_2 > \lambda_1$. If we let E_s be the color excess of a star as observed by Stebbins and Huffer, the ratios

$$\frac{E_s}{E_c} = \frac{\lambda_1^{-\alpha} - \lambda_2^{-\alpha}}{\lambda_4^{-\alpha} - \lambda_5^{-\alpha}} \text{ and } \frac{E_s}{E_m} = \frac{\lambda_1^{-\alpha} - \lambda_2^{-\alpha}}{\lambda_3^{-\alpha} - \lambda_5^{-\alpha}},$$

where $\lambda_1 = 0.426\ \mu$, $\lambda_2 = 0.477\ \mu$, $\lambda_3 = 0.550\ \mu$, $\lambda_4 = 0.611\ \mu$, and $\lambda_5 = 0.800\ \mu$. Since the effective wave-lengths are known to a first approximation, we can compute these ratios and compare them with the observed values for different values of α. The mean values of E_s, E_c, and E_m have been used in the computation of the observed ratios. The results are given in Table 3.

TABLE 3

α	Computed Ratio	
	E_s/E_c	E_s/E_m
4.0	2.34	1.30
2.0	1.00	0.64
1.0	0.65	0.44
0.6	0.55	0.38
Observed ratio	0.71	0.28

In making this comparison it is well to remember that we have again made the assumption that stars of the same spectral type have the same energy distribution and that k is not a function of λ. We make an additional assumption that the effective wave-lengths are independent of the color. This can only be regarded as a first ap-

proximation. The effective wave-lengths used for the color excesses found by Stebbins and Huffer[14] have not been corrected for two compensating factors: the energy distribution of early-type stars and the atmospheric extinction.

The data in Table 3 indicate that the computed ratios of color excess agree with the observed ratios when a is near unity. E_c is probably more reliable than E_m. Within the errors of measurement, E_a/E_c is constant for all reddened B stars in Table 2. Although we may not know the true cause of reddening, the fact that the data in Table 2 are consistent within themselves and agree well with those found for ζ Persei suggests that similar physical processes are involved for a number of stars.

SPROUL OBSERVATORY
SWARTHMORE COLLEGE
SWARTHMORE, PA.
February 1937

LINE CONTOURS OF THE ATMOSPHERIC OXYGEN BANDS*

C. W. ALLEN[1]

ABSTRACT

The breadth and structure of the atmospheric oxygen lines have been determined by studying the curves of growth of the three bands A, B, and α in the solar spectrum. True central intensities are thus computed as a function of the equivalent breadth. The absolute total absorption coefficients for the three bands have also been found.

INTRODUCTION

A considerable amount of experimental photometry of the atmospheric oxygen lines has led eventually to the conclusion that they are broadened essentially by molecular collisions and that the exponential law of absorption in the atmosphere is obeyed.[2, 3, 4, 5] Hence the complete contour of a line of a given intensity may be computed if the main constant of collision broadening (e.g., the effective collision diameter of the molecule) is known. Since such computed contours are narrower than solar lines but similar in other respects, they are ideal for determining the performance of a spectrograph when the contours of Fraunhofer lines are to be measured. The main broadening constant, however, has been determined only indirectly,[3] and hence a redetermination is necessary before the lines can be used for photometric control. The method used in the present paper is that of studying the curve of growth, i.e., the curve relating the logarithm of the equivalent breadth to the logarithm of the number of absorbing atoms.

THEORY

Theoretical curves of growth have been computed by using fixed collision broadening factors. The number of collisions per second, and

* *Contributions from the Mount Wilson Observatory, Carnegie Institution of Washington*, No. 566.

[1] Hackett Research Student.

[2] R. v. d. R. Woolley, *Mt. Wilson Contr.*, No. 420; *Ap. J.*, **73**, 185, 1931.

[3] W. H. J. Childs, *Ap. J.*, **77**, 212, 1933.

[4] *Ibid.*, *Phil. Mag.*, **14**, 1049, 1932.

[5] H. von Klüber, *Zs. f. Ap.*, **6**, 161, 1933.

hence the collision broadening, is proportional to the atmospheric pressure (the effect of variation in temperature being comparatively small). Suppose the collision breadth of the absorption coefficient to be $2b(p/p_0)$, where $2b$ is the breadth at normal pressure, and p and p_0 are the pressures at height h and at ground level. The absorption per centimeter for a line is

$$a_\nu = \frac{a}{\pi} \frac{b\,(p/p_0)}{(\nu - \nu_0)^2 + b^2\,p^2/p_0^2} \cdot \frac{p}{p_0},$$

where a is the total absorption for the line at normal pressure. Put $p = p_0 e^{-h/H}$, where H is the height of the homogeneous atmosphere; then

$$a_\nu = \frac{a}{\pi} \cdot \frac{be^{-2h/H}}{(\nu - \nu_0)^2 + b^2 e^{-2h/H}},$$

and the total absorption through the whole atmosphere is

$$\left.\begin{aligned} A_\nu &= \frac{ab}{\pi} \int_0^\infty \frac{e^{-2h/H} \sec z\, dh}{(\nu - \nu_0)^2 + b^2 e^{-2h/H}}, \\ &= \frac{aH \sec z}{2\pi b} \log_e \left\{ 1 + \frac{b^2}{(\nu - \nu_0)^2} \right\}, \end{aligned}\right\} \qquad (1)$$

where z is the sun's zenith distance.

This contour has a peak at $\nu - \nu_0 = 0$, but it is smoothed out in practice by Doppler broadening. The contour (1) was combined with Doppler broadening (assumed temperature 270° K) by numerical integration. With the absorption coefficients from the contour so obtained, absorption lines were plotted and the areas measured to derive equivalent breadths. The process was repeated for different values of a to obtain the curve of growth.

In order to derive the experimental curve of growth, it is necessary to determine the relative intensity of various lines in the band, i.e., the relative values of a. This is given by

$$a = CNie^{-E/kT}, \qquad (2)$$

where C is a constant, N the number of molecules capable of absorbing the band per cubic centimeter, $e^{-E/kT}$ the Boltzmann factor,

and i an intensity factor which is known for the oxygen bands.[6] The temperature of the atmosphere is irregular, but it is sufficient for our purpose to adopt the formula

$$T = T_0 \frac{5.3 \times 10^6}{h + 5.3 \times 10^6},$$

where h is the height in centimeters and T_0 the ground temperature. The absorption for a line at any height is then given by

$$a_h = CN_0 i e^{-E/kT} \frac{d}{d_0},$$

where N_0 is the value of N at normal temperature and pressure, and d and d_0, the densities of the atmosphere, are related by

$$\frac{d}{d_0} = e^{-h/9\times 10^5}.$$

The mean value of a to be used with a homogeneous atmosphere is then

$$\bar{a} = \frac{CN_0 i}{9 \times 10^5} \int_0^\infty \exp. \left\{ - \frac{E}{kT_0} \left(\frac{h + 5.3 \times 10^6}{5.3 \times 10^6} \right) - \frac{h}{9 \times 10^5} \right\} dh$$

$$= \frac{CN_0 i e^{-E/kT_0}}{1 + \dfrac{0.17E}{kT_0}}, \qquad (3)$$

which, except for the denominator, has the same form as (2). A somewhat similar expression was used by Mecke and Childs.[7]

OBSERVATIONS

A number of plates were secured with the tower telescope and 75-foot grating spectrograph of the Solar Laboratory of the Mount Wilson Observatory, situated in Pasadena at an altitude of about 700 feet. Photometric standardization was attained by use of step weakeners which had been calibrated at the Physical Laboratory at Utrecht. The weakeners were kindly lent by Dr. Mulders.

[6] W. H. J. Childs and R. Mecke, *Zs. f. Phys.*, **68**, 344, 1931.

[7] *Ibid.*, p. 362.

TABLE 1

INTENSITY DATA FOR THE OXYGEN BANDS A, B, AND α

LINE	EQUIVALENT BREADTH IN cm^{-1}			E.P. cm^{-1}	log $\bar{a}$
	A	B	α		
P_2 (0)	1.10	0.50	0.100	3	0.00
P_3 (2)	1.24	.56	.126	15	0.06
P_2 (2)	1.44	.66	.150	17	0.26
P_3 (4)	1.50	.62	.156	41	0.25
P_2 (4)	1.61	.77	.178	43	0.37
P_3 (6)	1.59	.67	.166	79	0.33
P_2 (6)	1.71	.70	.188	81	0.41
P_3 (8)	.....	.68	.168	127	0.32
P_2 (8)	.....	.72	.191	129	0.39
P_3 (10)	.....	.63	.156	188	0.27
P_2 (10)	.....	.67	.164	190	0.33
P_3 (12)	.....	.55	.133	260	0.18
P_2 (12)	1.39	.58	.140	262	0.22
P_3 (14)	1.25	.49	.121	343	0.05
P_2 (14)	.....	.52	.121	345	0.09
P (16)	1.06	.40	.085	439	−0.10
P (18)	.....	.33	.060	545	−0.30
P (20)	0.59	.....	.040	662	−0.52
P (22)	0.46	.170	.020	791	−0.78
P (24)	0.31	.128	.0126	931	−1.06
P (26)	0.21	.061	0.0075	1083	−1.37
P (28)	0.147	.038	.....	1246	−1.71
P (30)	0.104	0.023	.....	1420	−2.05
P (32)	0.042	.....	.....	1606	−2.46
P (34)	0.0156	.....	.....	1803	−2.86
P (36)	0.0064	.....	.....	2011	−3.30

Table 1 gives the observed values of equivalent breadth in wave-number units for the P_2 and P_3 branches of the bands A, B, and a situated at 7600, 6900, and 6300 A. The nomenclature is that used by Badger and Mecke.[8] Since up to $J = 14$ there is a measurable difference between the intensities of the two branches, both values are listed. The table also gives the excitation potentials in wave-

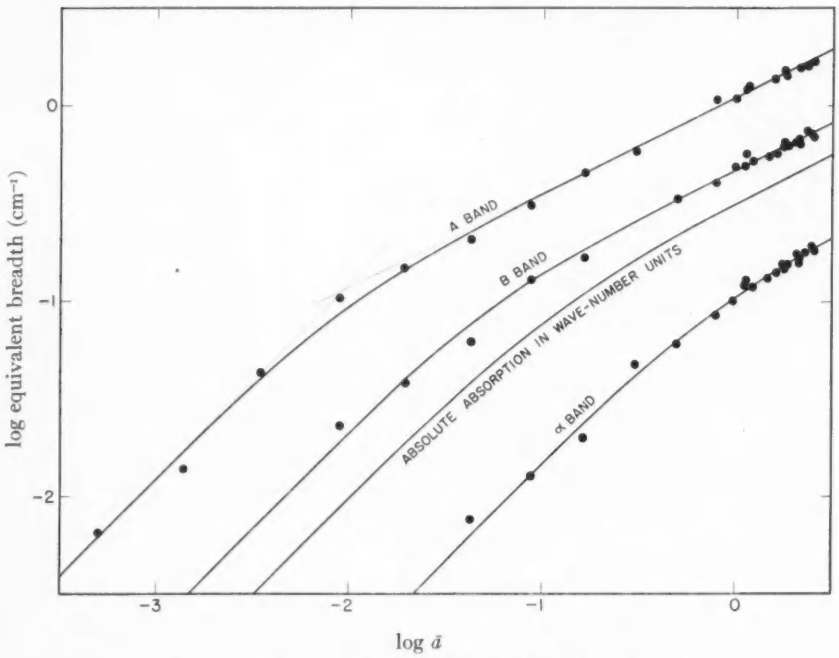

FIG. 1.—Curves of growth for atmospheric oxygen lines

number units,[9] and relative values of $\bar{a}$ computed from (3) and based on a ground temperature of 303° K. The actual mean temperature during the period of observation was 301° K, but this was increased slightly to allow for the peculiarities of the local temperature distribution. The air masses in terms of a homogeneous atmosphere at sea level were, respectively, 1.2, 2.9, and 5.0 for the bands A, B, and a. The observed curves of growth are plotted as points in Figure 1;

[8] *Zs. f. Phys.*, **60**, 59, 1930.

[9] Obtained from the measurements of G. H. Dieke and H. D. Babcock, *Proc. Nat. Acad.*, **13**, 670, 1927.

and, when fitted to a set of computed curves, the following values of b were obtained:

	Band		
	A	B	α
Value of b (cm^{-1})	0.047	0.049	0.050

The mean value of 0.049 cm^{-1} has been used for computing all the curves shown in Figure 1.

Two further checks have been made on this value of b. The α band has been measured in a solar spectrum taken on Mount Wilson (altitude 5715 feet); and, after correction for the decreased pressure, it gave a value of 0.051 cm^{-1}. The A band has also been measured in a 475-foot air-path spectrum taken on Mount Wilson with a tungsten strip lamp as source of light. In this case the pressure and temperature were practically constant over the length of the air path, so that the curve of growth is simpler to compute. It is very satisfactory to find a value of 0.048 cm^{-1} for b. The agreement with the values found for the whole atmosphere gives strong support to the assumption made above that the broadening increases with pressure.

CONTOURS OF ATMOSPHERIC LINES

When the value $b = 0.049$ cm^{-1} is introduced into (1) and a Doppler broadening equivalent to $T = 270°$ K and molecular weight 32 is superimposed upon this contour by numerical integration, the resulting frequency distribution of A_ν is that given in Table 2. Actual contours of exponential absorption lines with this value of A_ν have been plotted, and the relation between equivalent breadth and central intensity so obtained is shown in Table 3. This table should be useful in determining the performance of a high-dispersion spectrograph when used with absorption lines. If the altitude of the observing station is considerable, the lines will be somewhat narrower and the central intensities less. To obtain the value of the central intensity in this case from Table 3 the measured value

of the equivalent breadth should be divided by the reduction in pressure.

PHOTOMETRIC DATA FOR OXYGEN BANDS

The observations enable one to determine the following photometric constants of the oxygen bands: (*a*) the effective collision diameter of O_2 in air; (*b*) the relative absorption coefficient of the three bands *A*, *B*, and *a*; and (*c*) the absolute value of the absorption coefficient. Most of these constants have been studied already by Childs[3, 4] and hence will receive only brief mention.

TABLE 2

CONTOUR OF THE ABSORPTION COEFFICIENT A_ν OF OXYGEN ATMOSPHERIC BANDS

$\nu-\nu_0$ (cm^{-1})	A_ν
0.00	13.0
0.01	11.5
0.02	7.7
0.03	5.1
0.04	3.6
0.05	2.4
0.06	1.8
0.08	1.1
0.10	0.70
0.15	0.34
0.20	0.188
0.30	0.088
0.40	0.049
0.50	0.032
1.00	0.008
2.00	0.002

TABLE 3

RELATION BETWEEN CENTRAL INTENSITY r_c AND EQUIVALENT BREADTH *W* FOR OXYGEN BANDS

W(cm^{-1})	r_c
0.02	0.74
0.04	0.53
0.06	0.36
0.08	0.22
0.10	0.13
0.12	0.07
0.14	0.04
0.16	0.02
0.18	0.01
0.20	0.00

a) From Dennison's formula for broadening due to collisions[10] we may write

$$b(\text{sec}^{-1}) = 1.10 n\sigma^2 \sqrt{\frac{kT}{M}},$$

where n is the number of molecules per cubic centimeter, and σ the molecular diameter, and where k, T, and M have their usual mean-

[10] *Phys. Rev.*, **31**, 503, 1928, formula (1″).

ings. Introducing the numerical values, $n = 2.7 \times 10^{19}$, $k = 8.32 \times 10^{7}$, $T = 290^{\circ}$ K, $M = 30$, $b = 1.46 \times 10^{9}$ sec^{-1}, we find

$$\sigma = 4.2 \times 10^{-8} \text{ cm}.$$

This result may be compared with Childs's value obtained indirectly:

$$\sigma = 2.5 \times 10^{-8} \text{ cm}.$$

b) The relative absorption coefficient in the three bands, when corrected for the difference in air mass and expressed in wave-number units, is

A	:	B	:	a
13.5	:	1.00	:	0.039

This result is in agreement with the work of Childs, whose corresponding factor for the ratio A:B is 11.2.

c) Figure 1 includes a curve relating the equivalent breadth to the absolute absorption coefficient integrated over the breadth of

TABLE 4

	Absorption Coefficient per Centimeter of Normal Atmosphere	Molecular Absorption Coefficient
	cm^{-1}sec^{-1}	cm^{2}sec^{-1}
7620.087 A	4.2×10^{5}	7.3×10^{-14}
Total A band	2.7×10^{7}	4.7×10^{-12}
Total B band	2.0×10^{6}	3.5×10^{-13}
Total a band	7.8×10^{4}	1.4×10^{-14}

a line in wave-number units. Thus, for any measured line the absorption coefficient for the whole atmosphere may be read from this curve. Dividing this coefficient by $H \sec z$ and multiplying by c, the velocity of light, we find the absolute absorption coefficient in frequency units for an atmosphere of normal temperature and pressure. The molecular absorption coefficient is obtained by dividing again by the number of O_2 molecules per cubic centimeter at normal temperature and pressure. The results are as shown in Table 4.

The total absorption per centimeter at normal temperature and pressure for the A band has also been found from the 475-foot air-path plate. The result is 2.6×10^7 cm^{-1} sec^{-1}, in excellent agreement with the value obtained from the whole atmosphere. Childs and Mecke[6] obtained the value 4.8×10^7 cm^{-1} sec^{-1} for this constant.

In a forthcoming paper the oxygen-line contours will be used to determine the central intensities of Fraunhofer lines.

CARNEGIE INSTITUTION OF WASHINGTON
MOUNT WILSON OBSERVATORY
February 1937

CENTRAL INTENSITIES OF FRAUNHOFER LINES*

C. W. ALLEN[1]

ABSTRACT

The central intensities of 91 Fraunhofer lines in the red and infrared regions of the solar spectrum have been measured. The corrections for resolving power were obtained from a study of the atmospheric oxygen lines which appeared on the same plates as the solar lines.

By plotting the central intensity against the equivalent breadth it is found that all observed lines are consistently wider than theory predicts. In the main, the discrepancy may be overcome by assuming that the sun's reversing layer is subject to turbulent velocities of the order of 1.6 km/sec. The discussion deals with the nature of the turbulence, the change in the structure of Fraunhofer lines with wave-length, and the causes of abnormal sharpness and breadth in individual lines, and leads to the conclusion that the observations may be explained without departing from the simple method commonly used in computing Fraunhofer contours.

The intensity features of a Fraunhofer line may be described conveniently by the equivalent breadth and the central intensity. Numerous photographic observations of equivalent breadth have been published; but in order to observe central intensities by photographic photometry, one must overcome the difficulty of obtaining a suitable correction for the distortion of the absorption line by the spectrograph. Carroll[2] and Plaskett[3] have computed the corrections for ideal spectrographs giving theoretical resolving power, no ghosts, and no scattered light. Redman[4] and Thackeray[5] have eliminated ghosts and scattered light by using a monochromator. Shane[6] has employed interferometry to determine the correction, while the present author[7,8] has used fine emission lines. It has not been possible, however, to test the corrections so found on lines whose contours are known, and the disagreement between former results shows that the errors are considerable. In the present paper the corrections to be applied to solar lines are derived entirely from a

* *Contributions from the Mount Wilson Observatory, Carnegie Institution of Washington*, No. 567.

[1] Hackett Research Student.

[2] *M.N.*, **88**, 154, 1927.

[3] *Ibid.*, **91**, 870, 1931.

[4] *Ibid.*, **95**, 290, 1935.

[5] *Ibid.*, p. 293.

[6] *Lick Obs. Bull.*, **16** (No. 449), 76, 1932.

[7] *Mem. Commonwealth Solar Obs., Canberra*, No. 5, Part 1, p. 10, 1934.

[8] *M.N.*, **96**, 508, 1936.

study of atmospheric oxygen lines whose contours have recently been determined by the author;[9] and as a result, the effects of resolving power, light-scatter, and even Eberhard effect are eliminated.

OBSERVATIONS

Spectra of the center of the sun's disk have been obtained with the two 75-foot plane-grating spectrographs of the Mount Wilson Observatory. A Michelson 8-inch grating was used at the Solar Laboratory in Pasadena, and the Michelson 66 grating on Mount Wilson. Both spectrographs are fed by tower telescopes with equivalent focal lengths of 150 feet. The first, second, and third orders have been used in various regions, with dispersions ranging from 1.3 to 5.3 mm per angstrom. The theoretical resolving power is about 170,000 in the second order for both spectrographs. Eastman III F, 144 S, I N, and 144 N backed plates were used and were brushed during development with metol-borax for 5 minutes at 18° C. The developer was diluted considerably in order to decrease contrast, chemical fog, and Eberhard effect. Step-wedges, kindly lent by Dr. Mulders, were placed on the slit to give the plate-calibration. These wedges had been calibrated at the Physical Laboratory at Utrecht, but were recalibrated on Mount Wilson by photographic comparison with a step-slit; the two calibrations were in good agreement. The regions studied were 6122–6336, 6828–6925, and 7657–7788 A, the choice being such that atmospheric oxygen lines, as well as solar lines, appeared on the plates. The spectra were measured photometrically in the usual way with the Mount Wilson microphotometer constructed by Dr. Dunham. For each line, both solar and atmospheric, values were obtained of r_m, the uncorrected central intensity (with continuous background as unit), and of Δ_m, the measured breadth of the line at half its maximum depth. Using the results of an earlier paper,[9] we may obtain r_c, the true central intensity, for an atmospheric line from the equivalent breadth W, which for practical purposes is given by $W = 1.3\ \Delta_m (1 - r_m)$. The ratio of the measured to the true depth, i.e. $(1 - r_m)/(1 - r_c)$, represents the instrumental correction for atmospheric lines. The value of this

[9] *Mt. W. Contr.*, No. 566; *Ap. J.*, **85**, 156, 1937.

ratio, plotted as a function of Δ_m, defines a curve which may be used to determine a first approximation for the correction to solar lines.

The true central intensities of all atmospheric lines that are strong enough to be of importance are zero, and hence this method is not dependent on a very accurate determination of the structure found for the oxygen lines. There may be a small difference, however, between the correction-curves for atmospheric lines and for solar lines, owing to the differences in the line contours. In order to study this question, it has been necessary to obtain some idea of the in strumental contour, which we denote by $K(l)$, where l represents distance on the plate. The central part of $K(l)$ may be obtained from the computed resolving power and slit width of the spectrograph, but an appreciable wing intensity must be added to this result. By combining the estimated value of $K(l)$ with the known contour of atmospheric lines $I(l)$ and numerically integrating the standard equation

$$J(l) = \int_0^\infty K(\lambda - l)I(\lambda)d\lambda ,$$

we obtain $J(l)$, the observed contour; and by repeating the integration for lines of different intensity, we may compute a theoretical corrective-curve. Adjustments are then made in $K(l)$ until the theoretical curve agrees approximately with the observed curve. The final $K(l)$ may then be combined with lines of solar type to obtain another theoretical correction-curve; and the difference between these two theoretical curves indicates the adjustment that must be made in the observed correction-curve when it is to be used with solar lines. The adjustment has been applied, but our imperfect a priori knowledge of Fraunhofer contours leads to an ambiguity of 0.01, or perhaps 0.02, in the final values of r_c.

An indication of the statistical errors may be obtained from the variation in the individual values of r_c and the scatter in the points from which the correction-curves were obtained. The solar lines have been measured about ten times. In the 6300 A region the O_2 lines were not strong enough to provide values of Δ_m as large as those of the solar lines, and the correction-curve had to be extrapolated by comparison with the curve at 6900 A. In view of this

extrapolation and the ambiguity already mentioned, it would not be safe to compute the probable error of r_c from statistical considerations. This probable error is not likely, however, to be greater than 0.02, which is a considerable improvement on earlier observations in these regions.

The results obtained by the present method lie between the two sets of values already published by the author.[7,8] Evidently the values obtained from the prism spectrograph at Canberra[7] were undercorrected, a result which is not surprising; but the overcorrection of the grating observations made at Cambridge[8] requires some explanation. In the first place, the contour there assumed for the solar lines is not entirely suitable, and the blunter cores that Fraunhofer lines probably possess would necessitate a smaller correction. Secondly, the neon lines used to obtain the instrumental contour may not have been perfectly sharp. Neon spectra taken recently at Mount Wilson exhibit broader lines than can be attributed to instrumental effects. Whether this is due entirely to some feature of the particular discharge tube used at Mount Wilson is not certain, but at least it throws some suspicion on the use of the neon spectrum for the determination of the instrumental contour.

RESULTS

The results are set out in Tables 1, 2, and 3, in which the first three columns are taken from the *Revised Rowland*. The following columns give values of r_c obtained with different spectrographs: (*a*) first order and (*b*) second order, Michelson 8-inch grating, Solar Laboratory; (*c*) second order and (*d*) third order, Michelson 66 grating, Mount Wilson; (*e*) mean of earlier observations made at Canberra (prisms) and Cambridge (grating). Column (*e*) shows fair agreement with the other columns but has not been included in the final mean of r_c.

The values of the equivalent breadths W (unit, 0.001 A) have been averaged from all available material, including numerous remeasurements made in connection with the present research. For this purpose the formula $W = p\Delta_m(1 - r_m)$ has been found very useful, where p is a factor which depends to a small extent on the spectrograph and the nature of the line. For most cases p is between

TABLE 1

CENTRAL INTENSITY, EQUIVALENT BREADTH, AND SHARPNESS, 6122–6336 A

λ	Element	E.P.	r_c (b)	(c)	(d)	(e)	Mean	W mA	$10^6 W/\lambda$	d
6122.231...	*Ca*	1.878	0.16	0.16	.....	0.12	0.163	215	35.0	.....
6126.230...	Ti	1.062	.78	.77	.....	.78	.771	20	3.3	.....
6127.918...	*Fe*	.....	.....	.51	.....	.52	.514	47	7.7	1.00
6128.990...	*Ni*	1.669	.73	.72	.....	.76	.720	23	3.8	.....
6130.147...	*Ni*	4.248	.78	.78	.....	.79	.776	20	3.3	.....
6136.631...	*Fe*	2.443	.21	.20	.....	.12	.206	142	23.1	1.02
6137.709...	*Fe*	2.577	.20	.22	.....	.14	.205	138	22.5	1.02
6141.733...	*Ba*+*Fe*	0.701	.17	.18	.....	.24	.175	122	19.9	1.10
6142.499...	*Si*	5.595	.....	.74	.....	.....	.736	35	5.7	0.72
6149.255...	*Fe*+	3.873	.66	.64	.....	.66	.642	38	6.2	0.89
6151.630...	*Fe*	2.167	.47	.47	.....	.50	.467	47	7.6	1.10
6154.235...	*Na*	2.093	.....	.70	.....	.....	.701	35	5.7	0.80
6155.148...	*Si*	5.595	.....	.48	.....	.....	.483	84	13.6	0.76
6157.739...	*Fe*	.....	.....	.41	.....	.41	.410	60	9.8	1.04
6159.387...	.....	.....	.....	.87	.....	.....	.872	12	2.0	.....
6160.759...	*Na*	2.095	.....	.55	.....	.54	.552	54	8.8	0.85
6162.185...	*Ca*	1.891	.....	.13	.....	.11	.132	270	43.9	.....
6165.369...	*Fe*	.....	.....	.53	.....	.54	.532	45	7.3	1.02
6166.446...	*Ca*	2.510	.....	.40	.....	.34	.398	71	11.6	0.98
6169.050...	*Ca*	2.512	.32	.32	.....	.....	.317	90	14.6	0.98
6169.570...	*Ca*	2.515	.26	.28	.....	.20	.278	111	18.0	0.98
6173.348...	*Fe*	2.213	.35	.36	0.38	.35	.363	67	10.8	1.06
6176.822...	*Ni*	4.071	.45	.45	.44	.45	.449	63	10.2	0.94
6180.216...	*Fe*	2.716	.45	.45	.46	.47	.454	53	8.6	1.04
6186.725...	*Ni*	4.088	.....	.72	.72	.....	.716	27	4.4	.....
6188.002...	*Fe*	3.926	.54	.55	.52	.54	.542	45	7.3	1.00
6191.192...	*Ni*	1.669	.35	.36	.35	.34	.355	71	11.5	1.02
6191.577..	*Fe*	2.422	.22	.21	.22	.16	.216	137	22.2	1.01
6200.327...	*Fe*	2.597	.36	.39	.34	.38	.363	68	11.0	1.02
6213.443...	*Fe*	2.213	.31	.29	.32	.34	.307	81	13.0	1.04
6216.366...	*V*	0.274	.70	.68	.70	.72	.692	34	5.5	0.86
6219.294...	*Fe*	2.188	.28	.27	.28	.30	.277	88	14.2	1.04
6223.996...	*Ni*	4.088	.73	.72	.73	.72	.722	26	4.2	.....
6226.745...	*Fe*	3.867	.71	.70	.73	.71	.710	26	4.2	.....
6229.240...	*Fe*	2.833	.60	.60	.63	.64	.607	34	5.5	1.06
6230.111...	*Ni*	4.088	.81	.81	.83	.81	.817	17	2.7	.....
6230.742...	*Fe V*	2.548	.23	.21	.22	.18	.218	166	26.6	0.98
6232.655...	*Fe*	3.638	.35	.35	.37	.34	.354	83	13.4	0.97
6237.334...	.....	.....	.59	.59	.62	.54	.597	61	9.8	0.73
6240.659...	*Fe*	2.213	0.50	0.49	0.49	0.48	0.493	46	7.4	1.08

TABLE 1—*Continued*

λ	Element	E.P.	r_c					W mA	$10^6W/\lambda$	d
			(*b*)	(*c*)	(*d*)	(*e*)	Mean			
6246.333...	*Fe*	3.587	0.28	0.28	0.26	0.24	0.273	124	19.8	0.95
6247.569...	*Fe*+	3.875	.52	.51	.50	.48	.506	53	8.5	0.94
6251.845...	*V*	0.285	.....	.88	.87	.86	.874	13	2.1	.....
6252.572...	*Fe*	2.394	.....	.24	.23	.18	.235	123	19.7	0.99
6255.966...	*Fe*	.....	.....	.78	.80	.79	.787	18	2.9	.....
6259.598...	*Ni*	4.072	.....	.84	.84	.84	.843	15	2.4	.....
6261.112...	*Ti*	1.424	.....	.50	.54	.51	.518	48	7.7	0.98
6265.148...	*Fe*	2.167	.....	.30	.29	.30	.296	82	13.1	1.03
6270.237...	*Fe*	2.846	.....	.44	.46	.45	.449	53	8.5	1.04
6271.289...	*Fe*	3.318	.....	.76	.76	0.78	.757	21	3.3	.....
6297.808...	*Fe*	2.213	.30	.34	.35	.....	.331	71	11.2	1.07
6301.517...	*Fe*	3.638	.29	.28	.28	.....	.282	122	19.4	0.94
6302.508...	*Fe*	3.671	.37	.35	.34	.....	.352	81	12.8	0.98
6311.511...	*Fe*	2.819	.70	.70	.73	.....	.713	24	3.8	.....
6314.675...	*Ni*	1.927	.39	.40	.40	.....	.396	71	11.2	0.98
6318.036...	*Fe*	2.443	.30	.29	.28	.....	.291	104	16.4	0.98
6322.701...	*Fe*	2.577	.37	.36	.35	.....	.361	76	12.0	1.00
6327.613...	*Ni*	1.669	.60	.62	.64	.....	.619	35	5.5	1.03
6330.103...	*Cr*	0.937	.68	.70	.73	.....	.699	27	4.3	.....
6330.859...	*Fe*	.....	.66	.66	.68	.....	.662	33	5.2	0.96
6335.345...	*Fe*	2.188	.27	.27	.28	.....	.272	100	15.8	1.02
6336.837...	*Fe*	3.671	0.30	0.29	0.31	.....	0.298	108	17.0	0.95

TABLE 2

CENTRAL INTENSITY, EQUIVALENT BREADTH, AND SHARPNESS, 6828–6925 A

λ	Element	E.P.	r_c				W mA	$10^6W/\lambda$	d
			(*b*)	(*c*)	(*d*)	Mean			
6828.610.....	*Fe*	4.618	0.50	0.53	0.52	0.517	56	8.2	1.02
6839.847.....	*Fe*	2.548	.70	.73	.70	.710	28	4.1	.....
6841.355.....	*Fe*	4.587	.45	.49	.49	.480	64	9.3	1.01
6842.701.....	*Fe*?	.....	.63	.66	.66	.651	39	5.7	0.96
6843.672.....	*Fe*	.....	.47	.49	.49	.486	63	9.2	1.00
6882.530.....	*Cr*	3.423	.72	.73	.73	.725	30	4.3	.....
6898.307.....	*Fe*	4.202	.87	.84	.85	.856	14	2.0	.....
6914.578.....	*Ni*	1.942	.42	.42	.42	.422	80	11.6	0.98
6916.694.....	*Fe*	4.136	0.52	.52	.53	.522	56	8.1	1.00
6925.288.....	*Cr*	3.434	.....	0.69	0.70	0.694	35	5.1	.....

1.2 and 1.3; but for lines with very extensive wings, such as the solar hydrogen lines, it may be greater than 1.6.

Tables 1, 2, and 3 also give the quantity W/λ, which for some theoretical studies is more convenient than W itself, and, in the last column, d, which represents the difference in sharpness of Fraunhofer lines and might be called the "relative sharpness." It is

TABLE 3

CENTRAL INTENSITY, EQUIVALENT BREADTH, AND SHARPNESS, 7657–7788 A

λ	Element	E.P.	r_e			W mA	$10^6 W/\lambda$	d
			(a)	(c)	Mean			
7657.605	*Mg*	5.086	0.52	.....	0.522	100	13.1	0.85
7680.267	*Mn*	5.467	.57	0.54	.565	86	11.2	0.84
7691.562	*Mg*	5.728	.58	.56	.572	110	14.3	0.72
7698.977	*K*	0.000	.18	.18	.180	150	19.5	1.22
7710.367	*Fe*	4.202	.55	.54	.551	65	8.4	1.03
7711.737	*Fe*$^+$	3.887	.67	.65	.663	47	6.1	0.95
7714.309	*Ni*	1.927	.42	.43	.426	103	13.3	1.02
7715.577	*Ni*	3.683	.64	.64	.640	48	6.2	1.00
7723.211	*Fe*	2.269	.66	.66	.657	38	4.9	1.13
7727.616	*Ni*	3.663	.48	.46	.473	90	11.6	1.01
7742.722	*Fe*	4.970	.56	.57	.563	103	13.3	0.77
7748.284	*Fe*	2.936	.42	.41	.418	102	13.2	1.04
7748.894	*Ni*	3.690	.47	.47	.469	87	11.2	1.03
7751.117	*Fe*	4.970	.68	.67	.679	44	5.7	0.95
7771.954	*O*	9.106	.66	.67	.660	79	10.2	0.68
7774.177	*O*	9.106	.70	.70	.696	71	9.1	0.66
7775.394	*O*	9.106	.75	.76	.750	58	7.5	0.62
7780.567	*Fe*	4.454	.42	.42	.423	124	16.0	0.93
7788.933	*Ni*	1.942	0.50	0.45	0.490	90	11.6	0.98

defined as the ratio of the line depth $1 - r_e$ to the mean depth of other Fraunhofer lines of the same equivalent breadth and wave-length. These values of d are more accurate than those found hitherto, and now have some individual significance. The probable error is about 0.02.

GENERAL DISCUSSION

The first point of interest is to compare the observed central intensities with the values derived from the standard theories of Fraunhofer lines. The comparison may be made by plotting r_e

against W; but if W is in wave-length units, the characteristics of the different spectral regions are demonstrated more clearly by plotting r_c against W/λ. The experimental results are shown in Figure 1. The three regions near 6300, 6900, and 7700 A represent the data in Tables 1, 2, and 3; while the six lines near 5550 A are taken from the observations of Shane,[6] whose lines are not quite so deep as the author's. The 4500 A curve is from my earlier work[7] and may not be reliable. The scatter of the points in this diagram is real and represents the individual peculiarities of the Fraunhofer

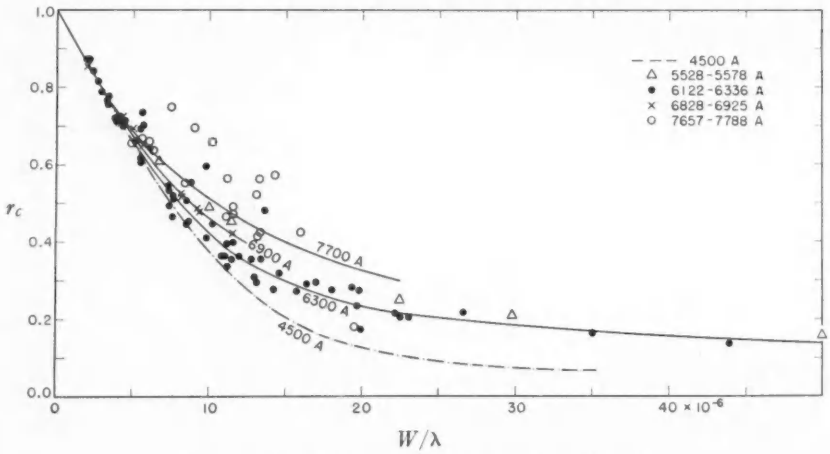

FIG. 1.—Correlation of central intensity with W/λ

lines. We are interested at present, however, only in the shape of the mean curves for the various regions, and in drawing these curves all lines that are obviously abnormal have been ignored. It is seen that the curves differ to some extent for the different regions but that they coincide for the weakest lines.

In order to obtain the corresponding computed relation between r_c and W/λ, it is necessary to know the Doppler broadening, the damping factor, and the F-curve (i.e., the curve relating the intensity r at any wave-length within a line to the logarithm of the line-scattering coefficient at that wave-length). Choosing thermal motion corresponding to $T = 6000°$ K and molecular weight 50 for the Doppler effect, a damping coefficient of $\omega = 2\pi \times$ damping breadth $= 4.2 \times 10^4/\lambda$ sec^{-1} (from curve of growth), and the F-curves

shown in Figure 2 representing (*a*) pure scattering,[10] (*b*) Eddington's formula[11] with $\epsilon = 0.0$, (*c*) same with $\epsilon = 0.1$, (*d*) a non-theoretical relation, we obtain the *A* group of curves in Figure 3. They are independent of wave-length, and we note that steeper *F*-curves form deeper or sharper lines. Now comparing the computed curves with the observed, we find at once the fainter observed lines are too wide by a factor of about 1.5. No reasonable *F*-curve will improve the agreement, the damping factor for faint lines has practically no influence, and the only way to bring about agreement is

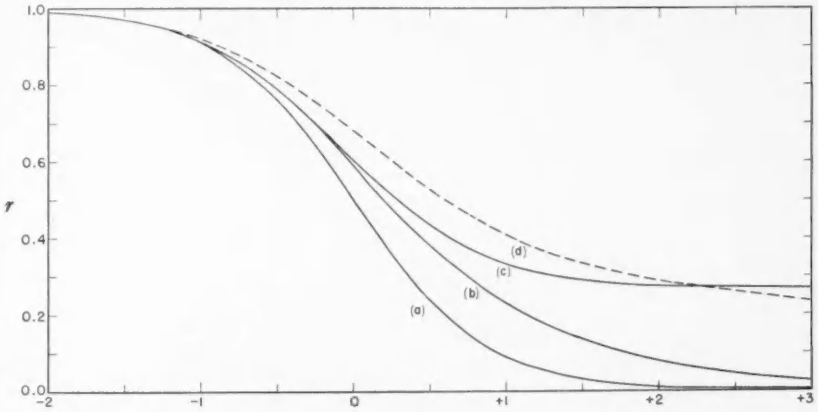

FIG. 2.—*F*-curves: (*a*) pure scattering, (*b*) Eddington's formula with $\epsilon = 0.0$, (*c*) same with $\epsilon = 0.1$, (*d*) a non-theoretical relation.

to adopt a larger Doppler broadening. This may be done by assuming that turbulent movements exist in the sun's atmosphere, the velocities of which are comparable with the thermal velocities. The consequences of such turbulence on the structure of Fraunhofer lines will be considered in some detail.

In order to study the effect of turbulence on the computed contours, it is necessary to decide whether the turbulence is on a large scale or a small scale in comparison with the depth of the sun's reversing layer.

For large-scale turbulence the lines emerging close to the sun's surface have a breadth determined by thermal motion alone, and

[10] A. Schuster, *Ap. J.*, **21**, 1, 1905. [11] A. S. Eddington, *M.N.*, **89**, 620, 1929.

the increased broadening that is actually observed in a terrestrial spectrograph is due to haphazard displacements of these lines. The *B* group of curves in Figure 3 shows the result of imposing large-scale turbulence with a Maxwellian velocity distribution and a most probable velocity of 1.8 km/sec. These curves agree fairly well with the observed curves and at least give the impression that close agreement could be obtained by a suitable choice of the *F*-curve. Such turbulence does not affect the equivalent breadth or the curve of growth, and hence the agreement with theory found for

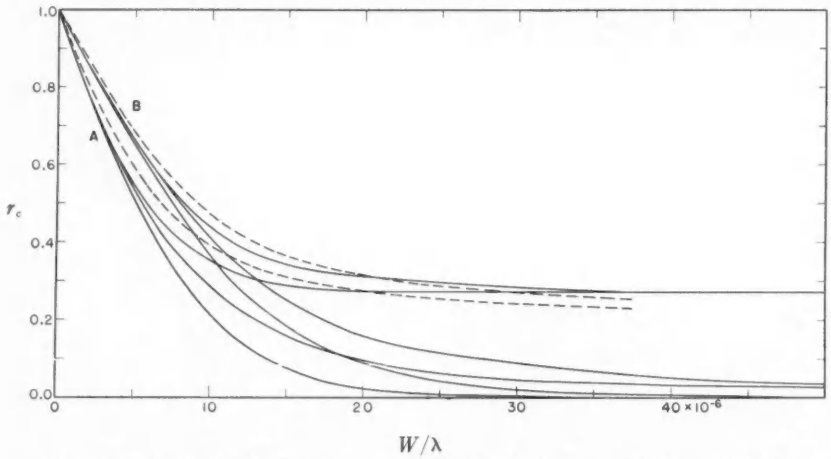

FIG. 3.—Calculated relation between r_c and W/λ for *F*-curves of Fig. 2, with (*A*) no turbulence and (*B*) large-scale turbulence of 1.8 km/sec.

the observed curve of growth[7,12] is still to be expected. One might expect, however, that a spectrogram of a well-focused solar image, taken with good observing conditions, would show measurable velocity shifts. Evershed[13] finds that shifts of the order of 0.3 km/sec are observable between center and limb but are rarely to be found right at the center of the disk. Even the velocity of 0.3 km/sec is too small to explain the line broadening, and hence it is at least doubtful whether the turbulent movements can involve complete granules.

If, on the other hand, it be assumed that the turbulence is on a small scale, the whole contour of the absorption coefficient for each line is broadened. Computing the relation between r_c and W/λ for

[12] D. H. Menzel, *Ap. J.*, **84**, 462, 1936.

[13] *M.N.*, **94**, 96, 1934.

this case and using a turbulent velocity of 1.5 km/sec, we obtain the results shown in Figure 4, which are rather similar to the *B*-curves in Figure 3. The experimental results are in fair agreement with both series of curves and do not permit a decision as to which is preferable. When the curve of growth is computed with the whole (turbulent + thermal) motion, it falls higher on the log W/λ axis and thus destroys the former agreement between theory and experiment.[7,12] It will be remembered, however, that these computations were made on the basis of *F*-curves representing either

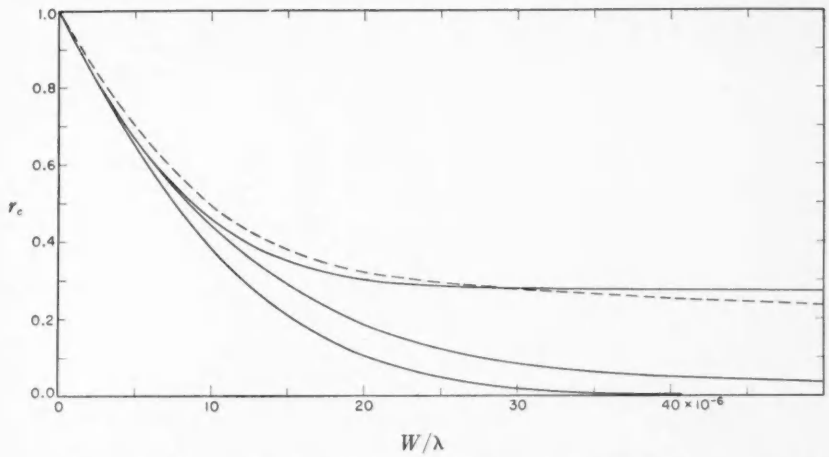

FIG. 4.—Calculated relation between r_c and W/λ for *F*-curves of Fig. 2, and small-scale turbulence of 1.5 km/sec.

Pannekoek's computations (case B) or pure scattering. If, instead, we use the *F*-curve representing Eddington's formula, which agrees rather better with observations,[7,14] the curve of growth is brought lower on the W/λ axis, and again agrees with observation. Figure 5 shows that the computed curve of growth based on Eddington's formula ($\epsilon = 0$) and a damping factor $\omega = 5.0 \times 10^4/\lambda$ agrees with my empirical curve. Thus the hypothesis of small-scale turbulence can fit the observations at least as well as large-scale turbulence, and at present it is scarcely possible to decide which alternative gives the better representation of the actual conditions.

The breadth of Fraunhofer lines is not the only evidence of

[14] M. Minnaert and J. Houtgast, *Zs. f. Ap.*, **12**, 81, 1936.

turbulence in a stellar atmosphere. Struve and Elvey[15] have found it necessary to adopt very large turbulent velocities to explain the curve of growth of some early-type stars. In the chromospheric spectrum also, Unsöld[16] has deduced turbulent velocities as high as 15 km/sec to explain the structure of Ca^+ lines. Even the appearance of the sun's granulated surface would lead one to expect a certain amount of turbulence in the reversing layer. The granulated areas themselves move with mean velocities of 8 km/sec,[17] and gas movements which are an appreciable fraction of this amount must be involved.

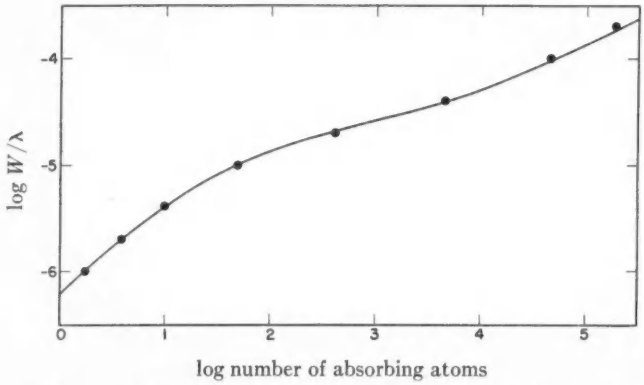

FIG. 5.—Curve of growth computed for a turbulent atmosphere and Eddington's formula. The points represent the observed curve.

It is well to consider briefly what other phenomena might produce the observed broadening of Fraunhofer lines. Hyperfine structure will widen a few lines and should have much the same effect on the curve of growth as small-scale turbulence, but would not affect all lines with the regularity shown in Figure 1. The existence of noncoherent radiation processes might result in light being absorbed in the wings of a line and re-emitted in the center with a consequent broadening effect. No adjustment of the F-curve would account for this phenomenon, and the simple method employed here for computing Fraunhofer contours breaks down. It will be for

[15] *Ap. J.*, **79**, 409, 1934.

[16] *Mt. W. Contr.*, No. 377; *Ap. J.*, **69**, 209, 1929.

[17] S. Chevalier, *Ann. Obs. Zô-sè*, **8**, 1912.

atomic theory to decide whether such a process could produce the effect described in this paper; and until such a theory is available, the breadth of lines cannot be regarded as a proof of turbulence.

In order to explain the variation with wave-length shown in Figure 1, it is necessary to assume that the slope of the *F*-curve decreases as one moves toward the red. Indications of such a change have been given before,[7] the cause of which is probably connected with the fluorescent transfer of radiation from the blue to the red by cyclic transitions.[18] The systematic decrease of equivalent breadth with wave-length is probably due to the same cause, and also the appearance of emission lines in the red of some stellar spectra.

INDIVIDUAL LINES

It is not difficult to account for the variety in the sharpness of individual Fraunhofer lines. For faint lines the atomic weight is the

TABLE 4

INFLUENCE OF ATOMIC WEIGHT ON RELATIVE SHARPNESS OF FAINT LINES

	Element					
	O	*Na, Mg*	*K, Ca*	*Ti*	*Fe*	*Ba*
Atomic weight	16	24	40	48	56	137
Relative sharpness, *d*	0.72	0.82	0.95	1.00	1.02	1.18

most important factor, and its influence on the relative sharpness, *d*, may be computed from the Doppler effect. Adopting a reversing layer at 6000° K and 1.6 km/sec turbulence, we obtain the sharpness for faint lines given in Table 4. As the lines become stronger, the influence of atomic weight is decreased until for $W/\lambda > 40 \times 10^{-6}$, *d* approaches 1.00 for nearly all atoms. Several of the very broad lines (i.e., small *d*) have a low atomic weight. For the great majority of lines, however, the atomic weight lies between 40 and 58, with, consequently, very little effect on relative sharpness; and most of the variations are to be attributed to changes in the *F*-

[18] R. v. d. R. Woolley, *M.N.*, **94**, 631, 1934.

curve. It will be noticed that there is more variety among the infrared lines than among the visible lines, which is just what would be expected if the *F*-curves have been influenced by fluorescent radiation transfer. If our explanation is correct, some lines must have very flat *F*-curves. Generally speaking, the damping factor influ-

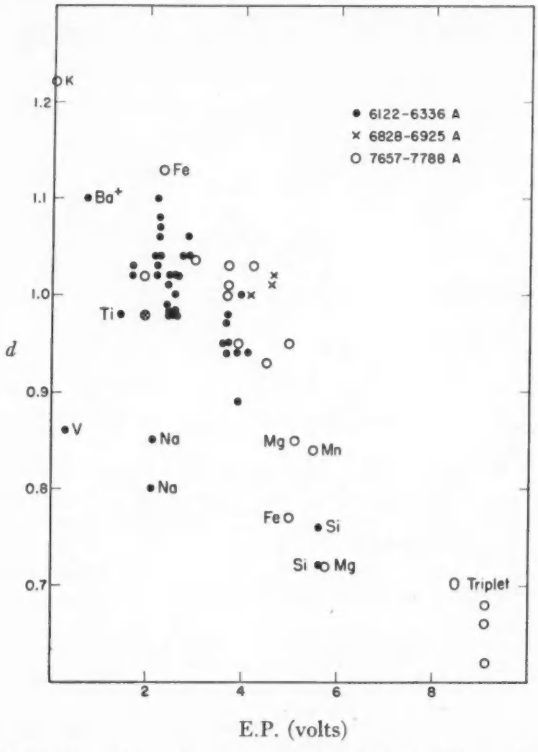

FIG. 6.—Correlation of relative sharpness (ordinate) with excitation potential (abscissa).

ences strong lines only; and for these the shape of the *F*-curve has so much greater influence that it is not possible to determine a damping factor from a single observation of central intensity. There may be a few cases where the damping factor is so large that the effect on faint lines is observable.

It has already been shown[7] that the sharpness depends statistically on the excitation potential, and the foregoing considerations show that this fact is probably connected with the dependence of

the F-curve on the excitation potential. When d is plotted against E.P., as in Figure 6, there is a larger scatter of points than can be attributed to varying atomic weight. Evidently the sharpness and F-curve shape are not governed simply by the excitation potential alone, but depend in a more complicated manner on the term structure.

Special attention may be drawn to the structure of the following lines:

a) The K line 7698 A (E.P. 0.0), although situated well within the infrared, is sharper than most lines in the visual region. Its unusual sharpness is undoubtedly associated with the fact that it is a resonance line; and it is tempting to conclude that all solar resonance lines have abnormally low central intensities. The observations so far published on the *Na* D lines[8] and the *Ca* g line[19] support this suggestion, but not the Ca^+ K line.[5]

b) The lines of the *O* triplet at 7771 A (E.P. 9.1) have an abnormally great breadth, due in part to the low atomic weight. Table 4 shows, however, that 0.72 is the lowest value of d that can be attributed to atomic weight alone, and the extra broadening required to give d a value as low as 0.62 must be associated with very high excitation potential and its consequent flat F-curve. The point that requires comment is that, if the F-curve is to affect lines as faint as these, the change of slope must set in for very weak absorption (as for curve d in Fig. 2). The introduction of a finite ϵ into Eddington's formula does not produce deviations in the F-curve which broaden such faint lines, and hence does not give a representation of the true conditions.

c) The broad V line at 6216 A (E.P. 0.3) is typical of the abnormality of V lines in the solar spectrum.

d) The sharpness of Ba^+ 6141 A (E.P. 0.7) is due both to high atomic weight and to low excitation potential. The contour is possibly affected by a blended *Fe* line.

e) All *Mg* and *Si* lines[20] in the lists are greatly broadened by virtue of both their low atomic weight and their high excitation potentials.

[19] Redman, *M.N.*, **95**, 742, 1935.

[20] I am indebted to Miss C. E. Moore for the identification of the silicon lines.

Moreover, Unsöld[21] has shown that the *Mg* lines have an abnormally large damping factor caused by Stark effect.

f) The breadth of the *Na* doublet at 6154 A (E.P. 2.1) is probably due entirely to low atomic weight.

Perhaps the main conclusion to be drawn from this work is that central intensities can be explained on the simple *F*-curve method of computing line contours, provided a turbulence of 1.6 km/sec be assumed to exist in the sun's reversing layer.

The author wishes to record thanks to Dr. W. S. Adams, director of the Mount Wilson Observatory, for the facilities placed at his disposal; to Dr. S. B. Nicholson for his interest and help with the apparatus; and to Dr. G. F. W. Mulders for the use of his step-wedges. The work was undertaken with the assistance of a Hackett Research Studentship granted by the University of Western Australia.

CARNEGIE INSTITUTION OF WASHINGTON
MOUNT WILSON OBSERVATORY
March 1937

[21] *Zs. f. Ap.*, **12**, 56, 1936.

NOTES ON SPECTRA OF CLASS Be

DEAN B. McLAUGHLIN

ABSTRACT

Observations of the relative intensities of components of double emission lines (V/R) and of the emission intensities relative to the continuous spectrum (E/C) are given for a number of the brighter Be stars, bringing a previous survey (1932) up to date.

During the twenty-five years of the Ann Arbor program, three stars previously constant in V/R have begun to vary, and three others, formerly conspicuously variable, have become constant. It is suggested that these represent different stages of the history of any V/R variable, and that periods of variation alternate with periods of constancy in most, if not all, Be spectra. The period of recurrence of variability is probably a century or more.

Several years ago the writer[1] published a summary of the Ann Arbor observations of the spectra of the brighter Be stars. The present paper brings the history of a number of these stars up to date. During the interval of five years, unexpected interesting and suggestive developments have occurred in the spectra of some of these objects. Their implications will be discussed at the end of this paper.

In the notes which follow, E/C refers to the estimated intensity of an emission line relative to the adjacent continuous spectrum outside the wings of the broad underlying absorption. V/R indicates the ratio of intensity of the violet to the red[2] component of the double emission lines.

γ CASSIOPEIAE ($0^h50^m.7$, $+60°11'$), $2^M.2$, Boe

Extensive studies by the late W. J. S. Lockyer[3] and by Cleminshaw[4] demonstrated that the spectrum was almost invariable from 1911 to 1928. Small variations then set in, and from 1932 to the present time the ratio V/R has varied conspicuously. A marked increase of intensity of the central absorption lines of hydrogen and

[1] *Pub. Obs. U. Michigan*, **4**, 175, 1932.

[2] "Violet" and "red" are used as convenient designations of the components of smaller and greater wave-length, respectively.

[3] *M.N.*, **93**, 362, 619, 1933; **95**, 520, 1935; **96**, 2, 1935.

[4] *Ap. J.*, **83**, 495, 1936.

helium was pointed out by the writer.[5] These reached maximum strength in May, 1936, almost simultaneously with equality of the emission components after the red component had been the stronger. Between June and August, 1936, these central absorption lines faded again. Since then the violet components of the hydrogen, *Fe* II, and *Si* II emissions have become relatively stronger; but those of helium have remained approximately equal to the red compo-

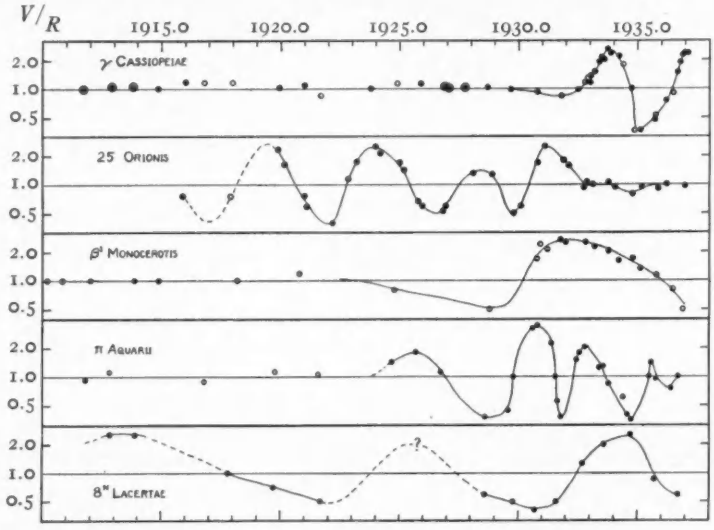

FIG. 1.—Variation-curves of V/R for Be stars. The points depend on means of $H\beta$ and $H\gamma$, except for β^1 Monocerotis, for which the points are based on $H\beta$ only. Open circles depend on only one or two plates, dots on three to nine, and ringed dots on ten or more plates.

nents. The emission structures of all lines have also become narrower; but those of hydrogen have shown the effect most conspicuously, so that $H\gamma$ is resolvable with difficulty. The spectrum may be about to repeat its anomalous behavior of 1934, when the emission lines appeared single on the Ann Arbor plates. The curve of variation of V/R is plotted in Figure 1.

ψ Persei ($3^h29^m.4$, $+47°51'$), $4^M.3$, B5e

One spectrogram, taken August 11, 1932, shows the red components of $H\beta$ and $H\gamma$ so much stronger as to be practically conclusive

[5] *Ibid.*, **84**, 235, 1936.

evidence of a temporary variation. Several other plates taken since then show V/R nearly 1.0. This star is shifted from the constant to the suspected class.

23 TAURI = MEROPE ($3^h40^m.4$, $+23°39'$), $4^M.3$, B5e

This star, previously variable in both E/C and V/R, has shown no marked activity since 1931.

X PERSEI ($3^h49^m.1$, $+30°45'$), $6^M.2$–$6^M.9$, Boe

The following observations have been obtained since the earlier survey:

Date	V/R	No. of Plates
1932.9	1.4	4
1933.8	2	3
1934.8	0.8	4
1935.8	2	2
1936.9	0.7	4

These data suggest a period a little longer than two years, but it does not satisfy the earlier observations. The variation is probably irregular.

11 CAMELOPARDALIS ($4^h57^m.4$, $+58°50'$), $5^M.3$, B3e

This star is one of the best examples of variable E/C. Recent data for several lines are given in the following table:

DATE	E/C				NO. OF PLATES
	$H\gamma$	$H\delta$	He	$H\zeta$	
1932.9	0.75	0.4	0.4	.....	3
1933.8	1.2	.8	.5	0.3	3
1935.1	1.5	.8	.7	.4	3
1936.0	1.6	.9	.6	.4	4
1936.9	1.6	0.95	0.7	0.5	4

The Ann Arbor data for $H\gamma$ are plotted in Figure 2. Minima of intensity were reached about 1920 and 1933. The emission has not yet recovered the maximum strength exhibited about in 1929. On

a plate taken December 14, 1936, the lines Hη, $H\theta$, and Hι have distinct but faint central absorption, which has never been detected before on Ann Arbor plates, though it has been carefully sought.

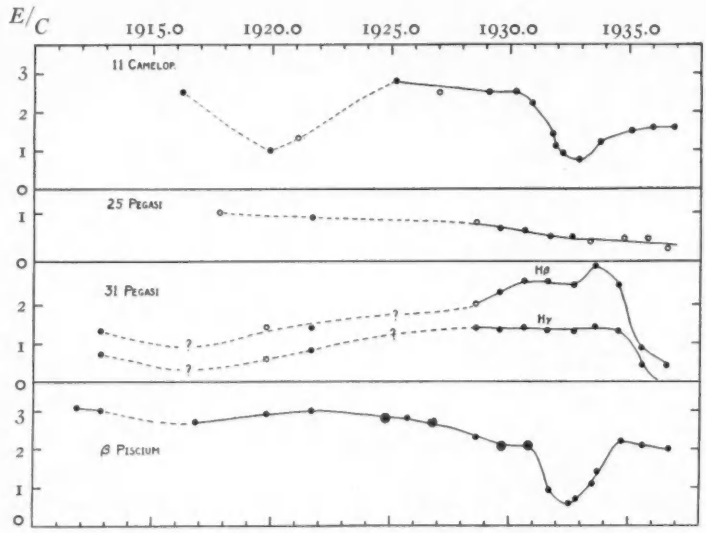

FIG. 2.—Variation-curves of E/C for Be stars. The points depend on $H\beta$, except for 31 Pegasi, for which curves of $H\beta$ and $H\gamma$ both are given. Open circles represent single plates, dots depend on two to nine plates, and ringed dots on ten or more plates.

105 TAURI (5^h02^m0, $+21°34'$), 6^M0, B3e

This star has fulfilled the expectation that it would prove to have variable V/R. The complete Ann Arbor data are as follows:

Date	V/R	No. of Plates
1930.8	0.6	2
1931.8	0.6	4
1932.8	0.65	1
1933.8	0.8	2
1934.8	1.2	1
1935.8	1.6	1
1936.9	1.5	1

The cycle of variation is evidently several years in length.

25 ORIONIS (5^h19^m6, $+1°45'$), 4^M7, B3e

A detailed discussion of the variations of this spectrum is given by Miss Dodson.[6] Observations subsequent to her study are given in the following table:

DATE	V/R		NO. OF PLATES
	$H\beta$	$H\gamma$	
1933.8	1.05	1.0	3
1934.05	0.95	0.9	3
1934.8	0.75	0.8	4
1935.2	0.9	1.0:	3
1935.9	0.8	1.1	4
1936.25	1.0	1.0	4
1937.0	0.9	1.0	3

The complete curve of V/R is plotted in Figure 1. The points represent means of $H\beta$ and $H\gamma$. Conspicuous changes of V/R continued from 1915 to 1932, in cycles varying in length from about 1800 to 1000 days. Since 1932, however, the star has been quiescent, with equal emission components.

120 TAURI (5^h27^m6, $+18°29'$), 5^M5, B3e

The complete Ann Arbor observations are as follows:

DATE	V/R		NO. OF PLATES
	$H\beta$	$H\gamma$	
1930.8	1.2	1.2	2
1931.8	1.2	1.1	3
1933.0	0.8	0.8	2
1933.8	0.8	1.0	2
1934.8	1.1	1.1	1
1935.9	0.8	0.9	2
1936.8	1.2	1.2	1

This spectrum is probably variable in V/R, with small range. A period of about three years is a possibility.

[6] *Ibid.*, p. 180.

HD 41335 ($5^h59^m.4$, $-6°42'$), $5^M.1$, B2e

In the previous note on this spectrum[7] the words "red" and "violet" should be interchanged. On plates taken in 1926, 1930, and every year thereafter until the present, the red components are much the stronger, though there has been a distinct change toward equality with probable secondary variations superimposed.

HD 44458 ($6^h16^m.8$, $-11°44'$), $5^M.5$, B2e

The data on this spectrum are fragmentary and indicate simply that V/R variation of moderate range has continued. The length of the cycle is still uncertain and is perhaps irregular.

β^1 MONOCEROTIS ($6^h24^m.0$, $-6°58'$), $4^M.7$, B2e

Recent Ann Arbor observations are given in the following table:

DATE	V/R		NO. OF PLATES
	$H\beta$	$H\gamma$	
1933.8	2.0	1.5	3
1934.2	1.6	1.3	3
1934.8	1.7	1.1	3
1935.1	1.3	1.1	3
1935.8	1.1	0.8	2
1936.3	0.8	0.75	2
1936.9	0.5	0.6	2

In the study of this spectrum by Miss Hawes[8] it was shown that V/R remained constant at 1.0 from 1905 to perhaps 1923. Between that time and 1928.8, V/R decreased to 0.5, and during the next two years the inequality was reversed. The foregoing table shows that the second reversal in 1935 occurred slowly, and that $H\gamma$ clearly preceded $H\beta$, as Miss Dodson has shown in the case of 25 Orionis. A curve of V/R for β^1 Monocerotis is given in Figure 1, for the interval 1910–1937.

κ DRACONIS ($12^h29^m.2$, $+70°20'$), $3^M.9$, B5e

Periods of thirty and twenty-three years have been suggested by Struve[9] and Jessup,[10] respectively, for the variation of E/C. Emis-

[7] *Pub. Obs. U. Michigan*, **4**, 182, 1932.

[8] *Pub. Vassar Obs.*, **4**, 29, 1934.

[9] *Pop. Astr.*, **33**, 596, 1925.

[10] *Ap. J.*, **76**, 75, 1932.

sion has completely disappeared at $H\beta$, and only a faint trace of bright $H\alpha$ is seen on wide absorption on a plate taken April 16, 1936.

20 VULPECULAE ($20^h07^m.8$, $+26°11'$), $5^M.9$, B8e

From about 1921 to 1932 the $H\beta$ emission increased through a small range. In 1936 its intensity was again about equal to that observed in 1921.

25 VULPECULAE ($20^h17^m.7$, $+24°07'$), $5^M.4$, B8e

The $H\beta$ emission appears to have faded slightly between 1931 and 1936.

λ CYGNI ($20^h43^m.5$, $+36°07'$), $4^M.5$, B5e

Weak single emission was present at $H\beta$ in 1926. In 1931 there was no emission, and plates taken each year after that showed $H\beta$ as a normal absorption line with a rather narrow central core. Four plates taken in 1936 show faint emission once more, and the absorption appears wide and ill defined, as in 1926.

HD 199356 ($20^h51^m.6$, $+39°51'$), $7^M.0$, Boe

There are only two spectrograms of this star, but they definitely establish the variation of V/R.

Date	V/R
1921 Aug. 6	0.6
1933 Aug. 11	1.2

f^1 CYGNI ($20^h56^m.4$, $+47°08'$), $4^M.9$, Boe

This interesting star lost its emission lines in 1912, regained them faintly in 1925 and strongly in 1927, and showed conspicuous variations of V/R in 1928–1930. The $H\beta$ emission faded again until it was just perceptible above the continuous spectrum in 1932. From that time to 1936 it remained quite inactive, without noticeable loss or gain of intensity.

υ CYGNI ($21^h13^m.8$, $34°29'$), $4^M.4$, B3e

This star shows definite V/R variation of small range. During 1929 the emission components were approximately equal. From

1930 to 1933 the red components were the stronger, and since 1934 the violet components have been slightly more conspicuous. If there is a period, it is of the order of eight or ten years.

6 CEPHEI ($21^h17^m.3$, $+64°27'$), $5^M.2$, B3e

From 1932 to 1936, E/C at $H\gamma$ changed from 1.0 to 0.75. A previous minimum of intensity, 0.7, occurred in 1921–1924. In 1936 the red component of $H\gamma$ was slightly the stronger, though in previous years the components were practically equal.

ϵ CAPRICORNI ($21^h31^m.5$, $-19°54'$), $4^M.7$, B5ep

This spectrum is characterized by well-defined hydrogen emission with strong sharp central absorption, and by variable enhanced metallic absorption lines. The latter emerged to visibility in 1929, faded in 1931, remained absent through 1935, and reappeared previous to September, 1936.

o AQUARII ($21^h58^m.1$, $-2°38'$), $4^M.7$, B5e

Twenty-seven plates taken between 1932 and 1936 show no indication of variation of either E/C or V/R.

25 PEGASI ($22^h03^m.1$, $+21°13'$), $5^M.7$, B5e

The following observations have been obtained:

Date	E/C ($H\beta$)	No. of Plates
1932.6	0.5	2
1933.6	.4	1
1934.8	.5−	1
1935.8	.5−	1
1936.6	0.25	1

The gradual fading of the emission previously noticed, between 1917 and 1931, has evidently continued. The curve of variation is shown in Figure 2.

31 PEGASI ($22^h16^m.6$, $+11°42'$), $4^M.9$, B3e

Recent Ann Arbor observations are summarized in the following table:

Date	E/C		No. of Plates
	$H\beta$	$H\gamma$	
1932.7	2.5	1.3	6
1933.6	3.0	1.4	5
1934.6	2.5	1.3	4
1935.6	1.0	0.4	4
1936.6	0.4	.....	6

Between 1933 and 1936 the emission faded from the brightest to the faintest ever recorded in this spectrum. A curve of variation is shown for $H\beta$ and $H\gamma$ in Figure 2. A previous minimum of emission occurred between 1912 and 1919.

π Aquarii ($22^h20^m.2$, $+0°52'$), $4^M.6$, B1e

Ann Arbor observations of V/R between 1911 and 1930 are tabulated in a previous paper.[11] During that interval the value of E/C at $H\beta$ was 2.3, with possible small fluctuations. Later observations of V/R and E/C are given in the following table:

Date	V/R		E/C ($H\beta$)	No. of Plates
	$H\beta$	$H\gamma$		
1931.4	2.8	1.5	2.0	1
1931.55	1.05	1.0	1.5	4
1931.65	0.44	0.62	1.4	5
1931.80	0.36	0.40	1.6	5
1932.45	1.5	1.5	1.3	5
1932.6	2.0	1.6	1.2	6
1932.8	2.3	1.8	1.4	5
1933.4	1.4	1.0	1.2	4
1933.6	1.6	1.0	1.2	4
1933.8	0.8	0.9	1.1	2
1934.4	0.6	0.6	1.4	2
1934.6	0.4	0.4	1.6	3
1934.75	0.3	0.4	2.0	4
1935.5	1:	1:	1.1	3
1935.6	1.5	1.4	1.1	5
1935.8	1.0	0.9	1.0	4
1936.4	0.75:	.....	1.0	3
1936.7	1:	1:	0.7?	7

[11] *Pub. Obs. U. Michigan*, **4**, 44, 1931.

The recent variations of V/R have been complicated by the fading of the emission, which rendered the numerical values unreliable although the direction of the inequality is definite enough. The data are in satisfactory accord with those given by Lockyer.[12]

The curve of V/R from 1911 to 1936 is shown in Figure 1. Unless the plates earlier than 1924 were taken, by remote chance, at times of equality of emission, the ratio V/R was constant near 1.0 from 1911 to 1923, and the large range of V/R is a comparatively recent development. This case is thus similar to those of γ Cassiopeiae and β^1 Monocerotis.

Another point of interest is shown by the tabular values of V/R in 1932–1933. $H\gamma$ passed through equality of components a few months before $H\beta$. This is similar to the behavior of these lines in 25 Orionis and β^1 Monocerotis.

8 Lacertae (North) ($22^h31^m.4$, $+39°07'$), $5^M.8$, B3e

Observations obtained since the previous survey are given in the following table:

Date	V/R		No. of Plates
	$H\beta$	$H\gamma$	
1932.7	1.3	1.2	4
1933.6	2	2	4
1934.7	2.8	2.2	3
1935.7	0.9	0.8	3
1936.7	0.5	0.7	6

The curve of variation of V/R is shown in Figure 1. A period of about eleven years appears to be a possibility.

HD 217050 ($22^h52^m.7$, $+48°09'$), $5^M.2$, B3ep

This star is a good example of a variable composite spectrum. Emission lines were absent in 1921. Since 1928 they have been strong, with sharp strong central absorption. With them an enhanced metallic absorption spectrum appeared, and it has persisted unaltered through 1936.

[12] *M.N.*, **96**, 480, 1936.

β Piscium (22^h58^m8, $+3°17'$), 4^M6, B5e

This star shows conspicuous E/C variation. Observations since the previous note are given in the following table:

Date	E/C			No. of Plates
	$H\beta$	$H\gamma$	$H\delta$	
1932.8	0.7	0.3	.....	4
1933.5	1.1	.5	0.25	4
1933.7	1.4	.7	.3	4
1934.7	2.2	.85	.35	6
1935.6	2.1	.8	.35	4
1936.7	2.0	0.8	0.3	4

The curve of variation is shown in Figure 2. In view of the relatively short duration of the recent minimum, observations about 1915 would be of considerable interest.

DISCUSSION

Several stars which have shown no new developments have been omitted from the preceding notes. The recent observations have resulted in a change of status of eleven stars. Some merely represent confirmation of suspected variation; others represent radical changes of behavior. The eleven stars are listed in the following table, with their classification as of 1932 and the revised classification of 1937.

Star	V/R		E/C	
	1932	1937	1932	1937
γ Cas	const?	var!!	const!	const!
ψ Per	const	var?	const!	const!
105 Tau	var!	var!	.....	const
25 Ori	var!!	var!!	const!	var?
120 Tau	var	var	.....	const
HD 41335	var!!	var!!	.....	const
HD 44458	var!!	var!!	.....	const
20 Vul	const?	const?	var?	var
25 Vul	const	const	const	var
6 Cep	const?	var?	var?	var
π Aqr	var!!	var!!	const!	var!

In addition to these, the star HD 199356, not included in the previous survey, has been found variable in V/R.

In the previous survey of forty-three Be stars (omitting the peculiar cases β Lyrae and υ Sagittarii), it was concluded that twenty showed variable V/R, eight were more or less strongly suspected of variation, six were certainly constant, and nine were uncertain because of insufficient data or single emission. Now, twenty-one are recognized as variable (γ Cassiopeiae added), eight are suspected (γ Cassiopeiae confirmed, ψ Persei added), five are constant, and the same nine are still unknown.

In 1932 the statistics of E/C were: twelve variable, three suspected, twenty constant, and eight unknown. These figures are now modified to: sixteen variable, two suspected, twenty-one constant, and four unknown.

The general conclusion that variability is the rule and constancy the exception among Be stars is slightly strengthened. The conclusion that no stars with large range of V/R show change of E/C is now disputed by the fading of emission in π Aquarii. It now appears more probable that it is only a question of time before all Be stars will show variable E/C. The irregularity of lengths of cycles serves to emphasize the earlier conclusion that binary motion as an explanation of the changes must be ruled out in most cases.

The present survey and work done, since the previous survey, on the earlier history of some of the stars has revealed cases of cessation of variation of V/R, as well as some cases of incidence of such variation in stars previously constant. Thus, on the one hand, we have ζ Tauri,[13] b^2 Cygni,[14] and 25 Orionis, which formerly showed large changes of V/R but are now constant. It may be mere coincidence that the last large inequality of components shown by all three of these stars was in the same direction, namely, V/R greater than 1.0.

On the other hand, three excellent examples of incidence of V/R variation are now recognized. These are: γ Cassiopeiae, β^1 Monocerotis, and π Aquarii. These do not present the same unanimity with regard to the direction of their first departure from V/R equal to 1.0 as did the previous three in their last large inequality.

It is possibly a coincidence that the numbers of cases of incidence

[13] Losh, *Pub. Obs. U. Michigan*, **4**, 3, 1931; McLaughlin, *ibid.*, **4**, 181, 1932.

[14] Losh, *ibid.*, **4**, 200, 1932.

and cessation are equal, but it has at least the suggestion of statistical equilibrium of the class. To the writer it is inconceivable that these observed changes represent *permanent* changes in the status of these stars. Rather, it seems very plausible that a given star may have alternate periods of activity and quiescence. In γ Cassiopeiae we have been privileged to observe the transition in one direction; in 25 Orionis the reverse change has been observed in detail. In the course of time we may hope to see the resumption of variation in the spectrum of 25 Orionis and its cessation in γ Cassiopeiae. When we consider the microscopic size of our time interval of observation compared with the life of a star, it would be illogical in the extreme to postulate a unidirectional change in any individual case when we observe equal numbers of cases in which the change has occurred in two opposite directions.

The present survey, added to the earlier work, shows that the periods of variation of E/C are, for the most part, many years in length, with ten years as a probable lower limit. Periods of two to twelve years would include almost all of the V/R variables, when we consider only the cycles of V/R. The periods of *recurrence* of variation or constancy of V/R are perhaps of the order of a century or more in length.

The fact that any given Be spectrum has shown no variation over an interval of twenty years or so is no guaranty that it will remain forever an uninteresting object. The case of γ Cassiopeiae is sufficiently recent to serve as a reminder that every Be star is at least potentially variable, and hence deserves reobservation at intervals sufficiently short to give warning of approaching activity. Only when we have a larger number of observations of incidence and cessation of variation will it be possible to generalize confidently with regard to the manner of such incidence or cessation, and only then will it be possible to attack the problem of physical causes with any considerable hope of success.

THE OBSERVATORY
UNIVERSITY OF MICHIGAN
February 27, 1937

ON THE INTERPRETATION OF THE SURFACE BRIGHTNESSES OF DIFFUSE GALACTIC NEBULAE

OTTO STRUVE

ABSTRACT

Observational results indicate that the surface brightnesses of many dark nebulae are not uniform but exhibit dark cores and more luminous edges. This effect cannot be due to uneven thickness or transparency of the dark nebula. The Lommel-Seeliger theory of diffuse reflection is extended to the case of an opaque spherical nebula consisting of particles which are characterized by different spherical albedos and phase functions. The surface brightness of the nebula is computed for different distances from the center, under the assumption that the illumination comes from the uniform brightness of the starlit sky. The results give values for the difference in stellar magnitudes between edge and center, from 0.03 mag. to 0.17 mag. The observations favor slightly a large albedo and a phase function which throws most of the light in the direction of the incident beam. The Lambert phase function can only be reconciled with the observations if the albedo is assumed to be unreasonably large.

The Lommel-Seeliger theory is next applied to the peculiar phenomenon of narrow bright rims frequently observed in emission nebulae but never found in nebulae having continuous spectra. A list of these objects is given, the most conspicuous of which is the rim on the west side of the Horse-head nebula, Barnard 33. If in the derivation of the Lommel-Seeliger formula the absorption coefficient of the incident radiation is k_1 and the absorption coefficient of the visible diffuse nebular light is k_2, then for a nebula in which the product of the radius by k_1 is very large, the surface brightness of the nebula is

$$I = \text{const} \frac{\cos i}{\cos \epsilon + (k_2/k_1) \cos i},$$

where i is the angle of incidence and ϵ is the angle between the line of sight and the perpendicular to the nebula. If k_2/k_1 is negligible, I is inversely proportional to $\cos \epsilon$, so that at the edge a narrow bright rim will be formed.

1. The principal purpose of a series of investigations now being carried on at the Yerkes Observatory is to obtain data concerning the nature of the particles which give rise to the scattered light of the nebulae. Henyey's recent paper[1] on this subject has elucidated the theory of nebular scattering and has shown how, with reasonable assumptions concerning the form of the phase function, the geometrical conditions of the problem and the albedos of the particles may be derived. From the observations of the colors of a few of the nebulae and from the small amount of radial polarization observed in two or three of them, we conclude that pure Rayleigh scattering de-

[1] *Ap. J.*, 85, 107, 1937.

pending upon λ^{-4} can, at most, contribute only a fraction—perhaps not more than one-half or one-third—to the total light of these reflection nebulae. It is, however, certain that some nebulae show selective reddening for transmitted light, so that scattering by small particles is not altogether negligible. The observations of the colors of the nebulae, of the amount of selective reddening for transmitted light, and of polarization really prove only that the majority of particles are not small enough to scatter in accordance with the symmetrical phase function $\varphi(\alpha) = 1 + \cos^2 \alpha$. The particles either may be large enough to have phase functions which return most of the light toward the source or may be sufficiently small to have phase functions which throw most of the light in the direction of the incident beam.

While Henyey and the writer have used the Lambert phase function without having encountered serious inconsistencies in the results, other phase functions would have served equally well. The trouble lies in the bewildering structural formations which are present in practically all diffuse nebulae and which tend to obliterate the effects produced by the geometrical conditions and by the form of the phase function. It will evidently be a difficult task to determine, even roughly, the form of the phase function. Yet, this is required if we are to make progress in our study of the physical properties of the nebular particles.

Since there are apparently no simple cases of nebulae where the phase function can be derived directly from the surface brightnesses at varying distances from the illuminating star, it will be necessary to pursue the laborious method of separating and interpreting those nebular features which are not merely a result of density fluctuations. The present investigation makes a first attempt in this direction. We shall show that while, even now, it is not possible to derive the phase function accurately, a number of interesting features, common to many nebulae, can be satisfactorily explained by the theory of diffuse scattering.

2. In a recent paper[2] it was shown that the dark nebula Barnard 15 has a dark core and slightly more luminous edges, although in all parts of the nebula the faint stars are completely blotted out.

[2] Struve and Elvey, *ibid.*, **83**, 172, 1936.

The total range is only 0.1 mag. between center and edge, and the observations are satisfactorily represented by a straight line. Photographs of B15 show conclusively that this effect is not produced by the increasing thickness of the nebula as we pass from the edge toward the center. Even at the adopted edge, marked by abscissa 1.0 in Figure 1, the absorption of starlight behind the nebula is still of the order of several magnitudes. Hence, the background of the starlit sky behind the nebula is effectively blocked out.

The photographs of the Milky Way by Barnard and by Ross reveal a large number of dark nebulae possessing similar dark cores.

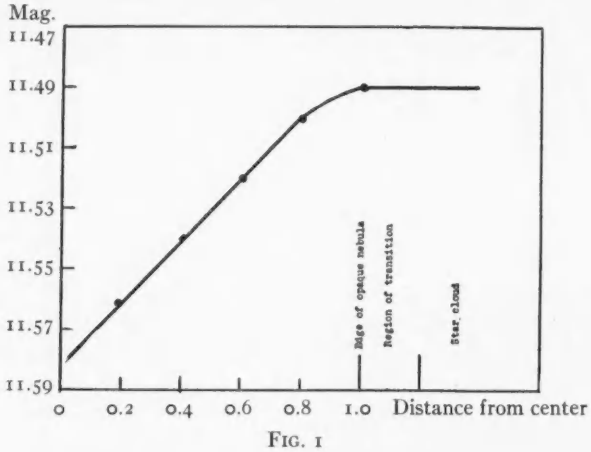

FIG. 1

Plate IV shows the extensive dark nebulae in Taurus, reproduced by E. L. McCarthy by superposing two original negatives taken by Professor Ross. The dark nebulae are very conspicuous, and the cores are quite prominent. Plate V shows the same region, reproduced from an original negative taken by Professor Barnard with the 6-inch Bruce telescope. The black cores are almost identical in the two illustrations. Finally, Plate VI is a reproduction obtained from the superposition of two original negatives by Barnard: it illustrates the dark nebulosities in the region of $\alpha\ 4^{h}10^{m}\ \delta + 54^{\circ}30'$. Barnard's dark nebulae B11, B12, and B13 have well-marked black cores; but a large starless region, B8, has a surface brightness which exceeds that of the cores and resembles that of the background in the denser star clouds. This region shows very clearly that there are marked differences in the surface brightnesses of dark nebulae.

PLATE IV

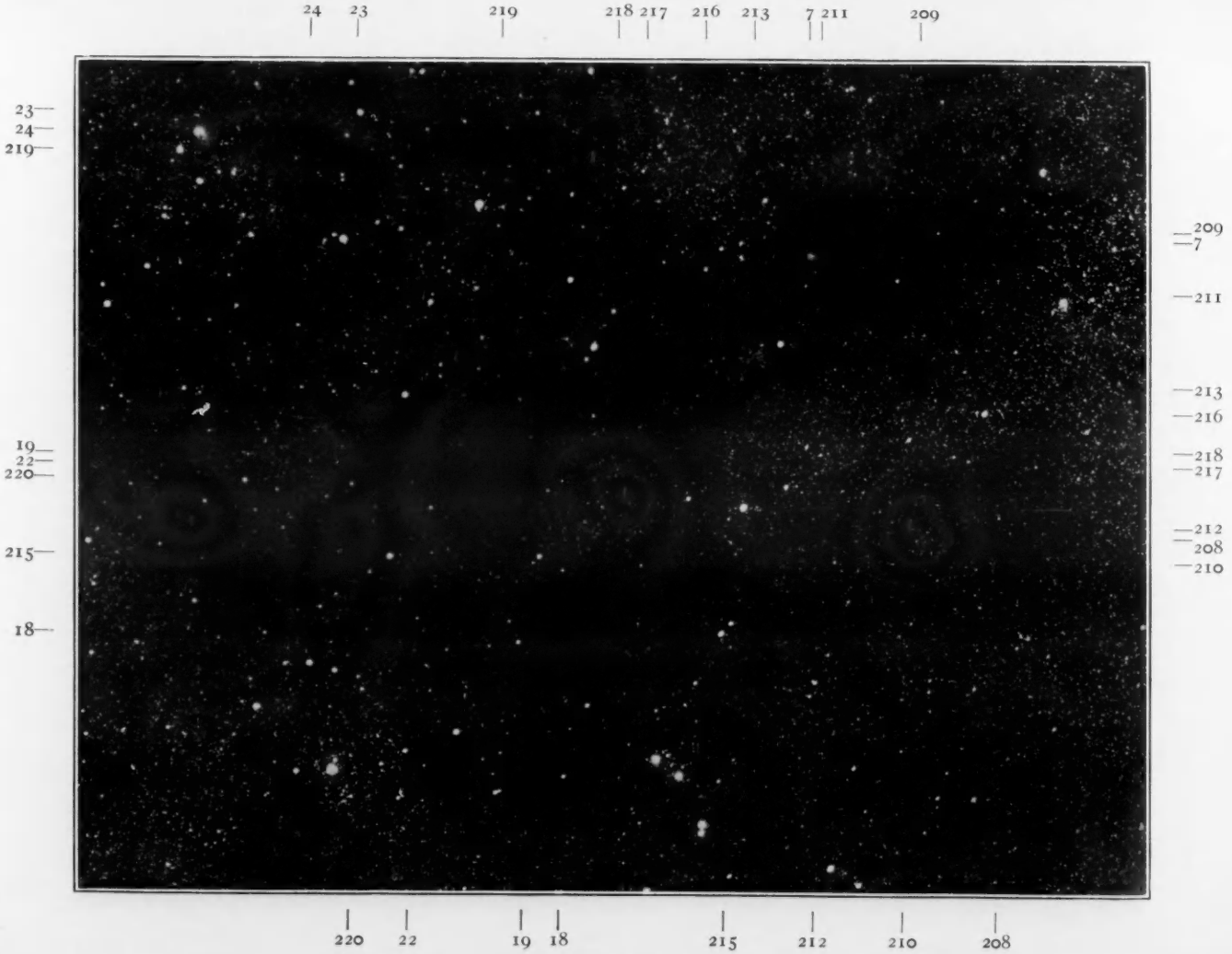

BARNARD'S DARK NEBULAE IN TAURUS

From photographs by F. E. Ross

PLATE V

BARNARD'S DARK NEBULAE IN TAURUS

From a photograph taken with the 6-inch Bruce telescope

(The numbers of Barnard's dark nebulae are shown on the margins)

PLATE VI

PLATE VI

BARNARD'S DARK NEBULAE IN CAMELOPARDUS

(The numbers of Barnard's dark nebulae are shown on the margins)

The color of the luminous edges surrounding the cores of dark nebulae is yellow. This was shown on photographs of the dark region north of 22 Scorpii, photographed with the Schmidt camera in yellow and in blue light.[3] More recent photographs of Barnard 216 confirm this result. The marking described by Barnard in his *Catalogue of 349 Dark Objects in the Sky* as a "dark spot in lane" has an appreciably smaller surface brightness than the surrounding starless region. It is equally well visible on an Eastman Process plate exposed without a filter and on an Eastman IC plate exposed with a red filter (Wratten 23 A). We conclude that the luminous portions of dark nebulae resemble in color the background of the night sky, and are therefore similar to the integrated light of the stars.

3. Since reasons have already been given for believing that an opaque mass of scattering particles in interstellar space illuminated by general starlight will be bright enough to produce a measurable amount of surface brightness on top of the luminous background of the sky, we shall follow up this hypothesis more closely and investigate whether it is possible to account for the uneven surface brightness of the dark nebulae.

Let us first consider the dark nebula as an opaque spherical body which acts as a diffusing screen obeying the law of Lambert. If the incident light is designated by L, we find for the surface brightness, per steradian, of the nebula

$$I = \frac{A}{\pi} L \cos i \, .$$

Here A is the Lambert albedo. If we imagine that L is uniformly spread over one hemisphere so that L_1 is the surface brightness per square degree of the sky, as seen from the nebula, such that

$$\frac{41{,}253}{4\pi} \int L_1 d\omega = L \, ,$$

we obtain for the surface brightness of the nebula per square degree

$$I_L = \frac{A}{\pi} L_1 \, 2\pi \int_0^{\pi/2} \cos i \sin i \, di = A L_1 \, .$$

[3] *Ibid.*, **84**, 223, 1936. Recent photographs in red light confirm this.

L_1 is not accurately known. The best we can do now is to use the value of $\int L_1 \, d\omega$ given by Seares, Van Rhijn, Joyner, and Richmond[4] for the total amount of starlight:

$$\frac{41{,}253}{4\pi} \int L_1 \, d\omega = 577 \text{ stars of photographic magnitude } 1.0 .$$

Hence, we find for one square degree of the sky a surface brightness of 56 stars of magnitude 10. This agrees quite closely with the results of Bottlinger.[5] The nebula receives, of course, more light because the units we have adopted refer to starlight which has passed through the atmosphere. Since, however, we observe the nebula also through the atmosphere, we can disregard the corresponding correction.

If we adopt $A = 0.3$, we find

$$I_L = 17 \text{ stars of magnitude 10 per square degree.}$$

This amount of light is superposed over the "terrestrial" background of the sky, for which we shall adopt a value of 4.4 pg. mag. per square degree, which is equivalent to 174 stars of magnitude 10. This value, due to Dufay,[6] must be corrected for the light of unresolved stars fainter than those which could be eliminated in his observations. This amount may be estimated at 20 per cent, leaving the equivalent of 140 stars per square degree for the "terrestrial" background. Consequently, if Lambert's law is adopted and if $A = 0.3$, the nebula should appear as a surface which is slightly brighter than the "terrestrial" sky background, the difference being

$$\Delta m_L = 2.5 \log \tfrac{157}{140} = 0.12 \text{ mag.}$$

While this value is quite plausible, Lambert's law leads to an expression for I_L which is independent of the angle ϵ between the line of sight and the perpendicular to the diffuse surface. Accordingly, I_L is constant for all ϵ, and there should be no variation in the surface brightness of a dark nebula. It is not likely that this inconsist-

[4] *Ibid.*, **62**, 373, 1925.

[5] *Zs. f. Ap.*, **4**, 373, 1932.

[6] *Etude de la lumière du fond du ciel nocturne*, Paris, 1934.

ency with the observations can be removed by dropping our simplifying assumption that the starlit sky, as seen from the nebula, appears uniformly bright and that its surface brightness is equal to the average surface brightness of all stars as seen from the earth. Hence, we are compelled to abandon Lambert's law.

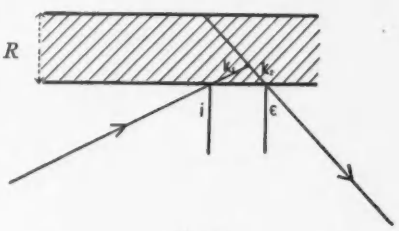

FIG. 2

4. We shall next use the law of diffuse reflection proposed by Lommel and by Seeliger. If the nebula is a uniform plane-parallel slab of diffuse material having an absorption coefficient k and a thickness R, the surface brightness is[7]

$$I = \frac{\mu}{k} L\varphi(a) \frac{\cos i}{\cos i + \cos \epsilon} [1 - e^{-Rk(\sec i + \sec \epsilon)}] .$$

The factor $\mu\varphi(a)$ measures the fraction of the incident light which is reflected by unit volume in the direction of the phase angle a. If the nebula is opaque, so that Rk is large, we have

$$I = \frac{\mu}{k} L\varphi(a) \frac{\cos i}{\cos i + \cos \epsilon} . \qquad (1)$$

No assumption has here been made concerning the nature of the nebular particles. If, however, we assume that we are dealing with fairly large spherical particles of radius ρ, we have

$$k = N\pi\rho^2 ,$$

$$\mu = N \frac{\gamma}{2\pi} \pi\rho^2 ,$$

$$\int \varphi(a) d\omega = 2\pi .$$

The albedo γ gives the fraction of the total light incident upon each particle which is reflected in all directions. Then

$$I = \frac{\gamma}{2\pi} L\varphi(a) \frac{\cos i}{\cos i + \cos \epsilon} ,$$

[7] Schoenberg, *Handbuch der Astrophysik*, 2, Part I, 35, 1929.

which is identical with Seeliger's expression adopted in our former paper,[8] where $\gamma = 2p$. If we again replace L by $L_1 d\omega$ and integrate over the hemisphere which is visible from the nebula, we obtain the surface-brightness I_s per square degree of the nebula as seen from the angle ϵ:

$$I_s = \frac{\gamma}{2\pi} L_1 \int \varphi(\alpha) \frac{\cos i}{\cos i + \cos \epsilon} d\omega \,. \tag{2}$$

Since the phase function is not known, we shall make three assumptions for it and compute the surface brightness of a nebula which is uniformly illuminated from all sides by starlight. The integration will therefore be carried out for six cases, as shown in the accompanying table.

	Phase Function		
	$\varphi_1(\alpha) = \cos^2 \frac{\alpha}{2}$	$\varphi_2(\alpha) = 0.5$	$\varphi(\alpha) = \sin^2 \frac{\alpha}{2}$
Case (1)	(1) $\epsilon = 0$	(3) $\epsilon = 0$	(5) $\epsilon = 0$
Case (2)	(2) $\epsilon = 90^\circ$	(4) $\epsilon = 90^\circ$	(6) $\epsilon = 90^\circ$

Case (1) is identical with the one computed in our former paper:

$$I_{s1} = 0.25 \gamma L_1 \,.$$

Our phase function $\varphi_1(\alpha)$ is that of Euler, which agrees reasonably well with the one by Lambert and throws most of the light in the direction opposite that of the incident beam. $\varphi_3(\alpha)$ throws most of the light in the direction of the incident beam; and while its form has no physical justification, it resembles the phase functions of moderately small particles computed by Blumer from the theory of Mie. $\varphi_2(\alpha)$ is an intermediate case. We shall assume that formula (2) holds for all three expressions of $\varphi(\alpha)$, although it was derived from the more general expression (1) under the assumption that the particles are large enough to permit us to use $k = N\pi\rho^2$. However, if we compare (1) with (2), we find that their forms are identical

[8] *Ap. J.*, **83**, 164, 1936.

and that only γ changes its meaning if the particles are so small that diffraction effects became serious.

It is obvious from the symmetrical shape of the three phase functions and from the identities

$$\tfrac{1}{2}[\varphi_1(a) + \varphi_1(a + 180°)] = 0.5\,,$$
$$\tfrac{1}{2}[\varphi_3(a) + \varphi_3(a + 180°)] = 0.5\,,$$
$$\varphi_2(a) = 0.5\,,$$

that at the edge ($\epsilon = 90°$), I_e will be the same for all three functions. The integrations are carried out as follows:

Case 1: See *Astrophysical Journal*, **83**, 166, 1936.

Case 2: Let β be the azimuth of the source as seen from the nebula. Then

$$\cos a = \sin i \cos \beta\,,$$
$$\varphi_1(a) = 0.5 + 0.5 \sin i \cos \beta\,.$$

The integral becomes, since $\dfrac{\cos i}{\cos i + \cos \epsilon} = 1$,

$$I = C \int_0^{\pi/2} \int_0^{2\pi} \varphi_1(a) \sin i \, di \, d\beta = C\pi\,.$$

Case 4: Similar to Case 2.

Case 6: Similar to Case 2.

Case 3: $\epsilon = 0$; $i = a$

$$I = 0.5C \; 2\pi \int_0^{\pi/2} \frac{\sin a \cos a}{1 + \cos a} \, da\,.$$

Substituting $1 + \cos a = z$,

$$I = 0.5C \; 2\pi \int_1^2 \frac{z - 1}{z} \, dz = z - lnz \Big|_1^2 = 0.307C\pi\,.$$

Case 5: $\epsilon = 0$; $i = a$

$$I = C \; 2\pi \int_0^{\pi/2} \frac{\sin^2 \frac{a}{2} \sin a \cos a}{1 + \cos a} \, da\,.$$

Substituting

$$\sin^2 \frac{a}{2} = 0.5 - 0.5 \cos a ,$$

$$1 + \cos a = z ,$$

$$I = C\, 2\pi \left\{ 0.5 \int_1^2 \frac{z-1}{z}\, dz - 0.5 \int_1^2 \frac{(z-1)^2}{z}\, dz \right\} = 0.057 C 2\pi .$$

Table 1 gives a summary of the results.

TABLE 1

Phase Function	Euler: $\varphi_1(a) = \cos^2 \frac{a}{2}$	Constant: $\varphi_2(a) = 0.5$	Small Particles: $\varphi_3(a) = \sin^2 \frac{a}{2}$
$\epsilon = 0$ $\epsilon = 90^\circ$	$I_{s1} = 0.25\gamma L_1$ $I_{s2} = 0.5\gamma L_1$	$I_{s3} = 0.15\gamma L_1$ $I_{s4} = 0.5\gamma L_1$	$I_{s5} = 0.06\gamma L_1$ $I_{s6} = 0.5\gamma L_1$
Ratio: Edge/Center	2.0	3.3	8.3

Assuming $\gamma = 0.3$ and $L_1 = 56$ stars of magnitude 10 per square degree,

$$I_{s1} = 4.2 , \quad I_{s3} = 2.5 , \quad I_{s5} = 1.0 ,$$

$$I_{s2} = 8.4 , \quad I_{s4} = 8.4 , \quad I_{s6} = 8.4 .$$

If we again adopt for the "terrestrial" background of the sky the equivalent of 140 stars of magnitude 10 per square degree, we obtain for the difference in magnitude between the edge and the center of a dark nebula the following values:

$$\text{For } \varphi_1(a): \gamma = 0.3;\ \Delta m = 2.5 \log \frac{148.4}{144.2} = 0.03 \text{ mag.}$$

$$\text{For } \varphi_2(a): \gamma = 0.3;\ \Delta m = 2.5 \log \frac{148.4}{142.5} = 0.04$$

$$\text{For } \varphi_3(a): \gamma = 0.3;\ \Delta m = 2.5 \log \frac{148.4}{141.0} = 0.06$$

The observed value is 0.1 mag., or twice the result computed for $\varphi_3(a)$. Increasing the value of γ to 0.6, which would correspond to a rather efficient scattering power of the nebula, we obtain:

For $\varphi_1(a)$: $\gamma = 0.6$; $\Delta m = 0.06$ mag.

For $\varphi_2(a)$: $\gamma = 0.6$; $\Delta m = 0.08$

For $\varphi_3(a)$: $\gamma = 0.6$; $\Delta m = 0.11$

The observations seem to favor the larger value of γ and the phase function $\varphi_3(a)$, which throws most of the light in the direction of the incident beam. It is possible, however, that γ is even larger, in which case $\varphi_2(a)$ or $\varphi_1(a)$ would give plausible values for Δm. Thus, for the unreasonably large value of $\gamma = 1.0$, we find:

For $\varphi_1(a)$: $\gamma = 1.0$; $\Delta m = 0.09$ mag.

For $\varphi_2(a)$: $\gamma = 1.0$; $\Delta m = 0.13$

For $\varphi_3(a)$: $\gamma = 1.0$; $\Delta m = 0.17$

Our result must be regarded as tentative because it is based upon uncertain values of the "terrestrial" background and of the real amount of starlight as seen from the nebula. Also, the observations are somewhat uncertain and should be repeated for a greater number of objects. Nevertheless, it is not very probable that we were able, with the Fabry photometer, to detect the full range of the variation in surface brightness. The computations give us the maximum range. Hence, our conclusions regarding γ and $\varphi(a)$ are probably correct.

5. In the derivation of the Lommel-Seeliger formula for diffuse reflection, the effect of the reflections of orders higher than the first is neglected. It is of interest to find to what extent the foregoing conclusions will be affected, if the reflections of the second order are allowed for. This can be done very simply by means of the formulae for diffuse reflection derived by Fessenkoff[9] and by Schoenberg.[10]

Fessenkoff adopts for the phase function Rayleigh's law:

$$\varphi_4(a) = 1 + \cos^2 a ,$$

[9] *Bull. Soc. Astr. de Russie*, May, 1916.

[10] *Op. cit.*, p. 37.

and derives an expression for the surface brightness, taking account of the second-order reflections. Schoenberg uses

$$\varphi_5(\alpha) = 1 - 2.7 \cos \alpha + 3 \cos^2 \alpha ,$$

which is the phase function for small drops of water resulting from Mie's theory. $\varphi_4(\alpha)$ is symmetrical with respect to both the line of sight and any straight line passing through the particle at right angles to the line of sight. Hence it should give results which are comparable to our $\varphi_2(\alpha)$. On the other hand, $\varphi_5(\alpha)$ throws most of the light in the direction of the incident beam, and is therefore somewhat similar to our $\varphi_3(\alpha)$.

Schoenberg has computed tables for both formulae, giving the value of the surface brightness of the diffusing screen at intervals of 10° in i and in ϵ, and at suitable intervals of the azimuth A. The integration for the hemisphere can therefore be carried out numerically: we first compute from the tables of Schoenberg the average surface brightness for each value of i. This eliminates the azimuth. Next we multiply each surface brightness thus computed by the area of the corresponding zone in i. The summation of the results for all zones gives the relative surface brightness of the nebula for any given ϵ. Setting the surface brightness at $\epsilon = 0$ equal to 1, we have

TABLE 2

ϵ	sin ϵ	1/cos ϵ	I (Fessenkoff)	I (Schoenberg)
0	0.00	1.00	1.00	1.00
10	0.17	1.02	1.01	1.04
20	0.34	1.06	1.03	1.14
30	0.50	1.15	1.07	1.34
40	0.64	1.31	1.13	1.65
50	0.77	1.56	1.22	2.09
60	0.87	2.00	1.36	2.72
70	0.94	2.92	1.55	3.64
80	0.98	5.76	1.85	5.00
90	1.00	∞	2.42	6.98

The results are shown in Figure 3, where the values of I have been plotted against sin ϵ as abscissa. The ratio Edge/Center is 2.4 for Fessenkoff's formula, instead of 3.3 as computed in section 4 with $\varphi_2(\alpha) = 0.5$. The same ratio for Schoenberg's formula is 7.0, instead

of 8.8, as computed in section 4 with $\varphi_3(\alpha) = \sin^2 \alpha/2$. The conclusions of section 4 are not materially altered.

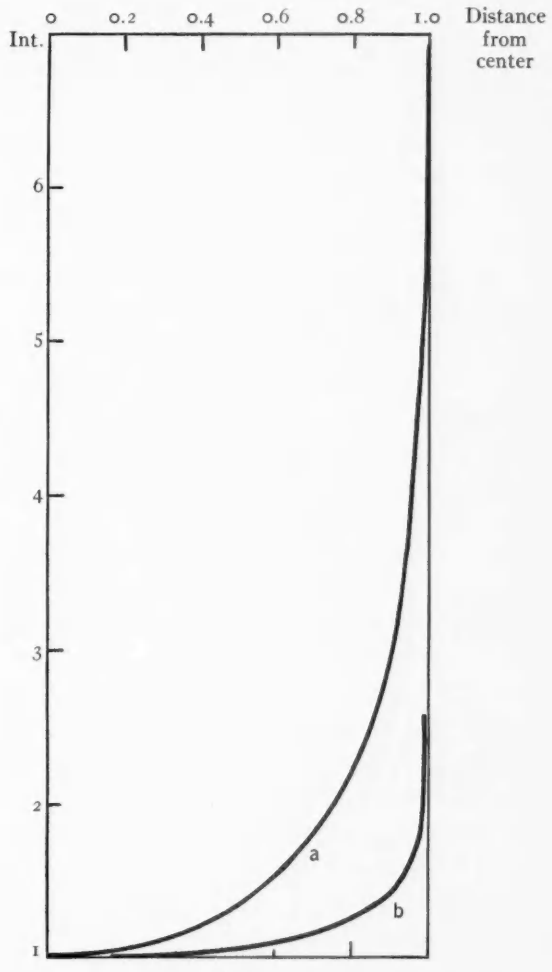

FIG. 3

There is an apparent discrepancy between the shape of the computed curves in Figure 3 and that of the observed curve in Figure 1. This is not serious, however. It is, of course, obvious from an examination of the photographs that the curve does not reach a sharp point in the center of the core. The bottom of the curve must be

flat. I have attempted to get a microphotometer tracing from photographs of the dark nebulae in Taurus; and while the result is not very satisfactory, the curve more nearly resembles Figure 3. I believe that more accurate observations will tend to confirm this result. The steep edges shown in Figure 3 are probably cut down by the decreasing thickness of the nebula and by the failure to obey our assumption that Rk is very large.

6. While the majority of cores in dark nebulae follow the general outlines of the nebula as depicted from their obscuring effect upon background stars, not all dark nebulae have cores. This is very clearly demonstrated by the lanes designated as Barnard 8 in Plate VI. If our explanation of the phenomenon of dark cores is correct, we must conclude that a lane which fails to show a dark core is, as a whole, inclined to the plane at right angles to the line of sight. The fact that there is a conspicuous core at B11, on the left side of B8, suggests that B8 is an elongated cloud, the nearer edge of which merges with B11 while the visible surface of the cloud extends toward the west and away from us.

7. In sections 4 and 5 we found that the observations favor a fairly large value of the spherical albedo, γ, and a phase function which throws most of the scattered light in the direction of the incident beam. A normal phase function of the Lambert, Euler, or Lommel-Seeliger type can only be allowed if γ is unreasonably large. It is difficult to estimate the uncertainty of this result. The amount and distribution of starlight may not be the same as that which is observed on the earth, although it is not probable that it will be materially different; the nebulae under consideration are not illuminated by nearby stars. The amount of the "terrestrial" background of the sky is rather uncertain, and so are the observations with the Fabry photometer. Nevertheless, there seems to be a rather definite tendency in nebular investigations to give a value of γ which is larger than that expected for ordinary spherical particles of rock. The albedos of the asteroids average about 0.1, while nebular particles give values ranging from about 0.5 to 1.0. This discrepancy does not necessarily mean that the material of the nebular particles is whiter than that of the asteroids. While in the latter we observe only the effects of diffuse scattering by

their surfaces, the particles of a nebula may be small enough to produce appreciable diffraction effects. In accordance with Mecke,[11] we may suppose that scattering by diffraction removes from the incident beam an amount equal to the cross-section of the particle. The total absorption coefficient is therefore $2N\pi\rho^2$. Of the total absorbed light, each cubic centimeter of the medium scatters one-half as diffracted light. The other half is partly transformed into heat, and only the fraction $\gamma N\pi\rho^2$ is scattered in accordance with the law of Lambert. If we consider only a single scattering process characterized by the phase function $\varphi(\alpha)$, the spherical albedo γ is an average between the ordinary value and unity—the latter representing the 100 per cent efficiency of the diffraction process.

8. One of the most interesting features of diffuse galactic nebulae, and one which suggests a definite phase effect, is the frequent occurrence of bright rims which partly surround dark masses of nebular material apparently projected against the structure of the bright nebula. The best known rim of this type is seen surrounding the Horse-head nebula, B33, from the northwest through the west and as far as the southwest. This rim does not belong to the underlying structure of the bright nebula IC 434.

Table 3 gives a list of the more conspicuous rims observed. It is very striking that, while many dark markings fail to show the rim effect, those that do show it always exhibit an exceedingly narrow crescent, often not more than 0.01 to 0.02 of the radius of the dark cloud in width. The transition along any such radius from dark to bright is exceedingly sudden. At the outer edge of the rim the brightness usually fades out more gradually. Wherever there is a definite symmetry in the underlying nebula, as in NGC 6523 or NGC 6514 (Trifid nebula), the brightest portion of each rim is in the direction of the exciting star. This alone proves that the dark clouds with their rims form a part of the bright diffuse nebula upon which they are seen projected. Most of these dark objects seem to be somewhat closer to us than the exciting stars; but the difference in distance cannot be very great, because in most cases the dark clouds are not completely black but exhibit varying degrees of illumination.

It is most surprising that the spectra of the nebulae exhibiting

[11] *Ann. d. Phys.*, **65**, 265, 1921.

bright rims are always of the emission type. Table 3, in which the nebular types are taken from Hubble, contains only one exception: IC 1274 a, c, is listed by Hubble as having a continuous spectrum,

TABLE 3

LIST OF BRIGHT RIMS*

Nebula	Exciting Stars	Sp. of Star	Sp. of Neb.	Description of Rims	Source
IC 434	ζ Orionis σ Orionis	Bo Bo	E	Excellent rims on the northwest, west, and southwest edges of B33 (Horse-head nebula), of the bay nebula near BD − 2°1343 and of the small bay nebula 6′ farther north. The entire structure of IC 434 may be considered as a rim of the large dark nebula to the east	J. C. Duncan *Ap. J.*, **53**, 392, 1921
NGC 6523 = M8	Cluster	Oe5 Bo	E	Several fine rims pointing toward exciting stars	Ross, *Ap. J.*, **77**, 246, 1933 Duncan, *Ap. J.*, **51**, 4, 1930 De Kerolyr, *L'Astronomie* **48**, 536, 1934
NGC 6611 = M16	Cluster	Oe5	E	Several fairly bright rims pointing toward brightest stars in cluster	Duncan, *Ap. J.*, **51**, 7, 1920
NGC 6514 = M20	−23°13804	Oe5	E	Several excellent rims in the southern part of the Trifid nebula pointing toward the exciting star	Duncan, *ibid.* **57**, 142, 1923
NGC 1977	c′ Orionis	B1	C+E	Fairly well-defined bright border around dark bay north of bright nebula; points toward c′ Orionis	Duncan, *ibid.*, p. 138
NGC 7000	α Cygni?	A3p	C+E	Several bright rims pointing west and north	Duncan, *ibid.*, p. 147
Nebula preceding NGC 7000	α Cygni?	A3p	E	Several faint rims surrounding dark nebulae	Duncan, *ibid.*, **63**, 122, 1926
IC 1274 a, b	−23°13997 −23°13998	B1 B1	c c	North rim of B91	Barnard, *Atlas*, No. 30
IC 1396	+56°2617	Oe5	e	Excellent border surrounding dark nebula covering stars +56°2598, +56°2604. Points toward +56°2617, if rim is considered to belong to dark (and not to bright) nebulosity	Barnard, *ibid.*, No. 49
NGC 1976	Trapezium	Oe5 Bo	E	Several confused rims	Ritchey, *Yerkes Pub.*, **1**, 389, 1903

* The original plates show numerous fine rims which are lost in the published reproductions.

but this was merely inferred by him from the spectrum, B1, of the exciting stars. The nebular spectrum proper has not been observed. It is quite possible that the spectral types of the stars are slightly in error and that the nebular spectrum is of the emission type. All

other nebulae listed in the table, except IC 1396, have been observed spectroscopically to contain emission lines. IC 1396 is excited by the Oe5 star +56°2617, and there can be no doubt that its spectrum is also of the emission type.

We conclude that the rims are strongest when $\epsilon = 90°$, and are absent when $i = 90°$. It is also obvious that we are not dealing with a normal phase effect, since the probability of observing so many objects at $i \approx 180°$ is too remote. Rather should we conclude from the symmetry of the structure of such nebulae as NGC 6523 that in most cases $i \approx 90°$. It is perhaps not an accident that rims are most often observed at rather large angular distances from the exciting stars.

If we retain the theory of scattering in spite of the fact that the spectra of these nebulae show emission lines, we are confronted with the fact that the illumination of an opaque spherical cloud of particles, according to the Lommel-Seeliger law, does not lead to very narrow rims except for i near 180°.[12] The same is, of course, true in the case of Lambert's law.

Perhaps we can find an explanation of the rims if we return to the derivation of the original Lommel-Seeliger formula. Following the original procedure of Seeliger, we shall assume that the absorption coefficient for the incident beam is k_1, while that for the scattered beam is k_2. Then:

$$I = \mu L\varphi(\alpha)\,\frac{\cos i}{k_1 \cos \epsilon + k_2 \cos i}\left[1 - e^{-R(k_1 \sec i + k_2 \sec \epsilon)}\right]. \qquad (3)$$

Let us now assume that k_2 is very much smaller than k_1. Then, if $R(k_1 \sec i + k_2 \sec \epsilon)$ is very large, we may write

$$I = \frac{\mu}{k_1} L\varphi(\alpha)\,\frac{\cos i}{\cos \epsilon + \dfrac{k_2}{k_1}\cos i}.$$

If $k_2/k_1 = 0$, we have $I \propto (1/\cos \epsilon)$, which is exactly the effect observed in the bright rims. If k_2/k_1 is very small, but not equal to zero, the rim will be less pronounced: for $\epsilon = 90°$,

$$I = C\,\frac{k_1}{k_2}.$$

[12] *Ibid.*, p. 74.

If $k_1/k_2 = 100$, the rim is already very greatly enhanced over the one which is shown in Figure 3 for Schoenberg's formula. The third column of Table 2 gives the reciprocals of cos ϵ which would apply to the case $k_1 = 0$.

Our explanation of the bright rims finds its most interesting confirmation in the consequences of Zanstra's theory of nebular radiation. It is now generally recognized that the absorption coefficient of a nebula for ultraviolet starlight beyond the Lyman limit is very large. After this radiation has been converted into visible radiation consisting largely of the Balmer lines and of the stronger forbidden nebular radiations, the absorption coefficient is greatly reduced[13] and the observed light passes relatively freely out of the nebula. Dr. Chandrasekhar has called my attention to the fact that it is not legitimate to put $k_2 = 0$. This is, of course, also shown by the observations: thus, B33 is not transparent to the visible light of IC 434 beneath it. But it is probably correct to assume $k_2 \ll k_1$. It is entirely possible that the ratio k_2/k_1 is not the same for all emission lines. It may be smaller for the forbidden nebular lines than for the Balmer lines. This suggests some interesting observational tests, which will, however, be difficult because of the faintness of the nebulae.

The physical interpretation of the phenomenon is rather simple. Since k_1 is large, the incident starlight penetrates to a small depth into the nebula. But k_2 is small; hence we can see into much deeper layers of the nebula, provided the layers are excited to luminosity by the incident radiation. For $\epsilon = 0$ our ability to penetrate to great depth yields us nothing because the exciting light, even for small values of i, fails to reach the deeper layers. For $\epsilon = 90°$, however, we look lengthwise through a narrow edge, all of which is reached by the exciting radiation and through which we can see to great depths because k_2 is small.

It is interesting to realize that from the photometric theory alone we could have concluded that $k_2 \ll k_1$ and that the visible radiation of the nebula is of an entirely different nature than the incident light from the star.

We still have to explain the gradual diminution in surface bright-

[13] Rosseland, *Theoretical Astrophysics*, p. 324, 1936.

ness of the rims as we pass along a radius away from the center of the dark cloud. This effect is probably due to the fact that at the extreme edge of a cloud, $R(k_1 \sec i + k_2 \sec \epsilon)$ in (3) can no longer be considered large. If it is small, we may expand the exponential[14] and use only the first term:

$$I = \mu RL\varphi(a) \frac{1}{\cos \epsilon} .$$

But this expression holds only for a nearly transparent plane-parallel nebula, in which $R/\cos \epsilon$ is the distance along the line of sight from the nearer to the farther surface. The relation between I and $1/\cos \epsilon$ is due to the increased path within the nebula, if observed slantwise. In a spherical nebula the factor $R/\cos \epsilon$ should be replaced by $2R_0 \cos \epsilon$, where R_0 is the radius. Accordingly, I decreases toward the edge of a transparent nebula with $\cos \epsilon$. This may even be accentuated by a decrease in nebular density toward the edge—a phenomenon accounted for in our formula by the factor μ which contains N, the number of particles per unit volume.

9. Two very remarkable bright nebulae appear in one of the most opaque parts of the dark cloud in Taurus. They are shown as B10 ($a = 4^h11^m.0$, $\delta = +28°.0$) and B14 ($a = 4^h32^m.3$, $\delta = +25°.5$) in Barnard's *Atlas of Selected Regions of the Milky Way*. Both nebulae are also shown in Plates IV–V. B10 is illuminated by a star of photographic magnitude about 15. The radius of the nebula is approximately 5′. It is evident that these values are not in agreement with Hubble's expression[15]

$$m_* + 5 \log a = 11 .$$

In order to satisfy the formula the star should have a magnitude of 7.5. Since the nebula exhibits little structure, it is not probable that the star is reduced in brightness by intervening clouds. The dimming of the starlight probably takes place in the nebula itself.

B14 has no star brighter than photographic magnitude 17. The radius $a = 1'.3$. Hence to satisfy Hubble's formula we should have

[14] Schoenberg, *op. cit.*, p. 36.

[15] Struve and Story, *Ap.J.*, **84**, 208, 1936.

$m_* = 10.5$. Evidently in this case the star is also dimmed in the nebula by 6 or 7 mag.

In both of these objects we are probably dealing with exceptionally dense and thick nebulae. The stars are so deeply imbedded in nebular material that only a small fraction of their light manages to penetrate. If τ is the optical thickness, the fraction $e^{-\tau}$ of the original starlight is observed. The diffuse light of the nebula, on the other hand, has a better chance to survive. If the nebular particles were perfectly white, so that $\gamma = 1$, the total light of the nebula would obviously be $1 - e^{-\tau}$. If γ is not equal to 1, the problem is more complicated. The analogous case of a planetary nebula has been solved by Chandrasekhar.[16] The problem of dense reflection nebulae is now under investigation by Dr. Henyey.

YERKES OBSERVATORY
February 19, 1937

[16] *Zs. f. Ap.*, **9**, 266, 1935.

A PHOTOELECTRIC STUDY OF THE LIGHT FROM THE NIGHT SKY*

C. T. ELVEY AND F. E. ROACH

ABSTRACT

Observations of the light from the night sky have been made with a recording photoelectric photometer. Records covering the entire hemisphere were made in about one hour. Observations were obtained at different hours of the night and at different seasons of the year, in order to determine the distribution of the various sources of radiation coming from the night sky.

Observations of certain regions of the sky were reduced by analytical methods to evaluate the unknowns. All of the tracings, however, were reduced by a graphical method, in which all radiations having similar distributions over the sky were grouped with respect to their co-ordinate systems.

Isophotes have been constructed for the zodiacal light, arranging the observations into four groups. There is a seasonal variation in the zodiacal light which might be interpreted as resulting from a cloud of meteoric particles which are in conjunction with the sun during the late winter months.

An analysis of the light associated with the galactic system shows that after the effect of the stars has been removed there is an excess of light, which we shall call the galactic light, and which is probably produced by the scattering of starlight by interstellar matter. It also includes the galactic nebulae. The mean amount of galactic light at latitude 0° is equal to 57 stars of the tenth photographic magnitude, or is equivalent to 5.6 mag. per square degree.

Applying a theoretical discussion of scattering by Struve, it is found that the spherical albedo is probably large and that in the galactic plane the medium is opaque.

The light from the night sky is composed of radiations coming from many sources, which we may enumerate as follows: direct starlight, scattered starlight, light originating in the upper atmosphere, which is termed the "permanent aurora," the polar aurora, the zodiacal light, light from galactic sources, which is probably starlight scattered by dust particles in interstellar space, and light scattered by our atmosphere from all these sources, as well as light scattered from terrestrial sources.

The distribution of the component radiations over the sky varies with each source, and consequently the photometric study of the light from the night sky offers a rather complex problem. The intensity is a function of so many variables that an analytical solution for the various components is impossible. However, with the aid of approximations and with observations obtained under certain con-

* *Contributions from the McDonald Observatory, University of Texas*, No. 3.

ditions it becomes possible to separate the various distributions and to determine them with some certainty.

The problem of the light from the night sky may be attacked in three ways, namely, by spectroscopy, by studies of polarization, and by photometry.

The spectroscopic results have been summarized recently by Georges Déjardin.[1] The emission spectrum of the night sky has received the most attention, since the feeble radiations are confined to narrow bands of wave-lengths and consequently are photographed much easier than is a continuous spectrum of the same total intensity. Déjardin discusses three regions of the spectrum—the visual, the photographic, and the ultraviolet. In the visual region the most prominent feature of the spectrum of the night sky is the green auroral line. In the photographic region, the one in which our work has been done (since our photometer contains a potassium photoelectric cell), a large number of radiations have been identified, mostly from the molecule of nitrogen. The most intense radiations are the Vegard-Kaplan bands of nitrogen, which have an excitation of 6.1 volts. Next in intensity are the bands from the first and second positive systems of nitrogen, with excitations of 7.4 and 11.0 volts, respectively. The fainter radiations are identified with those of the negative bands of nitrogen, the excitation potential being 19.6 volts. The relative intensities of these radiations from the night sky are exactly the reverse of those observed in the polar aurora. In the ultraviolet region of the spectrum of the night sky, in addition to the emissions, there is a continuous spectrum with absorption lines.

The foregoing studies are from spectrograms taken in regions of the sky where the zodiacal light or the Milky Way are not bright. The spectrum of the zodiacal light has been observed by E. A. Fath,[2] who found it to be like that of the sun, showing that it is scattered sunlight. Fath has also observed the spectrum of the integrated light from the Milky Way and found it to be of the solar type.

J. Dufay[3] has applied polarization methods to the study of the

[1] *Rev. Mod. Phys.*, **8**, 1, 1936.

[2] *Bull. Lick Obs.*, **5**, 141, 1909.

[3] *Bull. L'Obs. Lyon*, **10**, No. 9, 1928.

light from the night sky. The light originating from the upper atmosphere by emissions from atoms and molecules does not show polarization; but, on the other hand, the light scattered by the meteoric particles producing the zodiacal light should be polarized. Dufay has measured the amount of the polarization both in the intense parts of the zodiacal light and in the regions of the sky away from the ecliptic, and has shown that a part of the light over the entire sky can be attributed to an extension of the zodiacal light over those regions.

The third method of studying the light from the night sky, the photometric, has been used by P. J. Van Rhijn,[4] who made a long series of observations at Mount Wilson in 1913. The instrument employed is one described by L. Yntema.[5] The observations were made visually by comparing the background of the sky with a screen illuminated by a known source of light. Calibrations were obtained from observations of stars, with the aid of an artificial star. The observations were made in circles parallel to the horizon, and each series was compared with the light from the sky at the North Pole. This comparison was necessary since there are rather large and irregular variations in the amount of light from the North Pole, presumably caused by the variation in the intensity of the permanent aurora.

An inspection of Van Rhijn's table of observations shows that about eight points of the sky can be observed per hour; thus, to cover the entire sky with sufficient detail requires many hours of work. With the changing intensity of the auroral light it is quite possible that a considerable amount of uncertainty will enter into the observational data.

J. Dufay[3] has made extensive photometric investigations of the light from the night sky, particularly that coming from the region of the North Pole. He has used both a visual photometer, comparing the light from the sky with an illuminated screen, and a photographic method described by Charles Fabry[6] in 1910. The Fabry photometer is excellent for detailed studies of regions of the sky and gives precise results. However, in conducting an extensive survey of the

[4] *Pub. Astr. Lab. Groningen*, No. 31, 1921.

[5] *Ibid.*, No. 22, 1909.

[6] *C.R.*, **150**, 272, 1910.

sky, it has the same disadvantage as the visual observations, namely, it takes from 5 to 8 minutes to obtain a single observation.

In the photometric analysis of the light from the night sky we may take the brightness of a given region of the sky to be the sum of the intensities of the individual radiations as mentioned above:

$$B_0 = \frac{S}{F(z)} + \frac{A\varphi(z)}{F(z)} + \frac{ZL}{F(z)} + \frac{X}{F(z)} + S_T \times Sc(z) + T \times Sc(z) , \quad (1)$$

where all of the intensities are expressed as numbers of stars of the tenth photographic (or photoelectric) magnitude per square degree, and where B_0 is the observed brightness of a given region of the sky, S is the intensity of the direct starlight, A is the intensity of the permanent aurora at the zenith, $\varphi(z)$ is the law of variation of the permanent aurora with zenith distance, $F(z)$ is the extinction factor, ZL is the zodiacal light at the observed region, X is the unknown galactic radiation, $Sc(z)$ is the law of variation of scattering with zenith distance, and T is the total auroral, zodiacal, and galactic light over the hemisphere. The general solution of equation (1) is readily seen to be impossible. However, by a reasonable choice of assumptions and observing conditions the unknowns may be determined.

The contribution to the light from the night sky by the stars can be determined by star counts. However, such data are not available for all regions of the sky, and for the present we shall use the mean star counts as summarized by K. F. Bottlinger.[7] The deviations from the mean number of stars for regions of the sky at galactic latitudes greater than, say, 30°–40° will be small, and for the purposes of the present investigation we may neglect them.

The determination of the extinction factor, $F(z)$, has been made with the photoelectric photometer from observations of bright stars. For zenith distances less than 75° the factor varies as sec z, but at larger zenith distances the extinction deviates from the secant law. Our observations agree quite well with Bemporad's extinction theory.[8]

The intensity of the auroral light at the zenith, corrected for extinction, is no doubt a function of the physical state of the upper

[7] *Zs. f. Ap.*, **4**, 370, 1932. [8] *Handbuch d. Ap.*, **2**, Part 1.

atmosphere. There is little doubt that it varies with time, as observations of the integrated light from a region around the North Pole by Lord Rayleigh[9] and others show diurnal, seasonal, and long-period variations. Since it was necessary to make a series of observations over several hours in order to determine the law of variation of auroral light with zenith distance, we have assumed that a correction can be made for the diurnal variation from simultaneous observations of the light from a region of constant zenith distance, namely, the North Pole.

Van Rhijn[4] has developed an expression for the variation of the auroral light with zenith distance, the function $\varphi(z)$ in equation (1). He assumes that the light originates in a layer rather high in the atmosphere, that the layer is uniform over the region from which the observations are made, and that the light received from this layer is proportional to the thickness of the layer in the line of vision. The height to the layer is called h, which is expressed in units of the radius of the earth and is small in comparison with the latter. The thickness, ϵ, is assumed to be small enough so that in the development of the function the squared terms in ϵ are negligible. The resulting expression for the function is

$$\varphi(z) = \frac{1}{\sqrt{1 - \dfrac{\sin^2 z}{(1+h)^2}}}. \qquad (2)$$

This function reduces to sec z when the value of h is taken as zero.

It is seen that the intensity of the auroral light, $A\varphi(z)$, increases toward the horizon, the rate of increase being greater for smaller values of h, the height to the auroral layer. Since the extinction is produced by the atmospheric layers between us and the auroral layer, its variation with zenith distance will be more rapid than the increase in the thickness of the auroral layer; consequently there will be a tendency for the extinction to overcome the increase in the intensity of the auroral light toward the horizon. This produces a maximum of intensity of the auroral light a few degrees above the horizon, which we have noticed visually many times.

The zodiacal light is a function of the difference in longitude be-

[9] *Proc. R. Soc.*, Ser. A, **151**, 22, 1935.

tween the observed point and the sun, and of the latitude of the point. Numerous observations by visual observers, and our own records with the sky photometer, show that the zodiacal light is not symmetrical with respect to the ecliptic, the axis being as much as 5° north of the ecliptic. The work of both Van Rhijn and Dufay show that the zodiacal light is not merely confined to the region of the ecliptic but extends over the entire sky. Van Rhijn attributes a rather large portion of the light of the night sky to zodiacal light, while the studies of Dufay using polarized light indicate a much smaller percentage.

The quantity listed as unknown galactic radiations includes the diffuse galactic nebulae and any scattered light coming from interstellar matter. It is probable that this light is concentrated in low galactic latitudes and may be neglected at the higher ones.

The scattered light from all sources may be classed together, since we use the same scattering function, namely, that determined by C. G. Abbott[10] from observations made at Mount Wilson. However, since we have a value for the total number of stars, we shall correct our data for scattered starlight before proceeding with the analysis of the observations. In correcting for the scattered starlight, we make the assumption that the stars are distributed uniformly over the hemisphere; and we have modified Abbott's values of scattering in accordance with the wave-lengths of light used by us, namely, those of the photographic region.

The total auroral, zodiacal, and unknown sources of light which are scattered are grouped together as one term, T. Again, the assumption is made that they are distributed uniformly over the hemisphere.

Under the assumptions we have made, there remain four unknowns for which we must solve: A, the intensity of the auroral light at the zenith; ZL, the zodiacal light at the point in question; T, the total light (other than from stars); and h, the height to the auroral layer. Since the height to the auroral layer enters into the function $\varphi(z)$ in a rather complex manner, it is much easier to solve for it by approximations, thus leaving three unknowns.

[10] *A.J.*, **28**, 129, 1914.

PLATE VII

THE PHOTOELECTRIC SKY PHOTOMETER OF THE McDONALD OBSERVATORY

APPARATUS AND METHODS

A photoelectric photometer of the recording type was constructed for the purpose of making a comparatively rapid survey of the sky, thus eliminating one of the objectionable features of the visual observations. A series of tracings covering the entire sky could be made in about one hour. The sky photometer is shown in Plate VII. It is mounted on a table rotating on the vertical support, thus making it possible to observe in all azimuths at a given altitude. The lens forming the image of the sky on the photo-electric cell has its axis in the horizontal plane. By means of a mirror placed at an angle of 45° to the axis, light may be reflected into the photometer from any altitude. The photometer tube, a large brass cylinder, contains the Kunz photoelectric cell at one end and the amplifying tube, Pliotron FP-54, of the General Electric Company, in a compartment at the other end. The amplifier is of the balanced circuit type designed by Du Bridge and Brown.[11] The amplifying tube, with its grid resistor (4×10^{10} ohms), is located in the photometer tube, as near to the photoelectric cell as is possible. The remaining parts of the circuit are in the metal box shown on the table and are connected with the photometer by a shielded cable. The high-potential batteries for the photoelectric cell and the storage batteries for the amplifier circuit are in the box immediately behind the control box.

The output of the amplifier is measured with a Leeds and Northup high-sensitive galvanometer, the period being 1 second and the current sensitivity 5×10^{-9} amperes per millimeter at 1 meter. The deflections of the galvanometer are recorded with a beam of light from a motion-picture exciter lamp for sound reproduction which is reflected from the galvanometer mirror to the recorder mounted on the vertical support of the photometer. The recorder consists of a shield with a horizontal slit, and directly behind the shield is a holder containing bromide paper. The holder is connected by a pulley system to the photometer so that it is lowered past the slit as the photometer is rotated. The motion of the bromide paper is such as to make half a millimeter on the tracing equal to 1° of azi-

[11] *Rev. Sc. Instr.*, **4**, 532, 1933.

muth. Mounted at one end of the slit is a small light which is connected with contacts on the photometer so that the light is flashed as the instrument passes the cardinal points, thus giving the orientation. A check on the orientation is obtained by making tracings across Polaris and other bright stars.

A typical tracing is shown in Figure 1, a reproduction of a run made at a zenith distance of 70° on the morning of November 9, 1934. The tracing shows the zodiacal light in the east, the Milky Way, and several stars of medium brightness. The zero tracing shown at the bottom of the figure is placed on each sheet, inasmuch as it shows a departure from a straight line. The procedure is to make a short zero tracing with the photometer to the north, then open the shutter and make the circuit of the sky, and close the shutter and reverse the run to make the complete zero tracing. The apparently sinusoidal variation in the zero tracing was found to be due to the insufficient magnetic shielding of the Pliotron tube from the earth's magnetic field. Throughout any one night the zero tracings were reasonably constant; however, from night to night there were slight differences in amplitude, although the shape of the curve was the same.

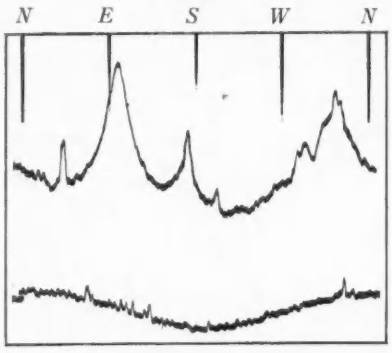

FIG. 1.—A tracing made with photoelectric photometer on November 9, 1934.

The observations consist partly of tracings covering the entire hemisphere and partly of a series of observations of individual regions of the sky for the purpose of determining the variations of the auroral and scattered light with zenith distance. Observations were taken for the purpose of calibrating the instrument, as well as for the determination of the extinction factor. All observations were made long enough before or after the rising or setting of the sun or moon so that no scattered light from these sources would interfere with the results. The observing station was near Mount Locke in the Davis Mountains, at an altitude of 6200 feet; and the distance to the nearest source of terrestrial illumination was 10

miles to Fort Davis, Texas, a small town without street lights and hidden at a lower altitude, behind the mountains. The nearest towns with street lights were: Alpine, 32 miles, Marfa, 26 miles, and Pecos, about 60 miles, all hidden from view by the mountains.

The observations were made on the best photometric nights; and if any change was seen in the appearance of the sky, it was noted in the records.

The normal procedure in securing a set of tracings of the sky was to observe a number of standard stars and regions of the sky before and after taking the set. The tracings were usually taken at zenith distances of 75°, 70°, 60°, 50°, 40°, and 30°. In general, it was our intention to obtain a series of observations for the evening and for the morning portions of the sky, each dark of the moon; but this was not always possible. Other series were taken at definite orientations of the sky in order to obtain the zodiacal light or the Milky Way under better conditions. At sidereal time 12^h40^m the Milky Way is practically on the horizon in our latitude, with the result that most of the entire set of tracings can be used to study the zodiacal light. For the study of the galactic light, tracings were taken when the Milky Way passed through the zenith near midnight, when the zodiacal light is weak. At the same time the plane of the Milky Way is nearly vertical, and the tracings are thus crossing the Milky Way at right angles. The auroral light for each tracing is constant, and the variation of intensity is practically all due to variation in galactic light.

To determine the extinction factor, observations were made on bright stars, α Lyrae, α Aquilae, α Virginis, and others, over a large range in zenith distance. Since the photometer received light from a large region of the sky around each star, it was necessary to obtain observations of the sky background on either side of the star. These background observations also gave data for studying the variation of the auroral light with zenith distance.

Additional observations of given regions of the sky over a large range in zenith distance were made for use in solving equation (1). The regions chosen were those for which star counts could be had, such as certain selected areas at high galactic latitudes. Two of the principal regions used were areas 52 and 58. Also, observations were

made of the north pole of the ecliptic. Throughout a series of observations, we observed the light from the North Pole at regular intervals in order to obtain a correction for the diurnal variations of the auroral light.

An examination of equation (1) shows that the observations taken near the horizon will have by far the greatest weight, and will be the ones determining the accuracy of the solution. Also, the observations made near the horizon will be subject to larger observational errors caused by small amounts of haze. For these reasons it seems best to combine observations of various regions of the sky into one least squares solution. This introduces the question of the variation in the amount of zodiacal light from place to place, as well as of the galactic light, when the observations are near the Milky Way. We have made corrections for these variations by reducing all observations to one region of the sky by the following empirical method. We made a diagram of the sky brightness plotted against zenith distance, drawing a smooth curve through the observations for each region of the sky. We then interpolated for the brightness of that region at any given zenith distance—say that of the North Pole. Under our assumption, the auroral light will be the same for a given zenith distance, as will also the scattered light. The variations in these brightnesses from different regions of the sky can be interpreted as being due to differences in zodiacal light and galactic light. From these data we can reduce all of the observations to one region of the sky, thus giving a larger number of points to be used in the least squares solution of equation (1).

As mentioned above, the function $\varphi(z)$ in equation (2) contains an unknown, h, the height to the auroral layer; but since it enters the function in a rather complex manner, it is necessary to solve for it by some other method than least squares. We have assumed values of h varying from 0.00 to 0.03. With each, a least squares solution was made for the other unknowns, from which we determined the residuals. The assumed values of h were then plotted against the sum of the squares of the residuals, and the point of minimum gives us the best value of h.

We have made analytical solutions of the foregoing equation for data from two nights in which there was considerable difference in

extinction, principally to guide us in the graphical evaluation of the major portion of our data to be described below. The values of h determined for these two nights are shown in Figure 2. The data for February 21, 1936, give a sharp minimum at a value of h equal to 0.008, or about 50 km; while the data from the night of October 2, 1935, give a broad minimum at 0.01, or 65 km.

These heights are somewhat lower than the minimum height usually observed for the polar aurora, that is, 80 km. No doubt we should expect the layer of the permanent aurora to be located in a different region of the atmosphere than the polar aurora, since there is a marked difference in the relative intensities of the radiations in the two spectra. It is also of interest to note that the observed heights of the auroral layer are somewhat lower than the height found for maximum frequency of meteors, which is also about 80 km.

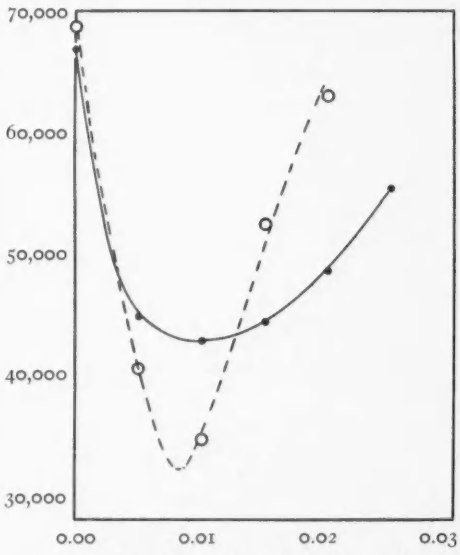

FIG. 2.—Graphical solutions for h, the height to the auroral layer. Abscissae are the values of h, and ordinates are sums of the squares of the residuals. The dots are for observations made on October 2, 1935; and the circles are for February 21, 1936.

Since the radiation known as the permanent aurora must originate in a region where the atoms or molecules are in an excited state, it is tempting to assign them to the region of the Kennelly-Heavyside layer. However, measurements made of the virtual heights to this layer (or layers, as we know now) show them all to be greater than that we have found for the auroral layer. The ionosphere is composed of several layers, and the height of each may be determined by the reflection of radio signals. Measurements show that the lower, or E layer, is 100–120 km in height, the F_1 layer, 200–230 km; and the F_2 region, about 240–500 km.[12] These meager data indicate

[12] *J. Res. Nat. Bur. Stand.*, **17**, 323, 1936.

that the auroral layer is considerably beneath the layers which reflect radio waves. It is impossible for us to draw definite conclusions from only two observations compared with the mean. It might be desirable to obtain simultaneous observations of the heights to the auroral layer and to the lower ionospheric layer.

The details of the solutions for the two nights of observations will not be given. The evaluation of the unknowns, A, ZL, and T, in the solution giving the best values of h is shown in Table 1. The agreement is closer than might be expected, except for T, the total light. The large value of T for October 2 is no doubt due to our failure to allow for an increase in the numerical value of the scattering function for a different value of the extinction. We have asumed that the variation of scattering with zenith distance is the same for each night; and consequently, the quantity T contains a factor which represents the variation in the scattering coefficient.

TABLE 1

Date	A	ZL (Pole)	T
Oct. 2, 1935.....	133	57	11.3×10^6
Feb. 21, 1936.....	136	45	8.0×10^6

The analytical solution has been applied only to the observations of individual regions of the sky. The majority of our observations are tracings which recorded the brightness of the sky in a circle parallel to the horizon. The reduction of these observations by an analytical method would be rather tedious; and since we are especially interested in studying the light which may originate from scattering in the galaxy, we have used a comparatively rapid graphical method. We shall group as units the sources of light whose distributions over the sky are functions of the same co-ordinate systems, that is, the alt-azimuth, the ecliptic, and the galactic co-ordinates.

We may best illustrate the method by following the reductions of an example. For this we shall take the observations of the evening of January 27, 1935, which afford a good example of the method we use in correcting for the aurora and for scattered light. Unfortunate-

ly, the tracings for this night were somewhat fogged by light during development and are not suitable for reproduction. The tracing in Figure 1, however, is typical; and we may refer to it. The abscissae of the tracings are azimuths, and the ordinates are deflections of the galvanometer. The lower tracing is that of the zero (no light on the cell), which, as mentioned before, is not a straight line, because of the influence of the earth's magnetic field. The rather sharp deflections in the zero tracing which are also present in the tracing for the sky are probably produced by ionization by cosmic rays in the air in the vicinity of the photoelectric cell and the amplifying tube. A. E. Whitford[13] found that it was necessary to evacuate the cell and the tube chamber in order to eliminate this unsteadiness. We decided against the evacuation of the apparatus because the equipment was in the field and because we were able to recognize the sporadic deflections on the tracings and to draw smooth curves to eliminate them. This is the first step in the reduction of a tracing. The next step is the elimination of the effects of the bright stars. A small celestial globe was set in the corresponding position of the sky at the time the observation was made, and with the aid of a spherical protractor and a knowledge of the size of the field of view of the photometer, about 9 square degrees, we could easily identify the deflections due to the brighter stars. All individual stars brighter than the third magnitude are eliminated with certainty.

After having drawn a smooth curve through the tracing, which represents the sky background, we next measured the tracing with the aid of a millimeter *réseau*, recording the deflection at every 5° of azimuth. The azimuth scale of the tracing was constructed so that each millimeter equals 2°.

Having measured the tracing, we must convert the deflections of the galvanometer into known units of intensity, which are numbers of stars of the tenth magnitude per square degree. We do this with the aid of the bright stars used for calibration and extinction determinations. We did not have accurate photoelectric magnitudes for these stars, and the photographic magnitudes were not satisfactory, many of them having been determined by applying the

[13] *Ap. J.*, **76**, 213, 1932.

mean color index of each spectral class to the visual magnitude. We have thought it best to apply the photoelectric colors of the individual stars to the visual magnitudes, which has given us fairly consistent results. For the photoelectric colors we have used the measures by K. F. Bottlinger[14] and W. Becker,[15] and the visual magnitudes are those of the *Harvard Revised Photometry*. We have checked the resulting magnitudes with our observations by comparing the standard stars with Polaris and applying a correction for the variation in light of the latter. The photoelectric magnitudes are not accurate enough to be listed as such but are sufficient for the purpose of this investigation.

The co-ordinates of the points which have been measured are all in the altitude-azimuth system. It is necessary to know the positions expressed in the other systems, and for this we have used graphical or mechanical methods of conversion. In changing from right ascension and declination to galactic co-ordinates, we have used the tables computed by P. Emanuelli.[16]

The observed intensities have all been corrected for the intensity of the direct starlight by making use of the tables of mean numbers of stars for various galactic latitudes by K. F. Bottlinger.[17] He has expressed his data in units which are numbers of tenth-magnitude stars per square degree. To make this correction it was necessary to take into account the extinction, which has been determined for each night from the observations of the standard stars. As mentioned before, this correction for direct starlight has been applied for all galactic latitudes; but the mean data are rigorous for latitudes greater than 30° or 40°.

A correction is applied, also, for the scattered starlight. The law of scattering with zenith distance is that determined by G. C. Abbott,[10] and the numerical value has been adjusted to the region of the spectrum to which the photoelectric cell is sensitive, namely, about 4500 A, assuming that the scattering is primarily according to Rayleigh's law. This is probably very close to the truth, since we have observed only on the best photometric nights; and at this

[14] *Veröf. Berlin-Babelsberg*, **3**, Part 4, 1923.

[15] *Ibid.*, **10**, Part 3, 1933.

[16] *Pub. Spec. Vaticana*, Ser. II, No. 14, 1929.

[17] *Zs. f. Ap.*, **4**, 370, 1932.

height above sea-level the sky is usually blue during the day, even near the horizon. As mentioned above, the additional assumption is made that the stars are distributed uniformly over the hemisphere; and we have taken for the total number of stars the value given by Seares, Van Rhijn, Joyner, and Richmond.[18] The correction for scattered starlight rarely, if ever, amounted to more than 4 or 5 per cent of the observed sky brightness.

After corrections have been applied for the direct and the scattered starlight, the data from each tracing parallel to the horizon are composed of a constant amount of auroral light (the so-called "permanent aurora"), a constant amount of scattered light, possibly a variable amount of polar aurora, and variable amounts of zodiacal light and radiations associated with the galaxy. Since we are primarily interested in determining the amount and distribution of the radiations associated with the galaxy, we can group the two sources of illumination which are functions of zenith distance and solve for the two together. This is readily done by a graphical method, since we can make the assumption that all the galactic radiations are at latitudes, say, less than 30° or 40°; and for higher latitudes the correction has been made for the stars. We are also reasonably certain that in the regions away from the sun, the variation of the zodiacal light over a short distance in longitude or latitude is rather small, and as a first approximation it may be considered constant. A part of the tracings for each zenith distance made on a given night cross the regions just mentioned, which lie in high galactic latitudes far from the sun. Within this region there should be a relatively constant amount of zodiacal light for which, as a first approximation, we can use the value determined for the North Pole or for the pole of the ecliptic.

The solution is best carried out by means of the diagram shown in Figure 3, which is a plot of the observed points on an equal area projection of the sphere. The co-ordinates are longitude and latitude. Every other observation has been omitted for convenience in making the illustration. The galactic equator is drawn, as are also the lines representing the limits of $\pm 30°$ galactic latitude. The observed intensity for each point is also given. By referring to Figure 3

[18] *Ap. J.*, **62**, 320, 1925.

it will be seen that the region north of the ecliptic at a longitude of 180° from the sun is far from the galactic plane, and that the vertical circles are roughly parallel to the circles of latitude. This will give

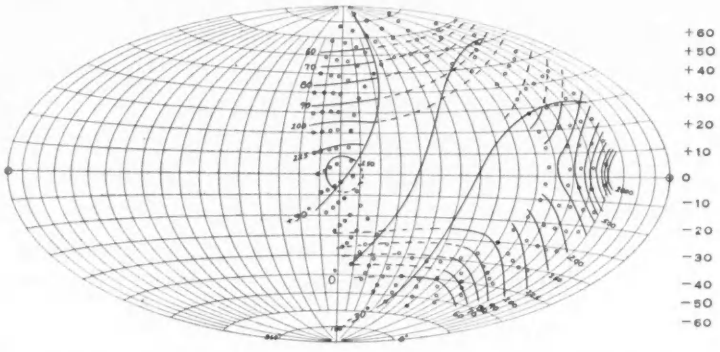

FIG. 3.—Plot of observations for January 27, 1935, to illustrate the method of determining the auroral and scattered light and the isophotes of the zodiacal light.

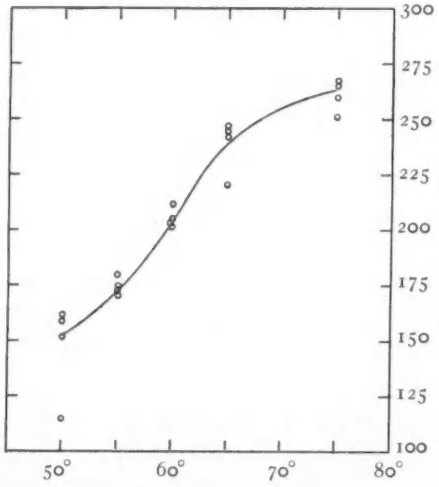

FIG. 4.—The variation of the aurora plus scattered light with zenith distance for the observations shown in Fig. 3.

a number of points at different zenith distances, while the zodiacal light remains roughly the same. Assuming values of the zodiacal light for the first approximation, we are able to plot the points corrected for the zodiacal light in Figure 4 with the corrected intensities

as ordinates and the zenith distances as abscissae. A smooth curve drawn through the points represents the variation of the sum of the permanent aurora plus scattered light. By correcting each set of observations on a circle parallel to the horizon by the respective amounts of auroral and scattered light, we obtain the values of the zodiacal light for the regions of the sky outside the limits of $\pm 30°$ galactic latitude. These isophotes are shown by the continuous

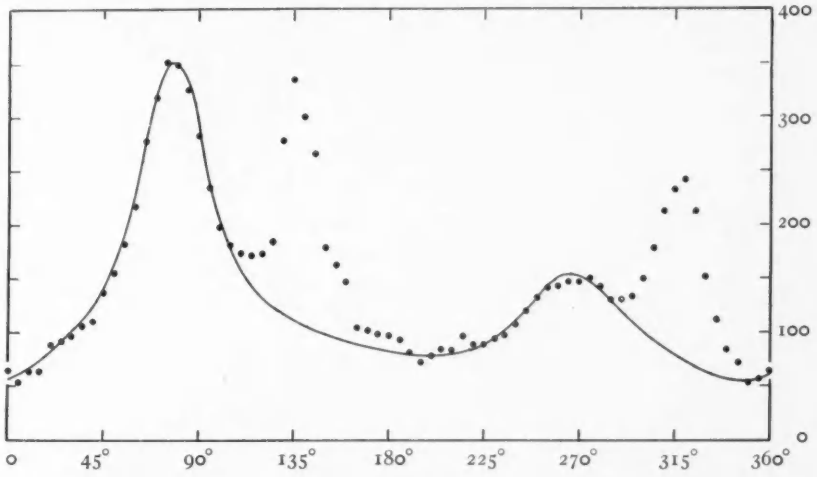

FIG. 5.—Plot of observations from one tracing made on January 27, 1935, after correction for auroral plus scattered light. The continuous curve shows the variation of zodiacal light obtained from Fig. 3. The difference between the points and the curve gives the galactic light.

lines in Figure 3. We can readily interpolate across the Milky Way for the intensities of the zodiacal light in that region.

Our data for any given tracing parallel to the horizon, corrected for scattered light plus auroral light, may then be plotted as in Figure 5, with the intensities as ordinates and the azimuths as abscissae. A continuous line is drawn through the points representing the intensity of the zodiacal light, obtained from Figure 3; and we can readily see that in crossing the Milky Way (azimuths 135° and 320°) there is an excess of light. This excess will be called the galactic light; it is caused by the deviations of the actual numbers of stars at each point from the mean for the corresponding galactic

latitude, by the light which originates in galactic nebulae, and by light scattered by interstellar matter.

THE POLAR AURORA

The plot of the observations made for the purpose of determining the galactic light sometimes (Fig. 5) shows an excess in the region of the north point. The polar aurora is very seldom seen at the latitude of Mount Locke. We have suspected occasionally that the northern horizon was slightly brighter than other regions, but at no time during our series of observations have we seen anything that might be called an auroral arch. However, on several of our tracings, as just mentioned, we have noticed an excess of light in the north which cannot be explained. In particular, the nights of January 25 and 27 and February 26 and 27 have shown a rather marked maximum around the north point for the tracings made at zenith distance 60° or greater. As a rule, the excess is larger for the tracing of greatest zenith distance and decreases with decreasing zenith distance. We have measured the point of maximum intensity on each of the tracings, and the mean is at azimuth 188° ±7° (m.e.). The azimuth of the magnetic north pole is about 192°.

THE ZODIACAL LIGHT

By the method described above we have obtained the isophotes of the zodiacal light for each night for which tracings have been made. On January 9, 1935, the set of observations was obtained when the Milky Way was on the horizon. This gave a good picture of the zodiacal light for the hemisphere. We made use of this information to reconstruct the regions of equal zodiacal light on other nights, in order to obtain the relationship of the auroral and scattered lights with zenith distance. It was soon evident that the zodiacal light was not constant with the seasons, and this night could be used as a guide for only a short interval. Other nights were chosen as we worked away from this date. It might be remarked that if our assumptions about the regions of equal zodiacal light were not exactly correct, we would obtain a scattering of the points. An empirical correction could be made if one tracing gave results consistently too high or too low with respect to the others.

The observations have been arranged in four groups. Figure 6

shows the data for six nights in November and December, 1934. Figure 7 is for six nights in January, February, and the first week in March, 1935. Figure 8 is for five nights in April and May, 1935, while Figure 9 contains the results for three nights in June and July, 1935.

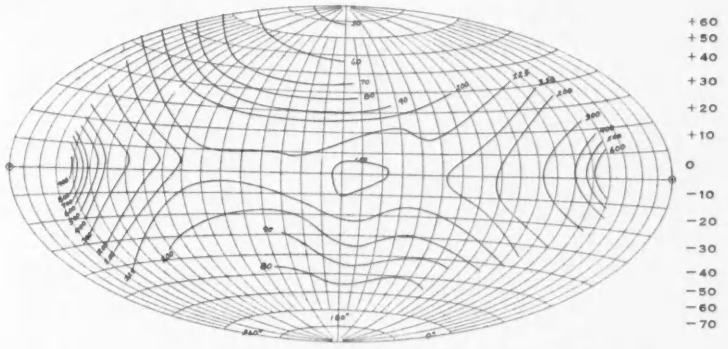

FIG. 6.—Isophotes of the zodiacal light for six nights in November and December, 1934.

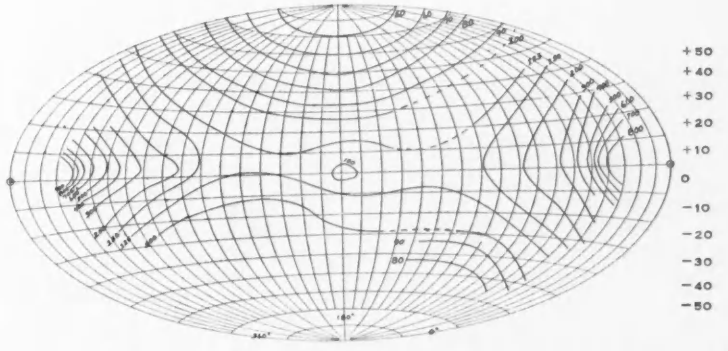

FIG. 7.—Isophotes for the zodiacal light for six nights in January, February, and March, 1935.

An inspection of Figures 5–8 shows the seasonal changes mentioned above. In November and December the evening zodiacal light was rather inconspicuous and the intensity increased toward the sun rather slowly, while the gradient of intensity for the morning zodiacal light was steeper. The isophotes for January and February show gradients of intensity with longitude of about the same order for the evening as for the morning light, with the morn-

ing light having a slightly greater intensity. In the figure for April and May we see that the evening zodiacal light has increased greatly, while that for the morning has decreased. The gradient has become quite steep for the evening light and distinctly weak for the morning light. The tracings for the months of June and July have the

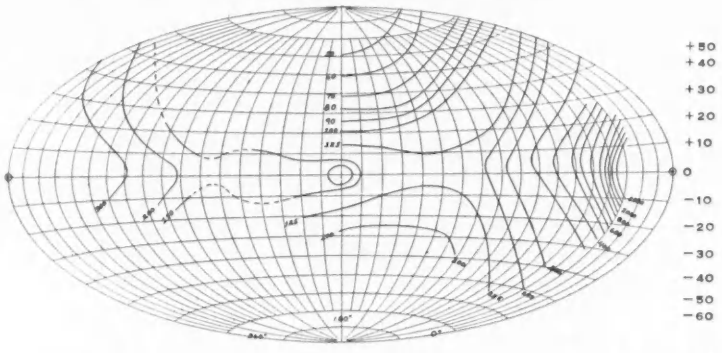

FIG. 8.—Isophotes for the zodiacal light for five nights in April and May, 1936

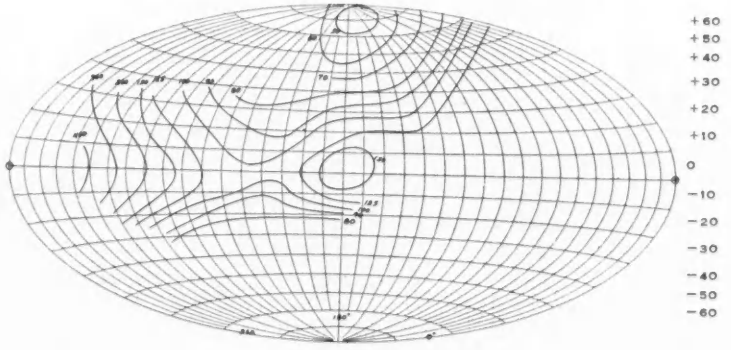

FIG. 9.—Isophotes for the zodiacal light for three nights in June and July, 1936

zodiacal light only for the morning. It is seen, however, that there is an increase in the gradient.

Another way to illustrate the changes in the zodiacal light is to take sections across the zodiacal light at longitudes from the sun, say, equal to 60° (evening zodiacal light) and to 300° (morning zodiacal light). These sections are shown in Figure 10, which has as abscissae the latitudes and as ordinates the intensity of the zodiacal

light. For the evening zodiacal light the greatest intensity is for the April–May series, while the least intense is the January–February series. The morning zodiacal light shows the reverse of the foregoing.

From the data we might conclude that there is a cloud of particles of greater than the average density in such a position that it is in conjunction with the sun during the late winter months. However, the data are too meager to justify an accurate determination. An accu-

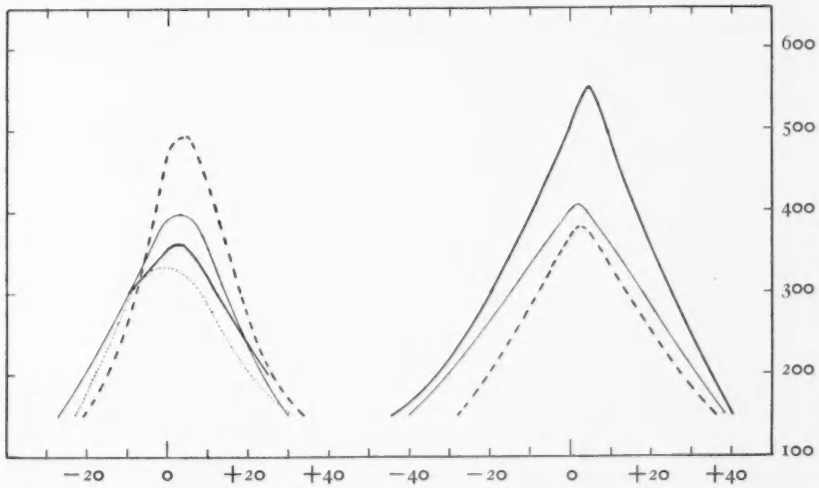

FIG. 10.—Sections across the evening and morning zodiacal light, at $\lambda - \lambda_{\odot} = 60°$ and 300°, respectively. The heavy continuous line represents the data for April and May. The heavy dashed line is for January and February. The narrow continuous line is for November and December; and the dotted line is for June and July.

rate set of the isophotes of the zodiacal light for each dark of the moon during the winter and spring months would undoubtedly give interesting information concerning the size and the parallax of the cloud.

THE GALACTIC LIGHT

In the preceding sections we have shown how to remove those components of the light from the night sky which are functions of the azimuthal and the ecliptical co-ordinate systems. The residuals are functions of the galactic co-ordinates. Since each of our observed points represents the light coming from an area of 9 square

degrees, there has been sufficient integration to obliterate the finer details of the Milky Way, and we have decided, for convenience in the construction of the isophotes of the galactic light, to average all points falling within a square of 5° on a side. This has been done in Figure 11, in which the isophotes were drawn from the mean values for the excess light plotted in the centers of every 25 square degrees, using the galactic co-ordinates. The first thing noticed is the lack of deficiencies. If we were dealing only with the deviations from the mean numbers of stars, then the plot should show nearly as many deficient areas as areas of excess. Before discussing the ob-

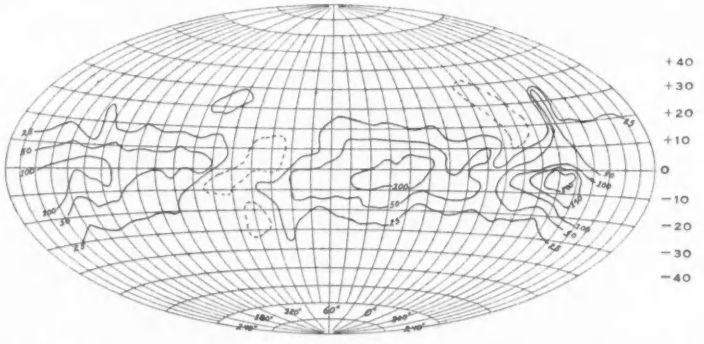

FIG. 11.—Isophotes of the excess light associated with the galactic system. This represents intensities due to deviations from the mean number of stars, to galactic nebulae, and to starlight scattered by interstellar matter.

servations, we must consider two assumptions which have been made in the reductions of the observations, namely, (1) that the light being scattered by our atmosphere is uniformly distributed over the hemisphere, and (2) that mean star counts were applied at low galactic latitudes.

Since a large number of observations have been obtained with the Milky Way in different positions in the sky, we have investigated the dependence of the excess light for a given region upon the zenith distance of the object during the observation. As the scattering is proportional to the air mass, which in turn is proportional to sec z, the intensities have been plotted against sec z. This should give an approximately straight line which can be extrapolated to sec $z = 0$, to give the correct value. The intensities of the various regions have been

adjusted so that the mean intensity is 100. Figure 12 shows such a diagram in which have been combined all data covering the Cygnus region of the Milky Way. We see from it that we should reduce our observed galactic light by 35 per cent. This amount seems rather large. However, if one considers that it includes scattered light from the stars in the Milky Way, as well as the galactic light, which is nearly as intense, the value seems more reasonable. The data shown in Figure 11 have been corrected by the foregoing amount.

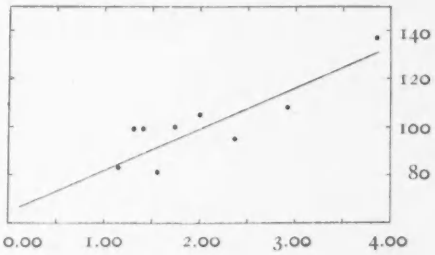

FIG. 12.—Variation with sec z of the excess light in the galactic system. Extrapolation to sec $z = 0$ shows that a correction must be applied to the observed excess light. This correction has been applied to the data plotted in Fig. 11.

Figure 11 shows the excess light to be strongest in the region of the Sagittarius cloud, longitude 300°, and to be faintest—really a deficiency—in the region of Auriga, longitude 120°.

TABLE 2

Regions	Galactic Latitude	Galactic Light
1	0°–5°	70
2	6 –10	62
3	11 –15	41
4	16 –20	29
5	21 –25	19
6	26 –30	9
7	31 –35	6
8	36 –40	4
I	3°	55
II	12½	32
III	21	18
IV	31	8

Since there are comparatively few individual star counts in the Milky Way, it is better to study the mean intensity of the excess light with respect to latitude. The mean distribution of the excess light, according to galactic latitude, is shown in Figure 13 and in

Table 2, Groups 1–8. The small circles and the dotted curve show the mean observed excess of galactic light over the mean number of stars, for the whole of our data. This, however, is not a fair test of the excess light, since our data cover the regions where the stars

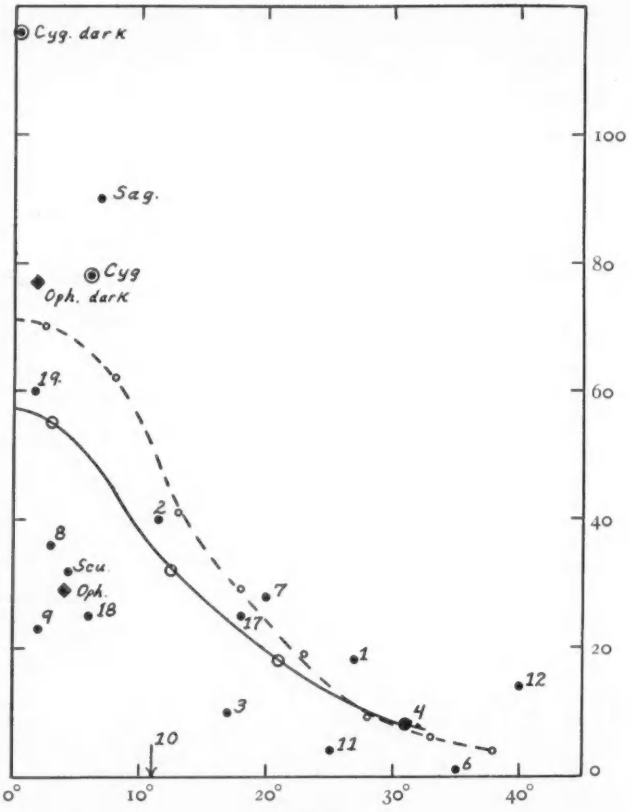

FIG. 13.—Plot of mean galactic light against galactic latitude. The dashed curve represents all the data. The continuous curve is for data from the same regions for which the mean star counts have been made. The individual points are for areas for which actual star counts have been used, and represent true galactic light.

are most numerous, namely, the Sagittarius cloud, while the data for the mean star counts do not include this region. A further comparison was made by grouping our data in such a way as to include only those which fall into the regions or groups of selected areas used in the determination of the mean number of stars.[18] The mean

excess is then shown by the continuous line in Figure 13, and by Groups I–IV in Table 2.

For certain selected regions we have individual star counts; consequently we can correct our excess for the observed deviation of the number of stars from the mean. Bottlinger[17] gives the total brightness of the direct starlight for the Sagittarius cloud, for the Cygnus cloud, both bright and dark, for a region in Ophiuchus, and for the Scutum cloud. Having corrected our data for these particular regions, for the deviation of the number of stars from the mean, we obtain the excess light in each region as shown in the diagram.

We were able to obtain data on the total amount of starlight from fourteen of the selected areas, making use of the information given in the *Bergedorfer Spektral-Durchmusterung*. Corrections to the excess in these regions for the deviations of the actual number of stars from the mean give the true excess. These have been plotted in Figure 12 by a dot with the number of the selected area beside it. All of the selected areas show an excess, with the exception of area 10, which has a small deficiency. This area is in Camelopardalis, just off the edge of the Milky Way where it is of the lowest density. In the chart of the isophotes of the galactic light this point falls in the region of deficiencies at longitude $+94°$ and $+11°$.

The data are shown also in Table 3. All the regions show an excess after all known sources of light except the galactic nebulae have been removed. The rather outstanding result that the dark regions show a greater excess than the regions of larger star density may be partly illusory since all points falling within a square of $5°$ have been averaged. This will obliterate much of the detail in the structure of the Milky Way. However, this smoothing of the observations is hardly enough to explain all the excess in some of the larger dark areas. Also, we should expect the dark areas to be somewhat luminous since they are clouds of cosmic particles which are obstructing the light of the stars behind them and are illuminated by the stars, much in the same way that a thin cloud in the night sky is illuminated by sky radiations rendering it no darker than the sky, although it obstructs a rather large amount of starlight.

Observations by Struve and Elvey[19] of some of Barnard's dark

[19] *Ibid.*, **83**, 162, 1936.

nebulae gave results which indicated considerable scattering of starlight by the material in interstellar space. Struve[20] has discussed the Rayleigh scattering of starlight by interstellar matter. Assuming that the number of particles per cubic centimeter is that

TABLE 3*

Region	Galactic Latitude	Galactic Light Corrected for the Actual Number of Stars
Region around Ophiuchus cloud	− 4°	29
Ophiuchus cloud, dark	+ 2	77
Cygnus cloud, bright	+ 6	78
Cygnus cloud, dark	0	116
Scutum cloud	− 4	32
Sagittarius cloud	− 7	90
Selected Area		
No. 1	+27	18
No. 2	+12	40
No. 3	+17	10
No. 4	+31	8
No. 6	+35	1
No. 7	+20	28
No. 8	− 3	36
No. 9	+ 2	23
No. 10	+11	− 14
No. 11	+25	4
No. 12	+40	14
No. 17	+18	35
No. 18	+ 6	25
No. 19	− 2	60

* The values in the last column are expressed in terms of the equivalent numbers of stars of magnitude 10 per square degree.

given by Gleissberg,[21] he obtained a rough value for the surface brightness of the galactic light which is somewhat greater than the observed value.

Struve's more recent results[22] can now be applied to the discussion of our observations, and we are indebted to him for the following

[20] *Ibid.*, **77**, 153, 1933.

[21] *A.N.*, **246**, 329, 1932.

[22] *Ap. J.*, **85**, 1937.

treatment. We may consider that each volume element in interstellar space receives, on the average, the same amount of starlight that an equal element in the solar system would receive from the entire celestial sphere. In other words, we shall assume that the surface brightness of the starlit sky as seen from each volume element is uniform and constant, equal to the surface brightness produced by all stars, as seen from the earth. Let this amount, L, be given in terms of the number of tenth-magnitude stars per square degree. Thus

$$L_0 = \frac{41{,}253}{4\pi}\int L d\omega = 577 \text{ stars of magnitude } 1.0 .$$

Obviously,

$$L = \frac{L_0}{41{,}253} = 56 \text{ stars of magnitude } 10.0 .$$

If only first-order reflections are considered, and if γ is the spherical albedo of each particle, ρ is its radius, N is the number of particles per cubic centimeter, and R is the extent of the diffuse medium in the line of sight, the surface brightness of the galactic light is given by

$$I_1 = L\gamma[1 - e^{-N\pi\rho^2 R}] ,$$

provided the phase function $\varphi(\alpha) = 0.5$. I_1 is expressed in numbers of tenth-magnitude stars per square degree.

The observations give $I = 57$. Hence

$$\gamma[1 - e^{-N\pi\rho^2 R}] = 1 .$$

This can only be satisfied if

$$N\pi\rho^2 R \approx \infty \qquad \text{and} \qquad \gamma \approx 1 .$$

In other words, the medium extends to very large distances R, so that the transmission, measured by $e^{-N\pi\rho^2 R}$, is effectively zero. Furthermore, the albedo is unexpectedly large. It should be emphasized here that the observational value, $I = 57$, is not very precise, and that γ measures not only the efficiency of ordinary scattering but also the fluorescence which give rise to emission nebulae.

Nevertheless, it seems desirable to extend the formula for I so that

it will include the second-order reflections. For this purpose we shall assume that each volume element in space, dv, is surrounded by an infinitely large sphere consisting of volume elements dv', each of which receives the same amount of light, $(41{,}253/4\pi)\int L d\omega$, from the starlit sky. If we again assume that the phase function $\varphi(a) = 0.5$, then the element dv' contributes the following amount of light to dv:

$$dq = 0.5\mu \int L d\omega \frac{e^{-k\Delta}}{\Delta^2} dv\, dv' ,$$

where Δ is the distance between dv and dv'. The other designations are the same as those used by Struve.[22] Of this amount, dv reflects toward the observer, at $\epsilon = 0$,

$$dq_1 = 0.25\mu^2 \int L d\omega \frac{e^{-k\Delta - kr}}{\Delta^2} dv\, dv' .$$

Since

$$dv = d\sigma dr ,$$

$$dv' = \Delta^2 \sin\theta d\Delta d\varphi d\theta ,$$

we have

$$Q = 0.25\mu^2\, d\sigma \int L d\omega \int\int\int\int e^{-k\Delta - kr} dr \sin\theta d\theta d\Delta d\varphi .$$

We integrate over the entire sphere, and from $\Delta = 0$ to $\Delta = \infty$ and from $r = 0$ to $r = \infty$. Struve[22] has shown that

$$\mu = N \frac{\gamma}{2\pi} \pi\rho^2 ,$$

$$k = N\pi\rho^2 .$$

Hence

$$I_2 = 0.25 \frac{\mu^2}{k^2} (4\pi)^2 L = \gamma^2 L .$$

Adding I_2 to I_1, we have

$$I = I_2 + I_1 = L\gamma(1 + \gamma) .$$

This would give $\gamma = 0.6$, if we again take $I/L = 1$.

It would not be profitable to continue this speculation by building up a power series in γ, for we have already made the untenable assumption that the diffuse matter extends to infinity in all directions from dv. Since in reality the scattering layer is thin, we cannot carry out the integration to $\Delta = \infty$ in all directions. It is not possible to determine γ without more information concerning the extent of the medium, and concerning the values of ρ and N, which become important when the upper limit of integration in Δ is finite. The only conclusion we can derive from our present data is that γ is not small enough to permit us to ignore completely the reflections of higher orders than the first, and that in the galactic plane $N\pi\rho^2 R$ is large enough to consider the medium as opaque. This agrees well with our current conception of the absorbing layer which gives rise to the zone of avoidance of extragalactic nebulae.[23]

We are indebted to our colleagues of the Yerkes Observatory for many helpful suggestions and for their assistance, and to Dr. F. H. Seares for information concerning star counts used in this paper. Mr. L. Henyey assisted in the construction of the photometer, and Mr. Theodor Immega has given valuable service in obtaining the observations. We are indebted to the Allan-Bradley Company, of Milwaukee, Wisconsin, for one of the high resistances used in the photometer.

McDONALD OBSERVATORY
UNIVERSITY OF TEXAS
February 25, 1937

[23] After this paper was written we received fasc. 19 of Vol. 1 of the *Publications de l'Observatoire de Lyon*, in which Wang Shih-Ky derives a theoretical value for the diffuse galactic light of about one-half of L. He has assumed Rayleigh scattering and has obtained the scattering coefficient from the observed value of the interstellar absorption. Considering the fact that his upper limit for I is equal to L, we can conclude that the theoretical data agree, as to order of magnitude, with the observations.

NOTE.—In equation 1, page 216, the fifth member on the right-hand side of the equation should be $S_T \times Sc(z)$ instead of $S \times Sc(z)$ since in this case the quantity is the total number of stars over the hemisphere.

RADIATION PRESSURE IN GALACTIC NEBULAE

JESSE L. GREENSTEIN

ABSTRACT

The existence of *small solid particles* with radii approaching the wave-length of light is indicated by the observed interstellar selective absorption. The recent investigations of Struve and his collaborators indicate that *particles much larger than the wave-length of light dominate in bright galactic nebulae*. The source of this difference is found in the *enormous radiation pressure of the hot stars* illuminating the nebulae. Figures 1–4 show the *dependence on spectral type of the sizes of the particles repelled* by a star. Further observations should yield information on the frequency function of particle sizes in space.

I. DISTRIBUTION OF PARTICLE SIZES IN INTERSTELLAR SPACE

The existence of selective absorption in the galactic plane indicates a considerable abundance of particles with radii of the order of, or less than, the wave-length of light. The fact that a low value is suggested by recent investigations[1, 2] for the ratio of the selective to the total absorption, and the spectrophotometric measurements of the distortion of the continuous radiation in early-type stars,[3, 4, 5] prove that Rayleigh scattering cannot be an important process. Some observational evidence on the frequency of particles of various radii is available from the distribution of interstellar hyperbolic meteors.[6] Over the observed range from 2.9×10^{-1} cm to 6.6×10^{-3} cm, Watson has shown that the frequency of meteoric particles in space increases uniformly with decreasing particle size.[7] The total absorption produced by such particles may be considerable, but the reddening will be zero. Particles capable of producing selective absorption would be meteors fainter than the sixteenth magnitude.

[1] Stebbins and Whitford, *Ap. J.*, **84**, 132, 1936.

[2] Greenstein, *Harvard Ann.*, **105**, 17, in press.

[3] Trumpler, *Pub. A.S.P.*, **42**, 267, 1930.

[4] Struve, Keenan, and Hynek, *Ap. J.*, **79**, 1, 1934.

[5] J. Rudnick, *ibid.*, **83**, 394, 1936.

[6] Watson, *Harvard Ann.*, **105**, 32, in press.

[7] The frequency and the velocity distribution of hyperbolic meteors will undoubtedly prove of great importance in the study of the interstellar medium.

The existence of selective absorption in the galaxy requires that the frequency function continue to increase at least as far as particles having radii of the order of the wave-length of light. The total density in space of these smaller particles may be less than that of the large particles, even though they dominate in the production of the total and selective absorption. The space density, ρ_i, of particles of radius a_i, required to produce a given total absorption coefficient, is of the form:

$$\rho_i \propto \frac{a_i}{K(a_i)} .$$

$K(a_i)$ is an efficiency factor, nearly unity except for $a_i < (\lambda/2\pi)$, when it is of the form (a/λ).[4]

The recent work of Struve and his collaborators,[8, 9] Collins[10] and other investigators on the colors of galactic nebulae with continuous spectra has yielded some interesting information as to the distribution of particle sizes in the neighborhood of hot stars. The observed agreement of the colors of these nebulae with the colors of the illuminating stars shows that the dominant process is diffuse reflection, or nonselective scattering. Any considerable dependence of scattering on wave-length for any large fraction of the scattered light, such as would exist for a $\leqslant\lambda$, is excluded by this observation. Struve and Story[11] have also shown that simple diffuse reflection from large particles ($a > \lambda$) will satisfactorily explain the observed relation between the brightness of the central star and the angular diameter of the nebula, found by Hubble.[12] This remarkable deviation from the form of the frequency function suggested above for interstellar space, in luminous nebulae which are associated with apparently normal obscuring clouds, can be simply interpreted as a result of the enormous radiation pressure exerted on small particles by hot stars of high luminosity.

[8] Struve, Elvey, and Keenan, *Ap. J.*, **77**, 274, 1933.

[9] Struve, Elvey, and Roach, *ibid.*, **84**, 219, 1936.

[10] *Pub. Amer. Astr. Soc.*, **8**, 240, 1936.

[11] *Ap. J.*, **84**, 203, 1936.

[12] *Ibid.*, **56**, 162 and 400, 1922.

II. RADIATION PRESSURE

The classical theory of the scattering of light by small, solid, spherical particles, developed by Mie,[13] has been applied by Debye[14] to the computation of the radiation pressure on such particles. Computations of the ratio of pressure to gravity, (P/G), by Gerasimovič,[15] as well as by Schoenberg and Jung,[16] have shown that this ratio can reach very high values ($\approx 10^4$). The value of the pressure varies with the ratio of the size of the particle to the wave-length, and is given by

$$P_\lambda = \frac{\pi a^2 E_\lambda}{c}\varphi(a); \qquad a = \frac{2\pi a}{\lambda}.$$

E_λ is the intensity; $\varphi(a)$ has been computed by Debye for several substances of differing optical properties, and depends on the index of refraction, ν, and the absorption coefficient of the substance. Schoenberg and Jung have given a table of (P/G) for a perfect conductor (perfect reflector), $\nu = \infty$. Their table for radii less than 10^{-6} cm gives too large values for the ratio (P/G) because of erroneous values they have adopted for $\varphi(a)$ for small values of a. Debye's theory gives a simple expression for very small particles, which was used in the present computations:

$$\varphi(a) = \tfrac{4}{3}a^4; \qquad a < 1, \nu = \infty.$$

On the assumption that the star radiates as a black body, the value of (P/G) for a particle of radius a and density s is

$$\left(\frac{P}{G}\right) = \frac{3R_*^2}{4cGsam_*}\int_0^\infty E_\lambda \varphi(a)d\lambda.$$

R_* and m_* are the radius and mass of the star; G is the gravitational constant; c is the velocity of light; and E_λ is the black-body energy corresponding to the effective temperature, Te. The values of (P/G) have been computed by numerical integration in a wide range of particle sizes and stellar temperatures for the substances

[13] *Ann. d. Phys.*, **25**, 377, 1908.
[14] *Ibid.*, **30**, 57, 1909.
[15] *Z. f. Ap.*, **4**, 265, 1932.
[16] *A.N.*, **247**, 413, 1932.

with the optical and physical properties given in Table 1. The errors arising from the lack of accurate values of $\varphi(a)$ and from the inaccuracies of the numerical integration are not larger than 10 per cent for most of the values of (P/G), except for $\nu = 1.1$. In any

TABLE 1

Refractive Index (ν)	Density (s)	Possible Substance
$\frac{\pi}{2}(1-\sqrt{-1})$....	5.0	Metals—iron, nickel, copper
1.1.....	0.5	Ice—Solid hydrogen, helium, or oxygen
1.5.....	2.0	Silica—stony meteors
Infinity.....	3.0	Perfect reflectors—"white body"

case, the results must be viewed as only approximate; the theory is developed for ideal smooth spherical particles with optical properties independent of the wave-length. The deviation for very small, coarse aggregates such as meteoric dust may be serious.

TABLE 2

Spectral Type	Effective Temperature (Degrees)	$\frac{m_*}{m_\odot}$	$\frac{R_*}{R_\odot}$
Bo.....	25,000:	19.5:	7.8:
B1.....	22,000:	13.0:	5.8:
B2.....	18,000:	8.6:	4.6:
B3.....	15,500	6.2	3.9
B5.....	13,000	4.7	3.3
Ao.....	9400	2.6	2.4
A5.....	7700	1.9	1.8
gF5.....	6000:	2.8:	5.5:
gG5.....	4500	3.6:	14.3:
gMo.....	3500	6.0:	53.7:

In order to determine the ratio (P/G) for typical stars of the spectral sequence, it was necessary to use values for the effective temperatures, radii, and masses of the stars. The adopted values in Table 2 are taken from a recent compilation of these data by Pilowski.[17]

[17] Pilowski, *A.N.*, **261**, 18, 1936

The detailed values of (P/G) so obtained will be published and discussed elsewhere, together with a treatment of the general problem of the stability of small particles in the galactic system. In the present discussion the results are given schematically for the various substances in Figures 1–4. The shaded areas in the figures indicate the range of particle radius, a, within which the ratio of pressure to gravity, (P/G), is greater than unity, as a function of spectral type. Particles for which this ratio is greater than unity cannot move in closed orbits around the central star, and will therefore be infre-

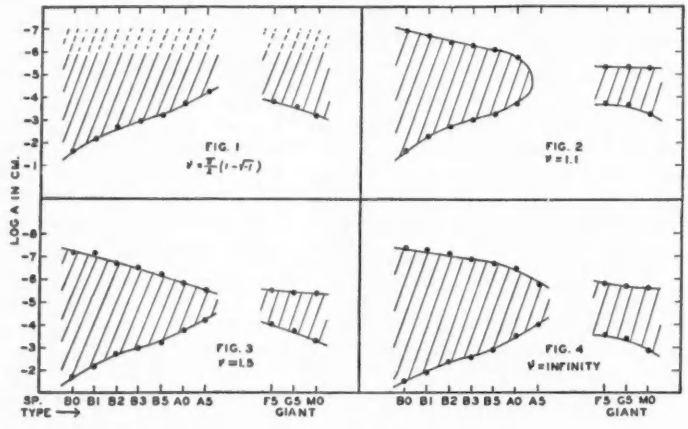

FIGS. 1–4

quent, if not entirely absent, at distances that are large compared with the usual sizes of luminous nebulae.

The ratio (P/G) depends on the total luminosity of the star and also on the wave-length of the energy maximum. The decreasing luminosity along the main sequence is the obvious origin of the features of that part of the diagrams. The late-type giants, though of high luminosity, have energy maxima strongly displaced toward the longer wave-lengths. The value of $\varphi(a)$ for a given particle size is therefore smaller for the red stars, reducing the pressure sharply for small particles. For metallic particles, the ratio (P/G) is independent of the radius for all particles of radius less than about 10^{-5} cm.

III. EFFECTS OF RADIATION PRESSURE IN GALACTIC NEBULAE

From these considerations it is obvious that the frequency function of particle sizes in space will be seriously affected near the very stars which most commonly excite nebulae. Particles whose radii nearly correspond to the wave-length of light are most subject to this effect and are absent from the nebulae. An examination of the figures indicates two general effects: (1) The total space density of interstellar matter will be decreased in the neighborhood of hot stars to a degree which depends on the spectral type. (2) Those particles capable of producing selective absorption ($\log a \approx -4.6$) are excluded from the neighborhood of stars of types Bo to A5, and gF5 to gMo.[18] Very small particles ($\log a < -6.0$) may be present near stars of types Ao and later, and of types gF5 to gMo.

1. Struve and Story[19] have shown that the total obscuration by dark material near emission-line nebulae is in fact less than that near reflection nebulae, indicating that the space density is lower near the hotter stars, in accordance with the theoretical predictions. The density of the scattering material present near emission nebulae must be less than that near reflection nebulae in order to explain the fact that the surface brightnesses of emission-line nebulae were no greater than those of reflection nebulae, in spite of the large amount of additional radiation in the strong nebular emission lines. This point was first noted by Struve.

2. The nonappearance of selective scattering in the nebulae so far observed may be due to the complete absence of small particles from the dark clouds with which the bright nebulae are associated. This is rendered rather improbable by the observed reddening of objects viewed through dark nebulae. The theory developed above will account simply for the distortion of the frequency function that is indicated by the agreement of the color of the nebulae with that of the illuminating star. A further prediction subject to observational test is that nebulae associated with stars as late as Ao, or with late-type giants, might show selective scattering and be

[18] Gerasimovič, *Ap. J.*, **78**, 298, 1933, has made a similar suggestion on the basis of less complete calculations.

[19] *Loc. cit.*

bluer than the illuminating star. The observational results are not definite as yet; the nebula near Antares[9] (cMo) seems to be nearly of the same color as Antares, while the nebula near γ Cygni[9] (F8p) is bluer than the star.[20] Such small particles are very inefficient scattering agents per unit mass, since the efficiency factor $K(a_i)$ is of the form $(a/\lambda)^4$. Therefore, only if the space density is very high will the nebula show strong selective scattering.

The importance of observations of the colors of nebulae near late-type stars cannot be overemphasized. Since space reddening may seriously affect some of the measured colors of nebulae, it is advisable to determine the color indices of the illuminating stars in the same manner as that of the nebulae. The frequency function for small particles can be investigated in this manner far beyond the range of sizes observable as meteors. Such data will prove of great importance in the discussion of the problems connected with the galactic absorption coefficient and the physical nature of the interstellar medium.

HARVARD COLLEGE OBSERVATORY
February 12, 1937

[20] A private communication from Struve and Elvey indicates that they suspect the existence of $H\alpha$ emission in the nebula near γ Cygni. Therefore the relative blueness of the nebula cannot be simply interpreted since other emission phenomena may exist.

NOTES

LINE STRENGTHS IN NEON I

ABSTRACT

The line strengths for the transition array $2p^5 4p - 2p^5 4s$ of neon I have been calculated in intermediate coupling, including the electrostatic and spin-orbit interactions.

The line strengths for the transition array $2p^5 3p - 2p^5 3s$ of neon I have been calculated by G. H. Shortley[1] in intermediate coupling, using the electrostatic and spin-orbit interaction terms and evaluating the radial integral parameters from the observed energy values. Similarly, the results of calculating the line strengths for the neon transition array $2p^5 4p - 2p^5 4s$ are given here.

Neon $2p^5 4s$ fits Houston's formulas well, so that the error in the line strengths introduced by the parameters from this configuration is probably less than 1 per cent. The radial integral parameters for neon $2p^5 4p$ have been calculated by C. L. Bartberger[2] in obtaining the energy-levels. Shortley found that a small change in the values of these parameters made a large change in the line strengths. However, as the calculated values of the energy-levels for $2p^5 4p$ agree better with the observed values than those for $2p^5 3p$, the radial integral parameters for $2p^5 4p$ should give more accurate values of the line strengths. The greatest deviation of a calculated level from an observed one was 70 cm^{-1} for $2p^5 3p$, 30 cm^{-1} for $2p^5 4p$; and the sum of the squares of all the deviations was 13,900 for $2p^5 3p$, 2900 for $2p^5 4p$, where $2p^5 3p$ has a spread of 4713 cm^{-1} between its lowest and highest energy-levels and $2p^5 4p$ a spread of 1768 cm^{-1}. It is convenient to estimate the error in calculating energy-levels by the ratio of the sum of the squares of the deviations to the spread of the configuration, which gives 294 per cent for $2p^5 3p$ and 164 per cent for $2p^5 4p$.

The values of the line strengths S(p, s) are given in Table 1. These are not the experimental intensities[3] of the lines but are re-

[1] *Phys. Rev.*, **47**, 295, 1935. [2] *Ibid.*, **48**, 682, 1935.

[3] E. U. Condon and G. H. Shortley, *The Theory of Atomic Spectra* (Cambridge University Press, 1935), § 7, pp. 97 and 240.

lated to the spontaneous transition probabilities A(p, s) of Einstein by the formula $S(p, s) = 3hc^3(2J_p + 1)\ A(p, s)/64\pi^4\nu^3$. ν is the frequency of the line, and the values of J_p are given as subscripts on the right of the Russell-Saunders notation for $2p^54p$. The Russell-Saunders level which occurs in largest proportion in each of the levels is used to denote that level. In addition, the original notation of Paschen and Götze is given for reference.

TABLE 1

LINE STRENGTHS IN THE TRANSITION ARRAY $2p^54p - 2p^54s$, NEON I

$2p^54s$	$2p^54p$									
	p_1	p_3	p_5	p_2	p_7	p_{10}	p_6	p_4	p_8	p_9
	$^1S_0$	$^3P_0$	$^3P_1$	$^1P_1$	$^3D_1$	$^3S_1$	$^3P_2$	$^1D_2$	$^3D_2$	$^3D_3$
$s_5\ ^3P_2$	.....	.....	17.4	1.6	2.7	8.3	19.8	28.1	2.1	70
$s_4\ ^3P_1$	0.7	9.3	8.3	9.0	1.0	11.7	30.2	18.4	1.4	.....
$s_2\ ^1P_1$	9.3	0.7	1.6	5.4	20.0	3.0	0.0	3.5	46.5	.....
$s_3\ ^3P_0$	.....	.....	2.7	14.0	6.3	7.0	.....	.....	.....	.....

C. W. UFFORD

ALLEGHENY COLLEGE
February 1937

NOTE ON PHOTOELECTRIC PHOTOMETRY

In a recent paper[1] I published observed magnitude differences between Vega and β Pegasi as a function of the mean wave-length. This mean wave-length corresponded to that at the center of the slits and not to the effective wave-length. Since the slits admitted 480 A at a time, the difference between the mean and the effective wave-length is not always negligible.

Smooth curves were drawn through the observed points in Figure 1.[2] The abscissa of this graph is the mean wave-length, and the ordinate is the electrometer deflection or the effective energy. By a simple graphical process the effective wave-length was found for each

[1] *Ap. J.*, **84**, 369, 1936. [2] *Ibid.*

star for each mean wave-length. Since the shape of each curve is well defined, it is possible to correct the energy observed at the effective wave-length to the value it would have at the mean wave-length. This process was carried through for both stars.

It was stated in the former paper[3] that these two radically different stars were compared primarily to test the efficacy of the apparatus in the determination of the effective wave-lengths when two color filters were used with the apparatus. Although these effective wave-lengths are not substantially changed by the corrections mentioned above, it seems worth while to give the corrected magnitude differences between these two stars.

In the following table the mean magnitude differences given in Table I[4] have been corrected in such a way that the wave-lengths are now effective wave-lengths. More than half of the corrections were 0.02 mag. or less, and none was more than 0.10 mag.

	Effective Wave-Length (μ)							
	0.454	0.478	0.501	0.525	0.549	0.573	0.597	0.621
β Peg–α Lyr. . . .	$+3^{M}63$	$3^{M}09$	$2^{M}90$	$2^{M}54$	$2^{M}30$	$2^{M}09$	$1^{M}92$	$1^{M}69$
(μ)	0.645	0.669	0.693	0.717	0.741	0.765	0.789	0.813
Δm	1.44	1.21	1.07	0.79	0.47	0.31	0.18	+0.06
(μ)	0.838	0.862	0.886	0.910	0.934	0.958	0.983	1.007
Δm	−0.06	0.15	0.17	0.30	0.23	0.36	0.44	−0.52

As a result of these corrections the observed difference in the color temperatures of these two stars is slightly larger. It still appears that if β Pegasi has a black-body temperature of 3000° K, the corresponding temperature of Vega is between 10,000° and 13,000°, depending on the spectral regions compared. If β Pegasi is hotter than 3000°, Vega is hotter than the foregoing figures indicate. This last statement was erroneously given in the original paper.

John S. Hall

Sproul Observatory
Swarthmore College
Swarthmore, Pennsylvania

[3] *Ibid.* [4] *Ibid.*

OBSERVATIONS OF THE SPECTRUM OF NOVA HERCULIS 1934

At the request of the editors of the *Astrophysical Journal* the directors of a number of observatories kindly communicated details of the spectrograms of Nova Herculis 1934 secured at their observatories between December 13, 1934, and April, 1935. On the formation of a subcommission on novae in the Commission on Stellar Spectra of the International Astronomical Union these details were passed on to the subcommission. They have been recently completed by returns from some outstanding observatories. Altogether 34 observatories obtained well over 3000 spectrograms between December 13, 1934, and April 20, 1935; and on every day in that interval at least one spectrogram was secured at some observatory. Most observatories are working up their own material, but in neverly every case the directors have expressed their willingness to send copies of plates to those investigators who are anxious to clear up difficulties arising from gaps in their own series. The complete list of observations is too long to publish, and a summarized statement may be more misleading than helpful. But the data are in my possession; and if any investigator wishes to know where he can find material to fill in a gap in his series of plates, I will, on receipt of a letter stating the dates and the region of the spectrum desired, send all relevant information in my possession.

F. J. M. STRATTON

GONVILLE AND CAIUS COLLEGE
CAMBRIDGE, ENGLAND

COLORS OF NEBULAE NEAR γ CYGNI

In a recent paper[1] the color index of the diffuse nebula near BD$+39^{\circ}4206$ was found to be -0.2 mag. If this nebula is produced by nonselective scattering of the light of γ Cygni, the color index should be roughly $+0.5$ mag. Since Henyey[2] found no measurable polarization in the light of this nebula, Rayleigh scattering by very small particles cannot account for its apparent blueness. In our determinations of the color index we used Eastman emulsion IG with

[1] *Ap. J.*, **84.**, 226, 1936.

[2] *Ibid.*, p. 617.

a yellow filter (Wratten No. 12, "minus blue"). This filter cuts off quite sharply at λ 5000, while emulsion IG cuts off at approximately λ 5800. This spectral region does not include any of the hydrogen lines, and the nebular line λ 5007 lies in the region where the filter begins to absorb appreciably. An emission nebula would appear to be quite faint if photographed with this combination. For the violet region we used Eastman Process or lantern-slide plates, which cover the region from λ 3000 to about λ 4700. All hydrogen lines from the Balmer limit to $H\gamma$ and many strong nebular lines are therefore included. In order to test whether the nebulae near γ Cygni are of the emission type we have taken several photographs on emulsion IC with a red filter (Wratten No. 23A). This combination includes the line $H\alpha$. The three nebulae near BD+41°3687, BD+39°4206, and BD+39°4186 are quite strong in red light. The spectral type of BD+41°3687 is Ko, but since no conspicuously red stars are near the other two nebulae, we tentatively infer that all three nebulae are of the emission type. If, as is probable, all three nebulae derive their light from the F8p star γ Cygni, we are confronted with the interesting problem of accounting for the emission. Unfortunately, these nebulae are so faint that we have not been able to obtain their spectra with the objective prism.

OTTO STRUVE
C. T. ELVEY

March 1937

THE MAGNITUDE OF THE COMPANION TO PROCYON

The companion to Procyon resembles in many ways the companion of Sirius: (1) the history of the discovery is similar; (2) the companions are very faint, compared with their primaries (we find that $\Delta m = 10$ mag. in both cases); (3) both companions are highly underluminous, as compared with ordinary stars of the same mass. This last feature indicates that both stars are white dwarfs, which is verified for the Sirius companion by its spectrum.

From the experience with gratings in measuring Δm in close double stars[1] the writer was convinced that the best method of

[1] *Pub. A.S.P.*, **46**, 99, 1934; **47**, 24 and 166, 1935.

measuring the brightness of the Procyon companion would be a determination of Δm with the aid of a double grating.[2]

At first a grating was made with a free opening of about 34 inches square, which gave first-order images 5.9 mag. fainter than the central image. When placed on the 40-inch telescope on a good night, this grating appeared to produce (1, 1) images too faint to be seen ($\Delta m = 2 \times 5.9 = 11.8$ mag.), whereas the companion was visible. Accordingly a new grating was made, giving $\Delta m = 2 \times 5.1 = 10.2$ mag. The wires are 0.1150 inches in diameter and are spaced by 1.300 inches (center to center), giving $\Delta m = 10.186$ mag. Twenty-five wires are placed in each co-ordinate, giving a square opening of $26 \times 1.3 = 33.8$ inches. The visual appearance of the patterns without and with grating is shown in Figure 1. Comparisons were made, with and without a yellow filter, between the images *a* and *B*, giving

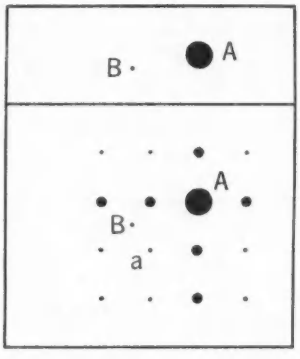

FIG. 1

$$B = a + 0^{m}.1 \pm 0^{m}.2,$$
$$\Delta m = 10.3 \pm 0.2 \text{ (m.e.)}.$$

The mean error is an estimate; it is considered very improbable that Δm lies outside the limits 10.0 mag. and 10.5 mag.

The apparent magnitude of Procyon B is therefore 10.8, and the absolute magnitude is 13.1, not nearly as faint as was often supposed.

The measurement of Procyon completes the writer's Δm determinations of the (roughly five hundred) visual binaries brighter than 6.50 mag., closer than 5".0, north of $-20°$ declination. The extension of the distance limit to 30" is being undertaken.

G. P. KUIPER

YERKES OBSERVATORY
March 29, 1937

[2] It turned out that Δm was considerably smaller than expected, and there would have been no objection to using a single grating; no very thin wires would have been needed.

A NEW BINARY OF LARGE PARALLAX

In the systematic micrometer work on the stars of large parallax, BD $-4^\circ 3665$ was found to have a distant companion which shares its proper motion, $0''.66$ in 261°. This is shown by the following measures:

1934.51.....	107°.3	15″.34	$m(B)=14.3$	36,	540×	seeing	3+
1935.51.....	108.3	15.23	15.3	36,	360		2+*
1937.27.....	107.0	15.35	14.8	40,	350		3
1935.81.....	107.4	15.32	14.8	3n			

* Half-weight, faint.

The position for 1900 is $\alpha = 14^h14^m.4$, $\delta = -4^\circ 41'$. The magnitude of A is 7.51 on the international photovisual scale, as determined from two sets of measures made at Leiden. The Mount Wilson spectrum is dK1, and the spectroscopically determined absolute magnitude is 5.5. The spectroscopic parallax is therefore $0''.040$.

The trigonometric parallax is $0''.053 \pm .006$ according to Schlesinger. Adopting this value, the absolute visual magnitude of the companion becomes 13.4; the spectroscopic parallax would make it 12.8 mag. The companion is, therefore, one of the faintest stars known.

G. P. KUIPER

YERKES OBSERVATORY
April 14, 1937

NOTE ON INTERSTELLAR SCATTERING

In a recent paper by Elvey and Roach[1] on the light from the night sky it was shown that the intensity of the light scattered by interstellar matter is very nearly the same as the intensity of the light coming to the earth from all the stars. In analyzing their data these writers made use of an approximate formula, derived by Struve,[2] giving the relationship between starlight and scattered light. It is the purpose of this note to derive an expression which is more rigorous.

[1] *Ap. J.*, **85**, 213, 1937. [2] *Ibid.*, p. 194

The equation of transfer governing the problem is

$$\frac{dI}{d\tau} + I = \int I\Phi d\omega + \int I_0 \Phi d\omega ,$$

where I and I_0 are the intensities of the scattered light and the starlight, respectively. Now if I_0 is taken to be everywhere equal to L, where L is the average intensity of starlight as seen from the earth, and if I is assumed isotropic, we have

$$\frac{dI}{d\tau} + (1 - \gamma)I = \gamma L ,$$

where γ is written for the albedo $\int \Phi d\omega$. The solution of this differential equation is

$$I = \frac{\gamma}{1 - \gamma} L \{ 1 - e^{-(1-\gamma)\tau} \} .$$

When $\tau \to \infty$ and when γ is small, this reduces, to within terms in γ^2, to the approximate expression referred to.

Since I and L are the same, the condition imposed on γ and τ by the observations is

$$1 = \frac{\gamma}{1 - \gamma} \{ 1 - e^{-(1-\gamma)\tau} \} .$$

Table 1 gives the values of τ for the values of γ compatible with the observations.

TABLE 1

γ	τ	γ	τ
0.5	∞ mag	0.8	1.6 mag
0.6	3.0	0.9	1.3
0.7	2.0	1.0	1.1

It will be seen that the albedo must, within the errors of observation, not exceed 0.5. Since it is not sensitive to the optical depth when the latter is large, it is likely that γ is about 0.5 or 0.6.

L. G. HENYEY

YERKES OBSERVATORY
WILLIAMS BAY, WIS.
April 1937